MARTIN MARIETTA ENERGY SYSTEMS LIBRARIES
3 4456 0064817 3

ORNL/TM-9678

ornl

OAK RIDGE NATIONAL LABORATORY

MARTIN MARIETTA

Application of the Finite Element Groundwater Model FEWA to Three Regional Aquifers

K-F.V. Wong
G. T Yeh

ENVIRONMENTAL SCIENCES DIVISION
PUBLICATION NO. 2616

OAK RIDGE NATIONAL LABORATORY
CENTRAL RESEARCH LIBRARY
CIRCULATION SECTION
4500N ROOM 175
LIBRARY LOAN COPY
DO NOT TRANSFER TO ANOTHER PERSON
If you wish someone else to see this report, send in name with report and the library will arrange a loan.

OPERATED BY
MARTIN MARIETTA ENERGY SYSTEMS, INC.
FOR THE UNITED STATES
DEPARTMENT OF ENERGY

Printed in the United States of America. Available from
National Technical Information Service
U.S. Department of Commerce
5285 Port Royal Road, Springfield, Virginia 22161
NTIS price codes—Printed Copy: A08; Microfiche A01

This report was prepared as an account of work sponsored by an agency of the United States Government. Neither the United States Government nor any agency thereof, nor any of their employees, makes any warranty, express or implied, or assumes any legal liability or responsibility for the accuracy, completeness, or usefulness of any information, apparatus, product, or process disclosed, or represents that its use would not infringe privately owned rights. Reference herein to any specific commercial product, process, or service by trade name, trademark, manufacturer, or otherwise, does not necessarily constitute or imply its endorsement, recommendation, or favoring by the United States Government or any agency thereof. The views and opinions of authors expressed herein do not necessarily state or reflect those of the United States Government or any agency thereof.

ORNL/TM-9678

ENVIRONMENTAL SCIENCES DIVISION

APPLICATION OF THE FINITE ELEMENT GROUNDWATER MODEL FEWA TO THREE REGIONAL AQUIFERS

K-F.V. Wong* and G. T Yeh

Environmental Sciences Division
Publication No. 2616

NUCLEAR AND CHEMICAL WASTE PROGRAMS
(Activity No. AR 05 15 15 0; ONL-WL14)

---

*University of Miami, Coral Gables, Florida 33124

Date issued - June 1986

Prepared for the
Office of Defense Waste and Transportation Management

Prepared by the
OAK RIDGE NATIONAL LABORATORY
Oak Ridge, Tennessee 37831
operated by
MARTIN MARIETTA ENERGY SYSTEMS, INC.
for the
U.S. DEPARTMENT OF ENERGY
under Contract No. DE-AC05-84OR21400

MARTIN MARIETTA ENERGY SYSTEMS LIBRARIES
3 4456 0064817 3

CONTENTS

	Page
LIST OF FIGURES	v
ABSTRACT	vii
1. INTRODUCTION	1
1.1 Background	1
1.2 Scope of Study	2
2. COMPARISON OF FEWA AND THE USGS TWO-DIMENSIONAL MODEL	4
2.1 Introduction	4
2.2 Similarities and Differences	5
2.3 Comparison of Results	8
3. APPLICATION OF FEWA TO LOVE CANAL, NEW YORK	14
3.1 Introduction	14
3.2 Lockport Dolomite	16
3.3 Major Assumptions	18
3.4 Application of FEWA	20
3.5 Comparison of Results	22
4. APPLICATION OF FEWA TO CONESVILLE, OHIO	28
4.1 Introduction	28
4.2 Conesville Study Area	28
4.3 Input Data	30
4.4 Application of FEWA	32
4.5 Comparison of Results	37
5. PREDICTIVE APPLICATION OF FEWA	40
5.1 Introduction	40
5.2 Biscayne Aquifer	41
5.3 Input Data	44
5.4 Model Calibration and Prediction	47
5.5 Comparison of Modeled Results to Field Data	50
6. SUMMARY AND CONCLUSIONS	54
REFERENCES	56
APPENDIX A FEWA INPUT DATA FOR USGS DATA SET	A-1
APPENDIX B FEWA INPUT DATA FOR LOVE CANAL, NEW YORK	B-1
APPENDIX C FEWA INPUT DATA FOR CONESVILLE, OHIO	C-1
APPENDIX D FEWA INPUT DATA FOR HIALEAH-PRESTON WELLS, MAY 3, 1977	D-1
APPENDIX E FEWA INPUT DATA FOR HIALEAH-PRESTON WELLS	E-1

LIST OF FIGURES

Figure		Page
1	Block-centered grid used for USGS two-dimensional model .	6
2	Finite element array used for FEWA simulation model . . .	7
3	Tabulated results from USGS 2-D model	9
4	Plotted results from USGS 2-D model	11
5	Tabulated results from FEWA model	12
6	Plotted results from FEWA model	13
7	Typical strata in the Love Canal landfill area	15
8	Generalized potentiometric surfaces for the Lockport Dolomite	17
9	Finite difference grid for the Lockport Dolomite	21
10	Tabulated results of GEOTRANS model, river head matrix . .	23
11	Computed potentiometric surface for the Lockport Dolomite using the USGS 2-D model	25
12	Computer potentiometric surface for the Lockport Dolomite using FEWA	26
13	Conesville power station study area	29
14	Conesville unconfined aquifer bottom contours	33
15	March 28, 1979 field-measured groundwater potential contours	34
16	Finite element array of Conesville area for input to FEWA	35
17	Finite element grid check of the Conesville area	36
18	March 28, 1979, model-predicted groundwater potential contours using VTT model	38
19	March 28, 1979, model-predicted groundwater potential contours using FEWA	39

Figure		Page
20	Measured potentiometric surface of the Hialeah-Preston wells on May 3, 1977	42
21	Measured potentiometric surface of the Hialeah-Preston wells on October 4, 1977	43
22	Structure contour map of Dade and Broward counties showing base of Biscayne aquifer	45
23	Monthly rainfall for 1977 and long-term average monthly rainfall	46
24	Finite element network of the study area	48
25	Grid check of the finite element network	49
26	Computed potentiometric surface of the Hialeah-Preston wells on May 3, 1977	51
27	Integrated flux at the wells and at the Miami Canal, May 3, 1977	52
28	Predicted potentiometric surface of the Hialeah-Preston wells on October 4, 1977	53

ABSTRACT

WONG, K-F V. and G. T. YEH. 1986. Application of the finite element groundwater model FEWA to three regional aquifers. ORNL/TM-9678. Oak Ridge National Laboratory, Oak Ridge, Tennessee. 126 pp.

This report documents the calibration with field data and predictive application of a finite element model of water through aquifers (FEWA). FEWA was described in a report written by G. T. Yeh and D. D. Huff in 1983. The model was first compared with the United States Geological Survey (USGS) two-dimensional model and found superior in treating anisotropic media when the coordinates cannot be made to coincide with the principal directions of hydraulic conductivities. In addition, there was no necessity to define nodal points outside the region, as required by the USGS model. FEWA was next calibrated with measured potentiometric surfaces from the Love Canal area in New York and the Conesville area in Ohio. There were satisfactory matches between computed results and available field data. The calibration and predictive runs of FEWA were then accomplished with the Hialeah-Preston well field data over the Biscayne aquifer in south Florida. The calibration run yielded two values of hydraulic conductivity in the area, and the predictive run gave results that matched well with available data.

1. INTRODUCTION

1.1 BACKGROUND

This report covers the calibration with field data and predictive application of FEWA: a finite element model of water flow through aquifers. For the purposes of this report, an aquifer is defined as a water-saturated stratum of permeable rocks, sand, or gravel. Thus, FEWA applies only to saturated geologic media.

Groundwater is not only a valuable resource, but an integral part of the environment. Population growth and industrial and agricultural production since World War II, coupled with the increased requirements for energy development, are generating ever larger quantities of hazardous and radioactive wastes. The groundwater environment is being loaded with an ever increasing number of contaminants and the potential for degradation of fresh groundwater exists. Choice of a waste disposal method requires attention to the possible damage to the environment.

Problems of groundwater quality degradation are difficult to overcome. First, owing to the heterogeneities inherent in subsurface systems, zones of degraded groundwater can be extremely hard to find. In addition, it ordinarily takes a long time before a groundwater problem becomes readily detectable. Finally, the flushing time for a contaminated aquifer is usually very long. Thus, it is important that groundwater dynamics be well understood and that models accurately predict the fate of contaminants within aquifers.

FEWA is a computer simulation model for the hydraulic aspects of aquifer systems. Its purpose is to model the effects of natural and artificial disturbances on the piezometric head distribution and groundwater flow in a system of aquifers. The model computes the temporal-spatial distributions of piezometric head and flow velocity in a two-dimensional areal plane. The velocity field is a necessary factor in determining the transport of contaminants in aquifer systems. Hence, the construction of FEWA is a necessary first step in the ultimate aim of building a model to simulate contaminant transport in subsurface media.

1.2 SCOPE OF STUDY

There are two major objectives in the present work; the first is to use field data to calibrate FEWA, while the second is to establish the predictive ability of the model.

In Chapter 2, the aquifer simulation data from the USGS two-dimensional model (Trescott et al. 1976), is used to run FEWA. The USGS model has been selected for comparison because it is a popular model and it has been around for quite some time.

In the following two chapters (Chapters 3 and 4), field data from the Love Canal area, New York, and from the Conesville area, Ohio, are used as input to FEWA. The Love Canal area was chosen for its notoriety as well as available data, while the Conesville area was investigated because a computer model, other than the USGS model, was used previously in its study.

Chapter 5 presents the work completed in pursuit of the second objective; that is an investigation of the predictive capabilities of FEWA. The site selected was part of the Biscayne aquifer in south Florida which is the United States Environmental Protection Agency (USEPA) number one priority for cleanup work under the superfund program.

2. COMPARISON OF FEWA AND THE USGS TWO-DIMENSIONAL MODEL

2.1 INTRODUCTION

The USGS two-dimensional finite difference model for aquifer simulation was written by Trescott, Pinder, and Larson (1976). The model simulates groundwater flow in an artesian aquifer, a water-table aquifer, or a combined artesian and water-table aquifer. The aquifer may be heterogeneous and anisotropic and have irregular boundaries. The source term in the flow equation may include well discharge, constant recharge, leakage from confining beds in which the effects of storage are considered, and evapotranspiration as a linear function of depth to water.

The theoretical development includes the appropriate flow equations and derivation of the finite-difference approximations (written for a variable grid) of the three numerical techniques available in the model. The strongly implicit procedure, in general, requires less computer time and has fewer numerical difficulties than do the iterative alternating-direction implicit procedure and line successive over relaxation (which includes a two-dimensional corrective procedure to accelerate convergence).

In this chapter the discussion is centered around the aquifer simulation published in the USGS two-dimensional finite difference model documentation (Trescott 1975). The input data from the USGS are used. After the appropriate modifications to the ORNL finite element model (FEWA), the similarities and differences are highlighted, and the results compared.

2.2 SIMILARITIES AND DIFFERENCES

For the user, the basic difference between the USGS 2-D model and FEWA is that the former is a finite difference model, and the latter is a finite element model. In the finite difference model, the generation of the grid is rather easy. The double array designation of node points is considerably easier than the single array designation of node points in the finite element model. In the finite element model, the coordinates of each of the nodes have to be entered as data input. It does not take much to show that if the number of elements goes beyond 300, the possibility of human error in establishing the coordinates can be rather high. Thus, the generation of coordinates for 1000 elements becomes tedious and almost impractical without a digitizer. This is the major drawback in using the finite element model.

On the other hand, the finite element method is capable of handling the situation that the finite difference method cannot. The finite difference method requires that the principal directions of anisotropy in an anisotropic formation parallel the coordinate directions. If there are two anisotropic formations in a flow field, each with different principal directions, the finite difference method is stymied, whereas the finite element method can provide a solution.

The USGS 2-D model uses a variable, block-centered grid approach. Figure 1 shows the grid used for the aquifer simulation. Figure 2 shows the corresponding elements array used for the same aquifer simulation with FEWA. There are two obvious differences besides the fact that one is block-centered and the other is corner-centered; the first is that, in the USGS 2-D model, the user has to define two extra

ORNL-DWG 85-11008

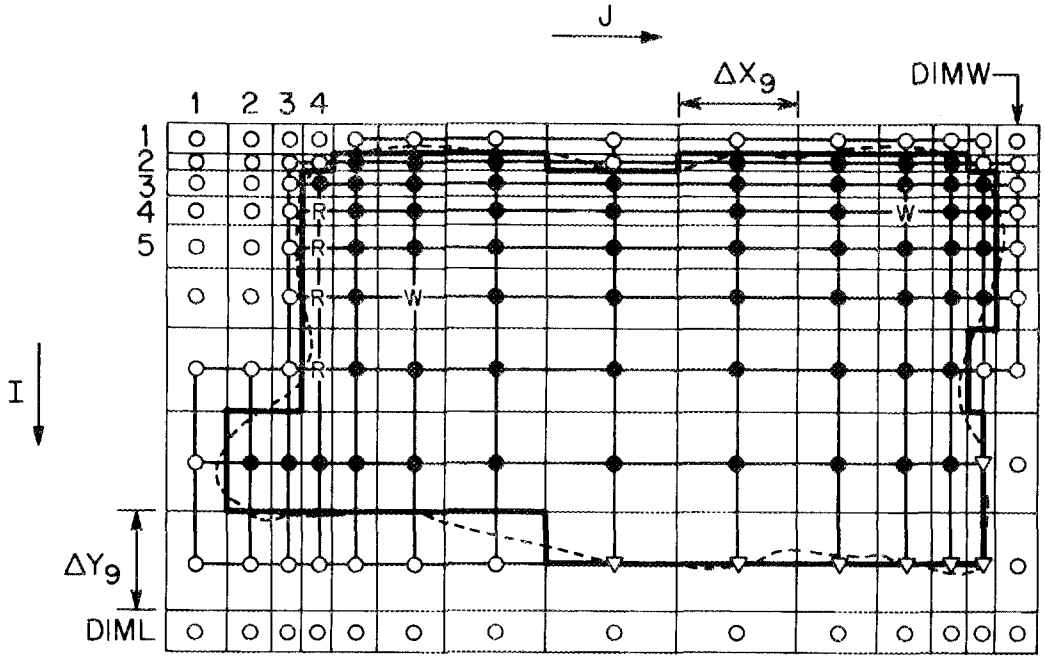

NODE SYMBOLS

INSIDE AQUIFER (TRANSMISSIVITY>0)

- W DISCHARGE WELL
- R RECHARGE WELL
- ▽ CONSTANT HEAD
- ● NODE WITHOUT WELLS OR SPECIFIED HEAD

OUTSIDE AQUIFIER

- ○ TRANSMISSIVITY = 0

--- AQUIFER BOUNDARY

— MATHEMATICAL BOUNDARY

DIML NUMBER OF ROWS

DIMW NUMBER OF COLUMNS

BOUNDARY CONDITIONS

CONSTANT HEAD

CONSTANT FLUX

$\partial h/\partial x = 0$

R $\partial h/\partial x = 0$

Fig. 1. Block-centered grid used for USGS two-dimensional model.

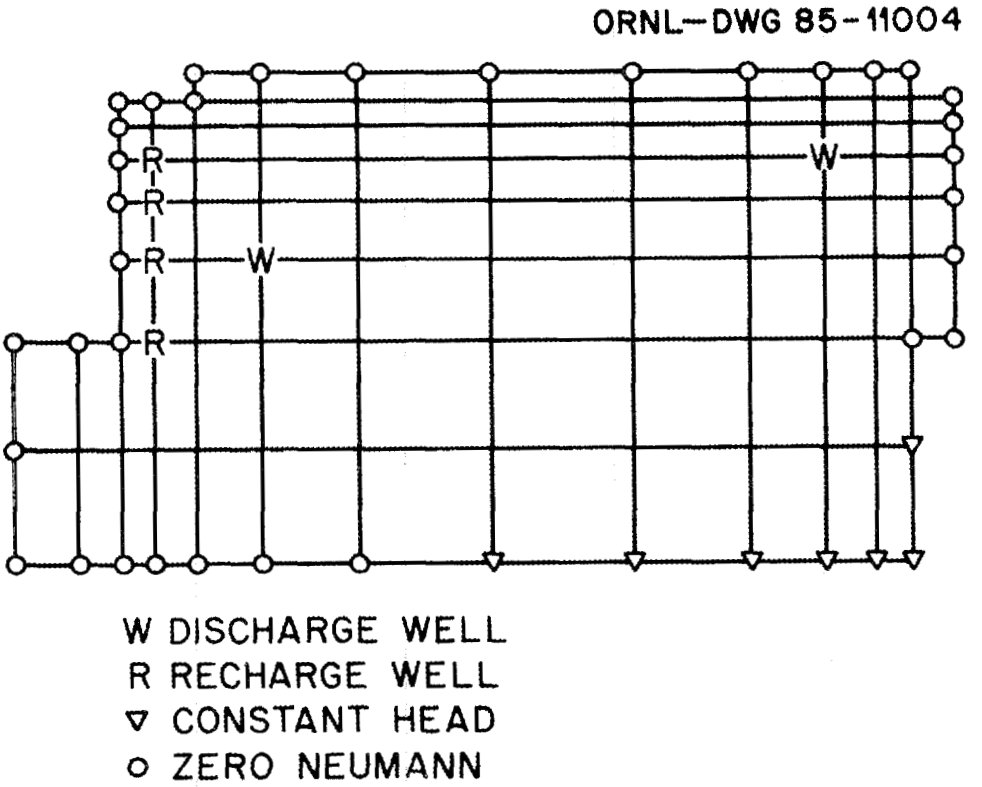

Fig. 2. Finite element array used for FEWA simulation.

external columns and two extra external rows when setting up the grid. There is no need for this with FEWA, resulting in a savings in computer memory storage space.

The second difference, though of no consequence to the aquifer simulation examined, is that the USGS 2-D model cannot handle grids other than rectangular or square ones. On the other hand, FEWA can handle irregular grids of any size as long as they are either four-sided or three-sided.

In the aquifer simulation under discussion, evapotranspiration is simulated because it is significant if the water table is within 4.3 m (14 ft) of the ground surface (Trescott 1975). There are two large pumping wells in the simulation. In the vicinity of these wells, evapotranspiration is not important because of the magnitude of the associated drawdown. Everywhere else, however, evapotranspiration has to be taken into account. Whereas the USGS model considers the evapotranspiration as a linear function of water depth from the surface, FEWA treats evapotranspiration as prescribed sinks. Therefore, the USGS model would require two sets of data to simulate this process: one is the evapotranspiration potential and the other is the depth below land surface at which evapotranspiration ceases. On the other hand, FEWA needs only one set of data to simulate this process, that is, the measured evapotranspiration rate.

2.3 COMPARISON OF RESULTS

The input data for FEWA is presented in Appendix A. The results of the aquifer simulation in the USGS 2-D model are tabulated in Fig. 3

HEAD MATRIX
(dimensions are in feet - 1 ft = 0.3 m)

1	100.0	100.0	100.0	100.0	100.0	100.0	100.0	100.0	100.0	100.0	100.0	100.0	100.0	100.0
2	100.0	100.0	100.0	100.0	79.0	79.5	82.7	100.0	85.9	80.2	72.6	74.3	100.0	100.0
3	100.0	100.0	100.0	78.9	78.9	79.4	82.8	86.8	86.1	80.4	71.7	74.6	76.1	100.0
4	100.0	100.0	100.0	78.8	78.6	78.7	82.8	86.9	86.5	81.1	67.9	75.3	76.9	100.0
5	100.0	100.0	100.0	78.4	78.0	77.0	82.7	87.3	87.5	83.8	78.6	79.8	80.1	100.0
6	100.0	100.0	100.0	78.6	77.5	72.1	83.0	88.3	89.2	87.4	85.5	84.9	84.0	100.0
7	100.0	100.0	100.0	81.5	81.4	81.6	85.4	90.1	91.4	91.1	90.9	90.9	100.0	100.0
8	100.0	84.0	83.9	83.9	84.0	84.8	87.6	93.4	95.1	95.7	96.6	98.1	100.0	100.0
9	100.0	100.0	100.0	100.0	100.0	100.0	100.0	100.0	100.0	100.0	100.0	100.0	100.0	100.0
10	100.0	100.0	100.0	100.0	100.0	100.0	100.0	100.0	100.0	100.0	100.0	100.0	100.0	100.0

Fig. 3. Tabulated results from USGS 2-D model.

and plotted in Fig. 4. The results obtained with FEWA are tabulated in Fig. 5 and computer plotted in Fig. 6. All the general trends are the same.

The head values throughout the region are comparable to each other. Since the ground surface is at 32 m (105 ft) and the evapotranspiration region is within 4.3 m (14 ft) of the ground surface, this mechanism is significant at 11 nodal points because, at these 11 nodal points, the head values are above 28 m (91 ft). Since no measured evapotranspiration rate is known for this hypothetical problem, it is not included in the simulation using FEWA. The neglect of evapotranspiration led to slight overprediction of head values by FEWA.

The above reason may account for the slight discrepancy in the head values at the two pumping wells. The USGS model gave head values of 21.9 m (72.1 ft) and 20.6 m (67.9 ft) at these wells, whereas FEWA gave head values of (22.4 m (73.6 ft) and 20.9 m (68.7 ft), respectively. The maximum discrepancy represented here is 2%.

ORNL—DWG 85-10995

RESULTS FROM USGS 2-D MODEL

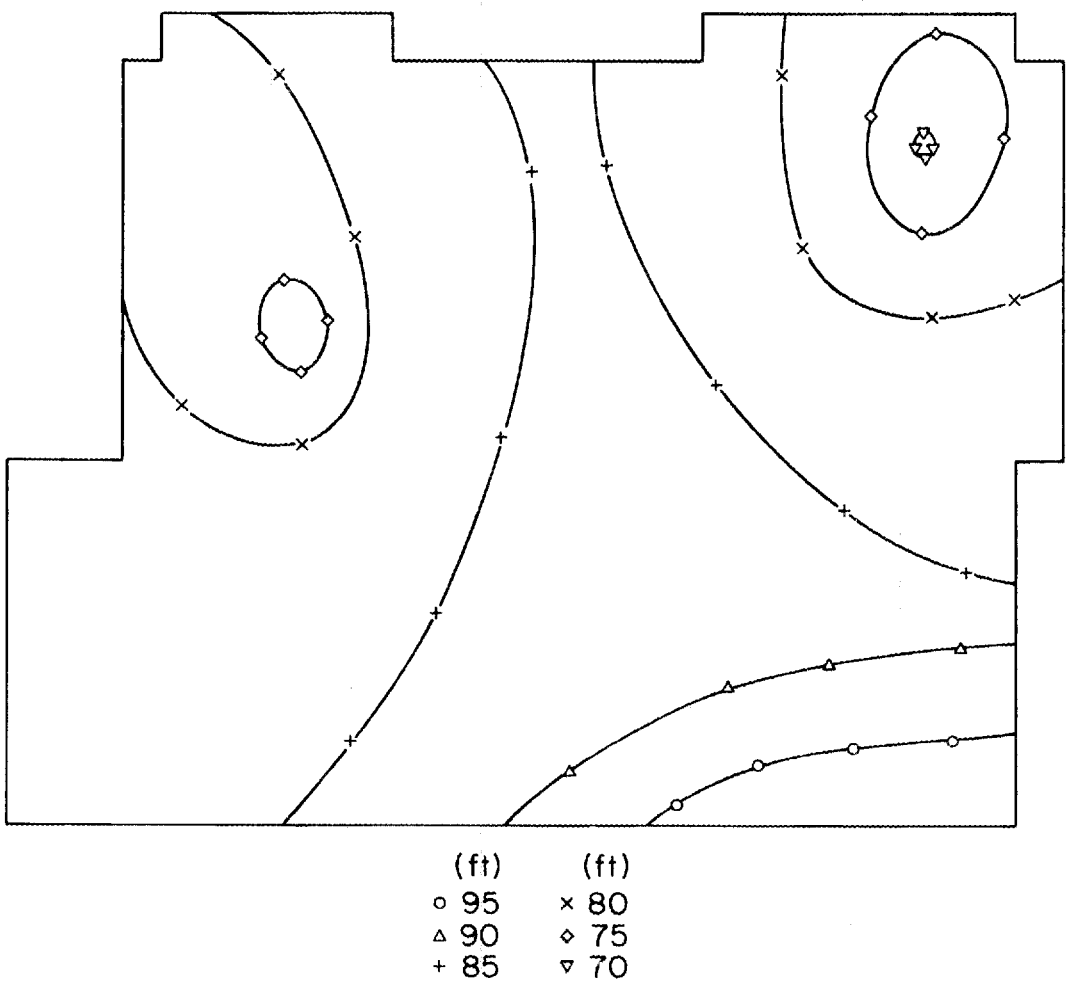

Fig. 4. Plotted results from USGS 2-D model.

Output Table 3. Hydraulic head (L) at time = 0.0, (Delt = 1,0000D-02), (Band width = 29) IT = 0
Steady-state initial conditions

Node I Hydraulic head of node I, I+1, ..., I+7

1	8.7639D	01	8.7738D	01	8.7911D	01	8.8138D	01	8.8532D	01	8.9498D	01	9.1561D	01	1.0000D	02
9	1.0000D	02	1.0000D	02	1.0000D	02	1.0000D	02	1.0000D	02	8.7363D	01	8.7360D	01	8.7442D	01
17	8.7541D	01	8.7846D	01	8.8585D	01	9.0989D	01	9.4036D	01	9.5717D	01	9.6120D	01	9.6757D	01
25	9.7980D	01	1.0000D	02	8.7007D	01	8.6700D	01	8.5947D	01	8.5458D	01	8.4842D	01	8.5324D	01
33	8.7169D	01	9.1457D	01	9.2874D	01	9.2931D	01	9.2893D	01	9.2639D	01	9.1673D	01	9.0513D	01
41	8.2819D	01	8.2667D	01	8.1612D	01	7.3501D	01	8.6047D	01	8.9666D	01	9.0542D	01	8.9123D	01
49	8.8119D	01	8.7743D	01	8.7715D	01	8.7905D	01	8.2238D	01	8.2020D	01	8.0762D	01	8.0422D	01
57	8.4807D	01	8.8661D	01	8.8707D	01	8.4934D	01	8.1313D	01	8.2039D	01	8.3403D	01	8.3765D	01
65	8.2296D	01	8.2268D	01	8.1977D	01	8.2300D	01	8.5241D	01	8.8104D	01	8.7440D	01	8.3965D	01
73	6.8686D	01	7.9830D	01	8.0909D	01	8.1462D	01	8.2413D	01	8.2405D	01	8.2435D	01	8.2948D	01
81	8.5353D	01	8.7890D	01	8.7099D	01	8.1986D	01	7.5596D	01	7.7966D	01	7.9875D	01	8.0465D	01
89	8.2427D	01	8.2494D	01	8.2614D	01	8.3208D	01	8.5276D	01	8.7931D	01	8.6781D	01	8.1676D	01
97	7.7222D	01	7.8042D	01	7.9247D	01	8.0376D	01	8.2577D	01	8.2677D	01	8.3380D	01	8.5011D	01
105	8.6390D	01	8.1663D	01	7.7795D	01	7.8159D	01	7.8623D	01						

Fig. 5. Tabulated results from FEWA model.

ORNL-DWG 85-10997

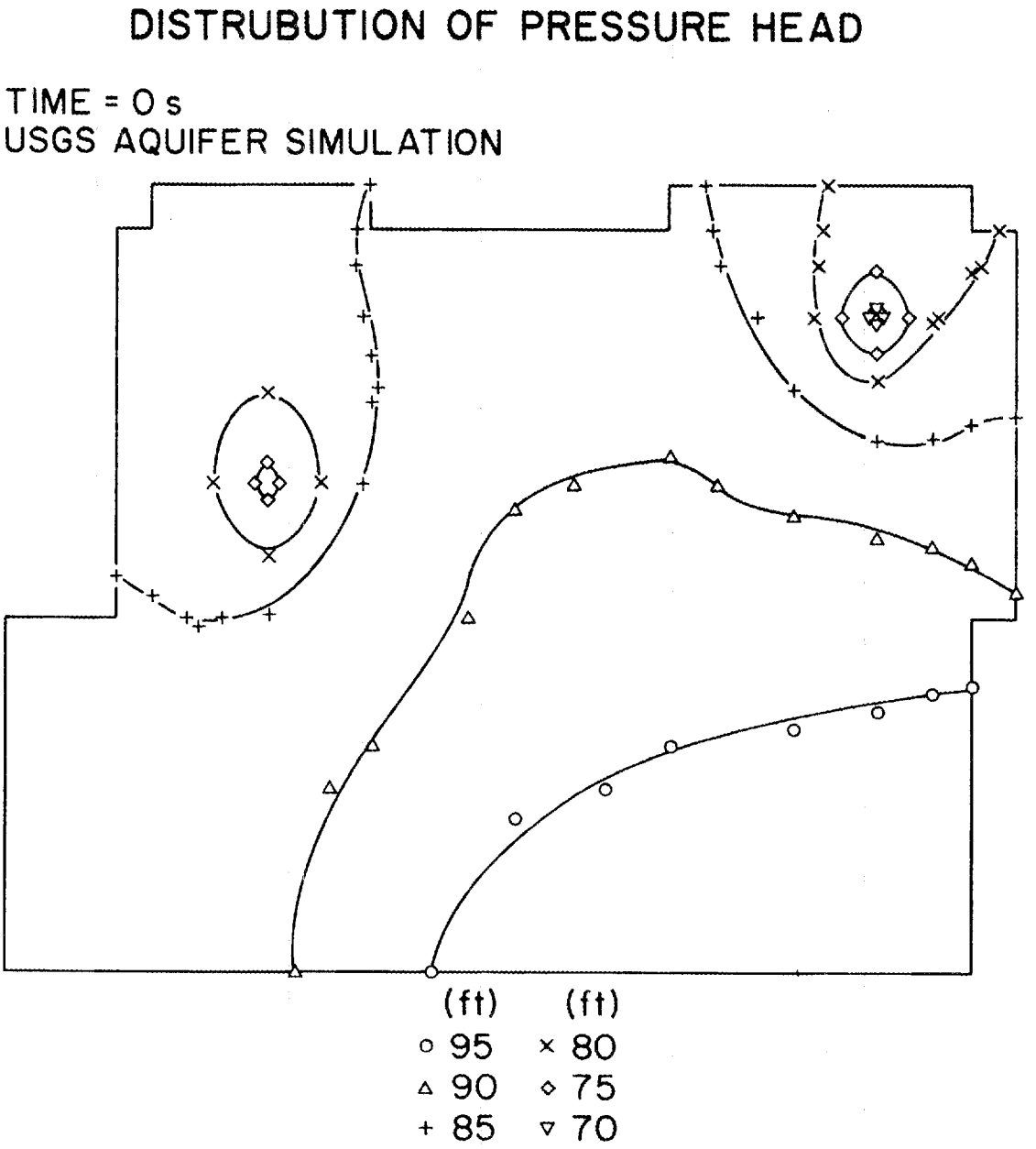

Fig. 6. Plotted results from FEWA model.

3. APPLICATION OF FEWA TO LOVE CANAL, NEW YORK

3.1 INTRODUCTION

A groundwater modeling study was conducted at the Love Canal area, Niagara Falls, New York during the fall of 1980 (Geotrans, Inc. 1981). The study was part of a comprehensive evaluation of the contamination at the Love Canal area. The hydrogeology underlying Love Canal consists of a shallow system of silts and fine sands underlain by confining layers of lacustrine and glacial clays which are underlain by the Lockport Dolomite, which is the local aquifer. The field data of the deeper Lockport Dolomite are used for the calibration of FEWA in this chapter. These field data have been used by Mercer et al. (1984) for a two-dimensional computer model also.

The Love Canal site is located on the east side of Niagara Falls, New York. The landfill of Love Canal was operated for a 25 to 30 year period, from 1923-1928 until 1953. The canal occupied a surface area of approximately 6.5 ha (16 acres) with the south end 400 m (0.25 mile) from the Niagara River near Cayuga Island. The canal varies from about 3 to 11 m (10 to 35 ft) in depth with the original soil cover varying from 0 to 1.8 m (0 to 6 ft) (in thickness (Leonard et al. 1977).

Figure 7 shows the typical strata at the Love Canal site. The soil layers are underlain by glacial till, which in turn is underlain by bedrock consisting of the Lockport Dolomite (USDA 1972). In general terms, the groundwater hydrology comprises: (1) a shallow system that is seasonally saturated and consists of the silt fill and silty sand,

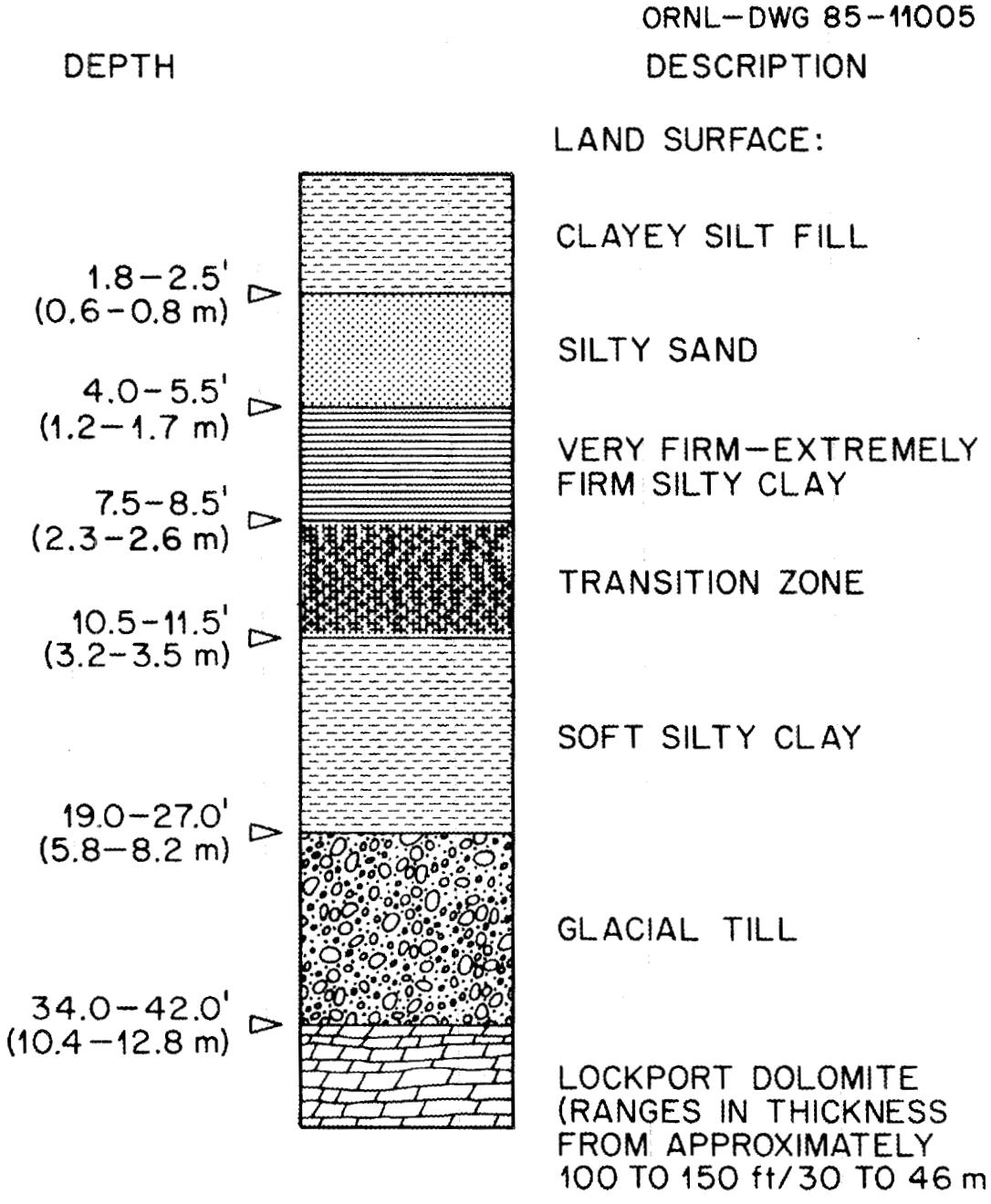

Fig. 7. Typical strata in the Love Canal landfill area.

and is underlain by (2) beds of confining material composed of clay and till that overlies (3) the Lockport Dolomite which is underlain by the relatively impermeable (4) Rochester Shale.

3.2 LOCKPORT DOLOMITE

The Lockport Dolomite is overlain by leaky confining beds and underlain by the relatively impermeable Rochester Shale (Johnston 1964). It is fairly continuous in the Niagara Falls area and is considered an aquifer with both confined and water-table conditions. It is a fractured system, with most of the permeability occurring in the top 3 to 4.6 m (10 to 15 feet) of the unit. The dolomite is probably bounded hydrogeologically in the Niagara Falls area to the south by the upper Niagara River (Fig. 8). It is bounded toward the west by the lower Niagara River and associated channel. The dolomite thins northward where it is bounded by the Niagara escarpment.

Recharge occurs at the junction with the upper Niagara River near the falls and at the high elevation just south of the Niagara River. Discharge occurred as seepage faces or springs at the lower Niagara River, along the Niagara escarpment, and along part of the upper Niagara River away from the falls. Annual precipitation is approximately 762 mm (30 in.).

A potentiometric map for the Lockport Dolomite is shown in Fig. 8. This was drawn using data from Johnston (1964). In many locations the potentiometric highs correspond to topographic highs. This is clearly evident near the Niagara escarpment where a recharge

ORNL-DWG 85-10999

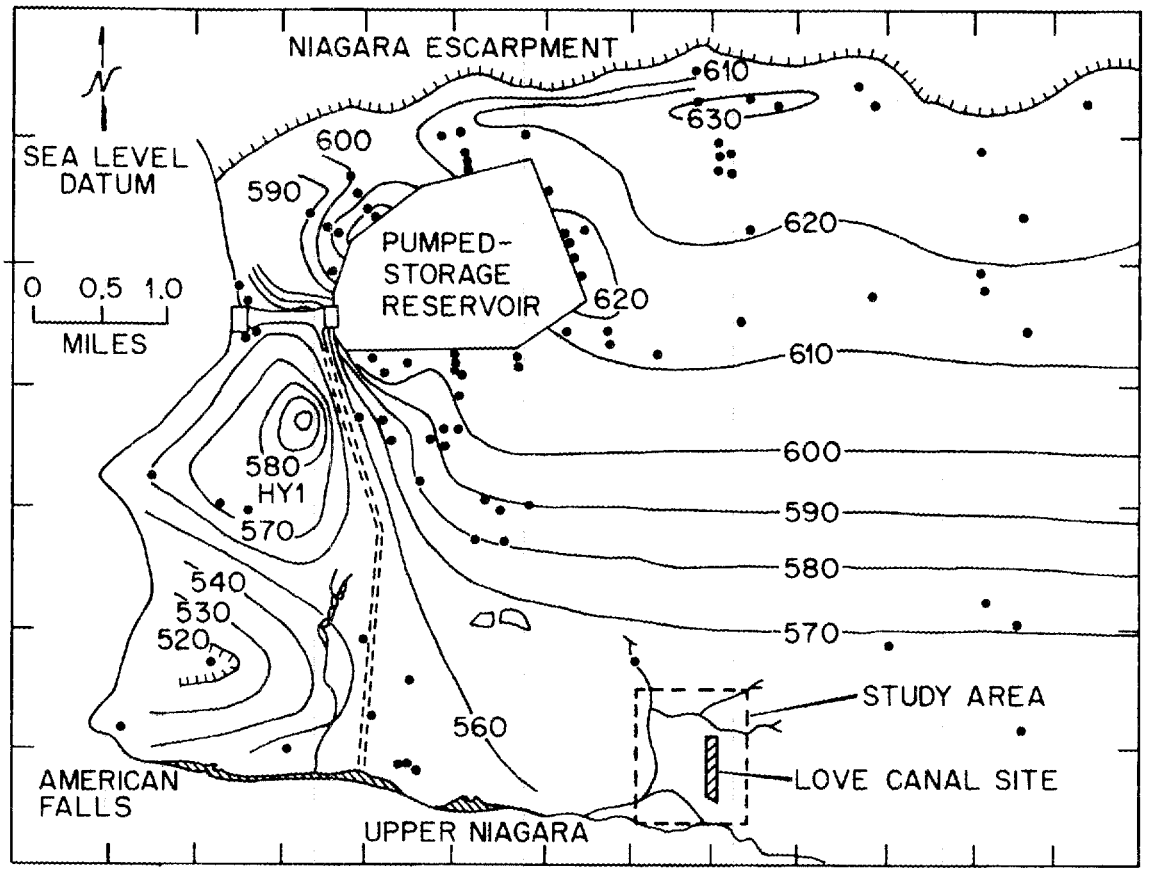

Fig. 8. Generalized potentiometric surfaces for the Lockport Dolomite (GEOTRANS 1981).

area produces flow toward the north, discharging as springs along the escarpment, and toward the south to the Love Canal site.

3.3 MAJOR ASSUMPTIONS

The groundwater flow model that was used by Geotrans Inc. (1981) was the USGS 2-D model presented by Trescott et al. (1976). The important assumptions made are as follows:

(1) The boundary condition at the bottom is no-flow since below the first 4.6 m (15 ft) extensive parts of the Lockport Dolomite are relatively impermeable. There is leakage through the upper confining beds.

(2) Groundwater flow and aquifer parameters in the Lockport Dolomite are vertically averaged.

(3) The flow is quasi-steady-state, although there are seasonal variations; over a long period of time the system does not change hydrologically from some seasonally averaged surface. This assumption is based upon the few well hydrographs available for this area.

(4) The aquifer in the Lockport Dolomite is considered to be confined, since that is the predominant condition.

(5) The aquifer transmissivity near the escarpment is taken to be 4.58×10^{-5} m^2/s (4.92×10^{-4} ft^2/s), determined by tests performed at the Love Canal site and the higher aquifer transmissivity near the river (Johnston 1964). A zone bordering the upper Niagara River was considered to have a transmissivity of 4.58×10^{-4} m^2/s (4.92×10^{-3} ft^2/s).

This value is about three times less than that obtained from the aquifer test analysis, yet slightly greater than previously reported values (Johnston 1964). This value for transmissivity was chosen since the aquifer test yielded a localized number for transmissivity, while the lower number used in the model is never representative of a larger area. The transmissivity is therefore isotropic, but nonhomogeneous.

(6) Water flows vertically into or out of the Lockport Dolomite through the overlying confining layer.

(7) The confining bed is 7.6 m (25 ft) thick.

(8) The hydraulic conductivity of the confining bed is 3.28×10^{-10} ft/s (10^{-10} m/s) (Leonard et al. 1977). Owing to the better drained soils near the Niagara escarpment (USDA 1972), the conductivity there was taken to be 3.28×10^{-9} ft/s (10^{-9} m/s). Thus, the hydraulic conductivity of the confining bed is isotropic, but nonhomogeneous.

(9) A potentiometric surface for the silty sand and silt fill (i.e. the shallow system) cannot be drawn because there is not enough well information. Work by Johnston (1964) shows that the water levels are approximately 3 m (10 ft) below land surface. Consequently, values obtained from a topographic map were used and 3.0 m (10 ft) subtracted to produce a shallow system potentiometric surface. This gave heads of 172 m (565 ft) in the Love Canal area.

(10) The heads in the shallow system represent an average value. Seasonal variations and imposed stresses are neglected.

(11) The few well hydrographs indicate that the pumped storage reservoir can be treated as providing constant head boundary points.

(12) The rock underlying the permeable part of the dolomite is treated as impermeable.

(13) The Lockport Dolomite can be modeled on a regional scale.

The area of interest was subdivided into rectangular blocks comprising the finite difference grid shown in Fig. 9. The grid consists of 21 columns and 23 rows. The northern boundary is considered no-flow because it is located along a recharge area (i.e., a groundwater divide). Discharge is through the confining bed. The eastern boundary is approximated as no-flow because it follows a flow line. The southern boundary is treated as constant head and corresponds approximately with the Upper Niagara River. The western boundary follows approximately the covered conduits of the pump-storage project and is considered constant head. The head values were determined from existing data (Johnston 1964; and Pasny 1965).

3.4 APPLICATION OF FEWA

The finite difference grid used by Geotrans Inc. (1981) is shown in Fig. 9. The finite elements used for FEWA matched the grid, however, since it is a finite element method, there was no necessity to store the grids that are shaded in Fig. 9. Furthermore, there was no necessity to define the two extra external rows and two extra external columns. Since the area was rather uniform, and all the elements were arranged in a regular array, there is no necessity to use a digitizer to locate the coordinates of each of the nodal points.

ORNL—DWG 85-11006

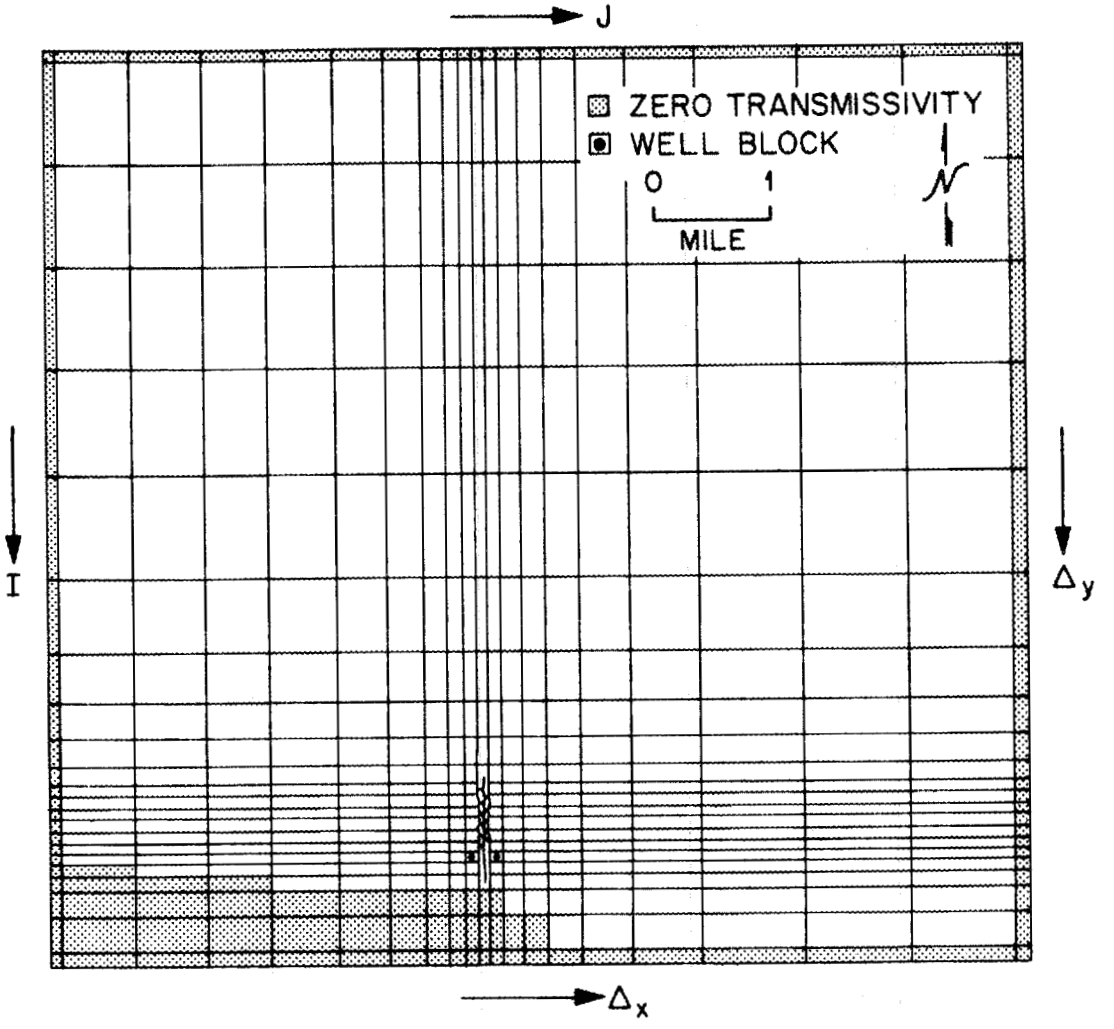

Fig. 9. Finite difference grid for the Lockport Dolomite Model.

The same values of the independent variables used by Geotrans Inc. (1981) were also used for FEWA. In essence, the same assumptions were made regarding the geohydrology of the Lockport Dolomite.

3.5 COMPARISON OF RESULTS

The input data for FEWA is presented in Appendix B. The results of the Geotrans model (1981) are tabulated in Fig. 10 and plotted in Fig. 11 (Mercer 1984). The results obtained with FEWA are computer drawn and shown in Fig. 12. Compared to Fig. 8, it can be seen that FEWA produced a good match on a regional scale, with the gradient in the Love Canal being toward the south and southwest. In terms of spatial distribution, leakage into the Lockport Dolomite occurred near the topographic high in the northern part of the study area. Leakage out occurred toward the escarpment and down-gradient toward the Upper Niagara River. In the Love Canal area, the gradient was generally into the Lockport Dolomite.

From the simulated results of Geotrans in Fig. 10, it is obvious that the manual plot in Fig. 11 is not an accurate representation of the computed results. Firstly, the highest head of 630 ft is computed only as a semi-elliptical area by the USGS model and also by FEWA, not a full elliptical area as depicted in Fig. 11. One can only conclude that the manual plot was influenced by the presence of the field data. Secondly, the potentiometric lines of 560, 570, 580, 590, and 600 ft should end at the reservoir or at the boundary, not within the boundary as shown in Fig. 11.

CONFINING BED THICKNESS = 25.00000
RIVER HEAD MATRIX
(dimensions are in feet - 1 ft = 0.3 m)

1	0.0	0.0	0.0	0.0	0.0	0.0	0.0	0.0	0.0	0.0	0.0	0.0	0.0	0.0	0.0	0.0	0.0	0.0	0.0	0.0
	0.0																			
2	0.0	600.0	610.0	610.0	620.0	620.0	620.0	620.0	620.0	630.0	630.0	630.0	630.0	640.0	640.0	630.0	620.0	620.0	620.0	620.0
3	0.0	620.0	640.0	640.0	620.0	620.0	620.0	620.0	620.0	620.0	620.0	620.0	620.0	620.0	620.0	620.0	620.0	620.0	620.0	620.0
	0.0																			
4	0.0	620.0	640.0	640.0	620.0	620.0	620.0	620.0	620.0	620.0	620.0	620.0	620.0	620.0	620.0	620.0	620.0	620.0	620.0	620.0
	0.0																			
5	0.0	590.0	590.0	600.0	610.0	610.0	610.0	620.0	610.0	610.0	610.0	610.0	610.0	610.0	610.0	610.0	610.0	610.0	610.0	610.0
	0.0																			
6	0.0	580.0	580.0	590.0	590.0	590.0	590.0	590.0	590.0	590.0	590.0	590.0	590.0	590.0	590.0	590.0	590.0	590.0	590.0	590.0
	0.0																			
7	0.0	570.0	580.0	580.0	570.0	570.0	570.0	570.0	570.0	570.0	570.0	570.0	570.0	570.0	570.0	570.0	570.0	570.0	570.0	570.0
	0.0																			
8	0.0	570.0	570.0	580.0	565.0	565.0	565.0	565.0	565.0	565.0	565.0	565.0	565.0	570.0	570.0	570.0	565.0	565.0	565.0	565.0
9	0.0	565.0	565.0	570.0	565.0	565.0	565.0	565.0	565.0	565.0	565.0	565.0	565.0	565.0	565.0	565.0	565.0	565.0	565.0	565.0
	0.0																			
10	0.0	565.0	565.0	565.0	565.0	565.0	565.0	565.0	565.0	565.0	565.0	565.0	565.0	565.0	565.0	565.0	565.0	565.0	565.0	565.0
	0.0																			
11	0.0	565.0	565.0	565.0	565.0	565.0	565.0	565.0	565.0	565.0	565.0	565.0	565.0	565.0	565.0	565.0	565.0	565.0	565.0	565.0
	0.0																			
12	0.0	565.0	565.0	565.0	565.0	565.0	565.0	565.0	565.0	565.0	565.0	565.0	565.0	565.0	565.0	565.0	565.0	565.0	565.0	565.0
	0.0																			

Fig. 10. Tabulated results of Geotrans model, river head matrix.

CONFINING BED THICKNESS = 25.00000
RIVER HEAD MATRIX
(dimensions are in feet - 1 ft = 0.3 m)

13	0.0	565.0	565.0	565.0	565.0	565.0	565.0	565.0	565.0	565.0	565.0	565.0	565.0	565.0	565.0	565.0	565.0	565.0	565.0	565.0
	0.0																			
14	0.0	565.0	565.0	565.0	565.0	565.0	565.0	565.0	565.0	565.0	565.0	565.0	565.0	565.0	565.0	565.0	565.0	565.0	565.0	565.0
	0.0																			
15	0.0	565.0	565.0	565.0	565.0	565.0	565.0	565.0	565.0	565.0	565.0	565.0	565.0	565.0	565.0	565.0	565.0	565.0	565.0	565.0
	0.0																			
16	0.0	565.0	565.0	565.0	565.0	565.0	565.0	565.0	565.0	565.0	565.0	565.0	565.0	565.0	565.0	565.0	565.0	565.0	565.0	565.0
	0.0																			
17	0.0	565.0	565.0	565.0	565.0	565.0	565.0	565.0	565.0	565.0	565.0	565.0	565.0	565.0	565.0	565.0	565.0	565.0	565.0	565.0
	0.0																			
18	0.0	565.0	565.0	565.0	565.0	565.0	565.0	565.0	565.0	565.0	565.0	565.0	565.0	565.0	565.0	565.0	565.0	565.0	565.0	565.0
	0.0																			
19	0.0	0.0	565.0	565.0	565.0	565.0	565.0	565.0	565.0	565.0	565.0	565.0	565.0	565.0	565.0	565.0	565.0	565.0	565.0	565.0
	0.0																			
20	0.0	0.0	0.0	0.0	565.0	565.0	565.0	565.0	565.0	565.0	565.0	565.0	565.0	565.0	565.0	565.0	565.0	565.0	565.0	565.0
	0.0																			
21	0.0	0.0	0.0	0.0	0.0	0.0	0.0	0.0	0.0	0.0	0.0	0.0	565.0	565.0	565.0	565.0	565.0	565.0	565.0	565.0
	0.0																			
22	0.0	0.0	0.0	0.0	0.0	0.0	0.0	0.0	0.0	0.0	0.0	0.0	0.0	0.0	565.0	565.0	565.0	565.0	565.0	565.0
	0.0																			
23	0.0	0.0	0.0	0.0	0.0	0.0	0.0	0.0	0.0	0.0	0.0	0.0	0.0	0.0	0.0	0.0	0.0	0.0	0.0	0.0
	0.0																			

Fig. 10 (continued)

ORNL-DWG 85-10998

COMPUTED STEADY STATE POTENTIOMETRIC SURFACE
LOCKPORT DOLOMITE
FEET ABOVE MSL

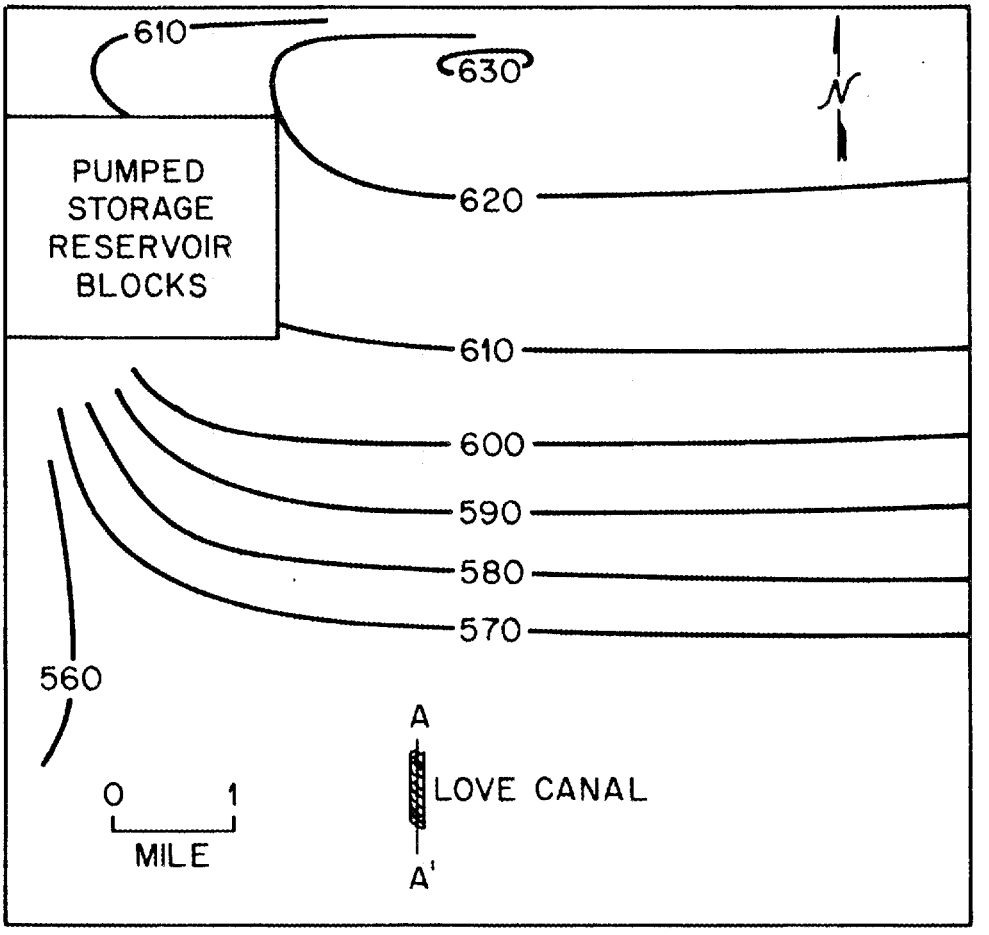

Fig. 11. Computed potentiometric surface for the Lockport Dolomite using the USGS 2-D model (Geotrans 1981).

ORNL-DWG 86-1558

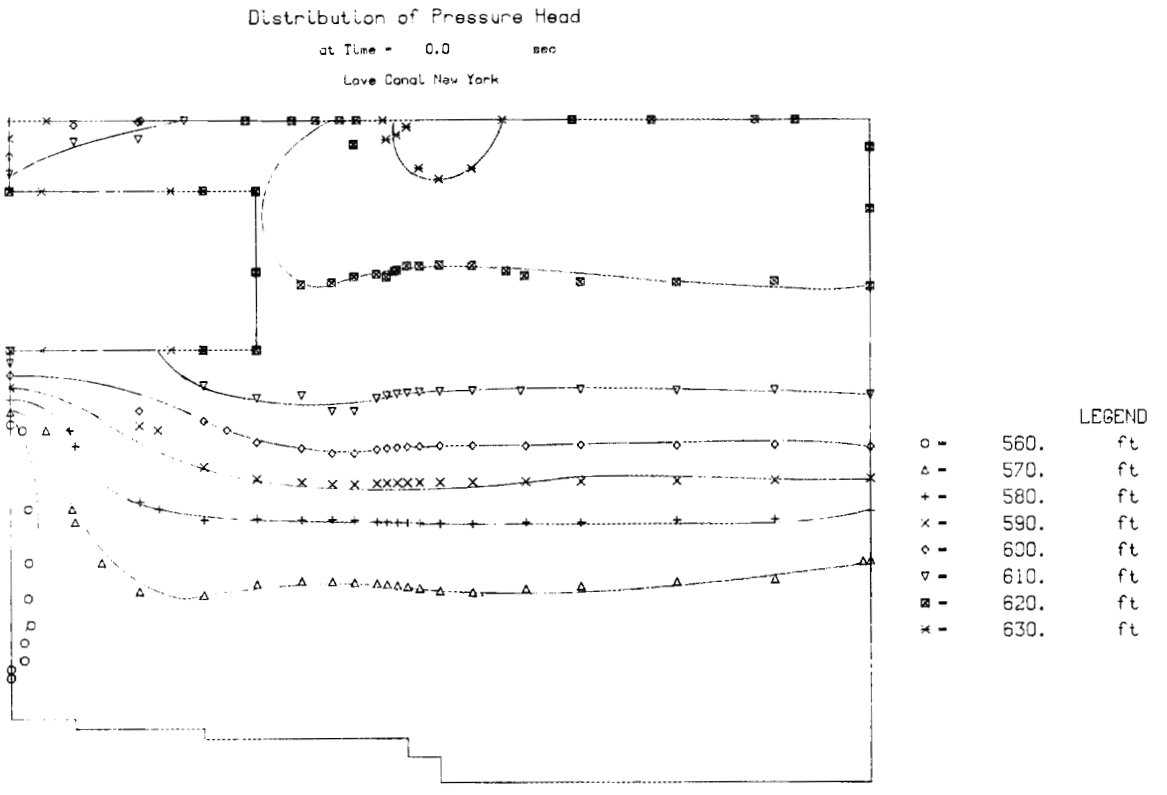

Fig. 12. Computer potentiometric surface for the Lockport Dolomite using FEWA.

In Fig. 12 it is noted that FEWA computes a highest head of 630 ft as a semi-elliptical area. The computer plot of the 630 ft potentiometric line does not close onto itself, but ends at the boundary. In addition, all the other potentiometric lines end at the boundaries.

4. APPLICATION OF FEWA TO CONESVILLE, OHIO

4.1 INTRODUCTION

The leaching and potential groundwater contamination aspects of flue gas desulfurization (FGD) sludge disposal at the Conesville site were studied (Bond 1980) to provide information useful to authorities making decisions regarding the disposal of FGD sludges. The Conesville generating station is located on the east bank of the Muskingum River in Coshocton County, Ohio. The study region, Fig. 13, is approximately 5.29 km^2 (2.3 $mile^2$) in size and consists of the plant facilities, the disposal area for ash and sludge (Poz-O-Tec), sedimentation and holding water ponds, and surrounding agricultural fields. The station is situated near the center of a small glacial-outwash filled valley surrounded by hilly terrain. The aquifer considered in the study is unconfined and ranges in thickness from 46 m (150 ft) near the center of the valley to zero where the bedrock (aquifer bottom) crops out along the face of the surrounding hills. The unconfined aquifer composed of the glacial outwash material is the main site aquifer of interest here. The bedrock below the unconfined aquifer comprises the Conemaugh and Allegheny Series of the Pennsylvania system. These series are composed mainly of beds of sandstone, shale, and limestone (Bond 1980).

4.2 CONESVILLE STUDY AREA

The actual study area comprises the power plant facilities, the disposal areas for ash and sludge (Poz-O-Tec), sedimentation and

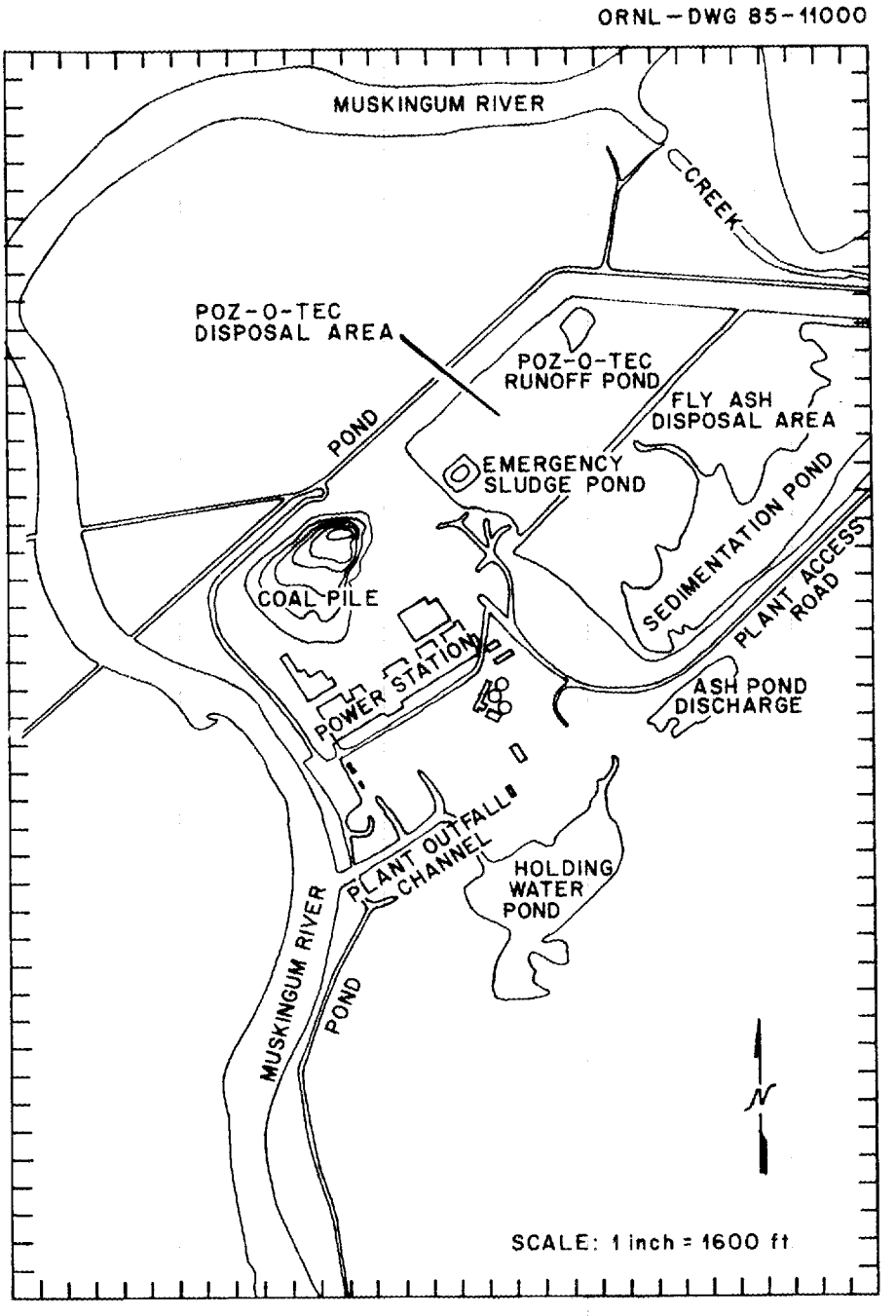

Fig. 13. Conesville power station study area (Bond 1980).

holding water ponds, and surrounding agricultural fields (Fig. 13). The area is approximately 6 km^2 (2.3 $miles^2$) in size, with the Muskingum River forming the north and west boundary, and the low hills forming the boundary to the east and south. An unnamed creek to the northeast is hydraulically connected to the groundwater aquifer and was used as a boundary.

Water is ponded in an area along the northeastern perimeter of the Poz-O-Tec disposal area. All drainage in the area is directed to the Poz-O-Tec runoff collection pond which is approximately 0.4 ha (1 acre) in size. The pond is a surface expression of the regional groundwater system (Bond 1980).

The regional groundwater flow pattern in the study area is from the low hills west and northwest to the Muskingum River. The gradient is very small over most of the study area and increases rapidly near the hills. The Muskingum River, the creek to the northeast, the Poz-O-Tec pond, the ash sedimentation pond, and the holding water pond are all hydraulically connected to the groundwater system. The Muskingum River and the creek are natural, while the remainder of the surface-water bodies are man-made.

4.3 INPUT DATA

The two-dimensional variable thickness transient (VTT) model (Kipp et al. 1972) was used by Bond (1980) to study the Conesville area. Natural recharge to the Conesville generating station model region consists of rainfall, underflow (groundwater flow from the hills to the east), and/or underflow from the Muskingum River to the west and

north (depending on river stage). Natural discharge from the model region takes the forms of evapotranspiration and underflow to the Muskingum River.

For modeling purposes, the recharge rate to the aquifer is taken as 54.8 ft^3/d (1.55 m^3/d) at each interior node of this model region which represents an area of 40,054 ft^2 (3721 m^2). This rate is computed from the average precipitation, the actual potential evapotranspiration (AET) (Thornthwaite and Wilm 1944), and the surface runoff.

The water level at the nodes representing the Muskingum River is held at the field-determined river elevations. The majority of the eastern boundary is either represented by stationary elevations at nodes or is assumed to have little or no underflow moving across it. However, there is a considerable amount of subsurface recharge in the small region between the ash pond and the creek directly to the north of the pond. It was estimated by Bond (1980) that the total subsurface flow over this 183 m (600 ft) boundary was 100,000 ft/d (2831 m/d).

The man-made sedimentation pond in the ash disposal area is hydraulically connected to the water table. For this reason the pond was set as a held potential boundary. There is a single pumping well in the region; however, the well is within 75 m (246 ft) of the river in highly permeable material. Since it pulls most of the water from the river (Bond 1980), the discharge from the well was discounted.

Bond (1980) determined the transmissivity distribution in the Conesville study area. Due to uncertainties in the pump tests and

analyses, he naturally used the transmissivity to be the principal variable adjusted when calibrating the model. Rather than change the model to agree with the measured transmissivities, the pump test results were used as a starting point and changes were made in the process of model calibration. After calibration and verification the final transmissivity surface was determined by Bond (1980). On the average, this corresponded to a saturated hydraulic conductivity of 0.0145 ft/sec over much of the area. The area of the fly ash disposal pond had a hydraulic conductivity of 0.003 ft/sec.

The aquifer studied here is a single unconfined aquifer. As such, the aquifer top is the land surface elevation which can be obtained from a topographic map of the region. The top was set at 245 m (800 ft) above sea level. The aquifer bottom surface is shown in Fig. 14. The bottom surface consists of silt, clay, or bedrock and, thus, is considered to be impermeable.

4.4 APPLICATION OF FEWA

The March 28, 1979 field-measured groundwater potential contours are presented in Fig. 15. This region was divided into finite elements, and a digitizer board was used to input the coordinates of the nodes. The finite elements are shown in Fig. 16. A grid check was done to ensure that there were no errors in setting up the coordinates. The output from this grid check is presented in Fig. 17. An error is indicated if two lines cross.

ORNL-DWG 86-1559

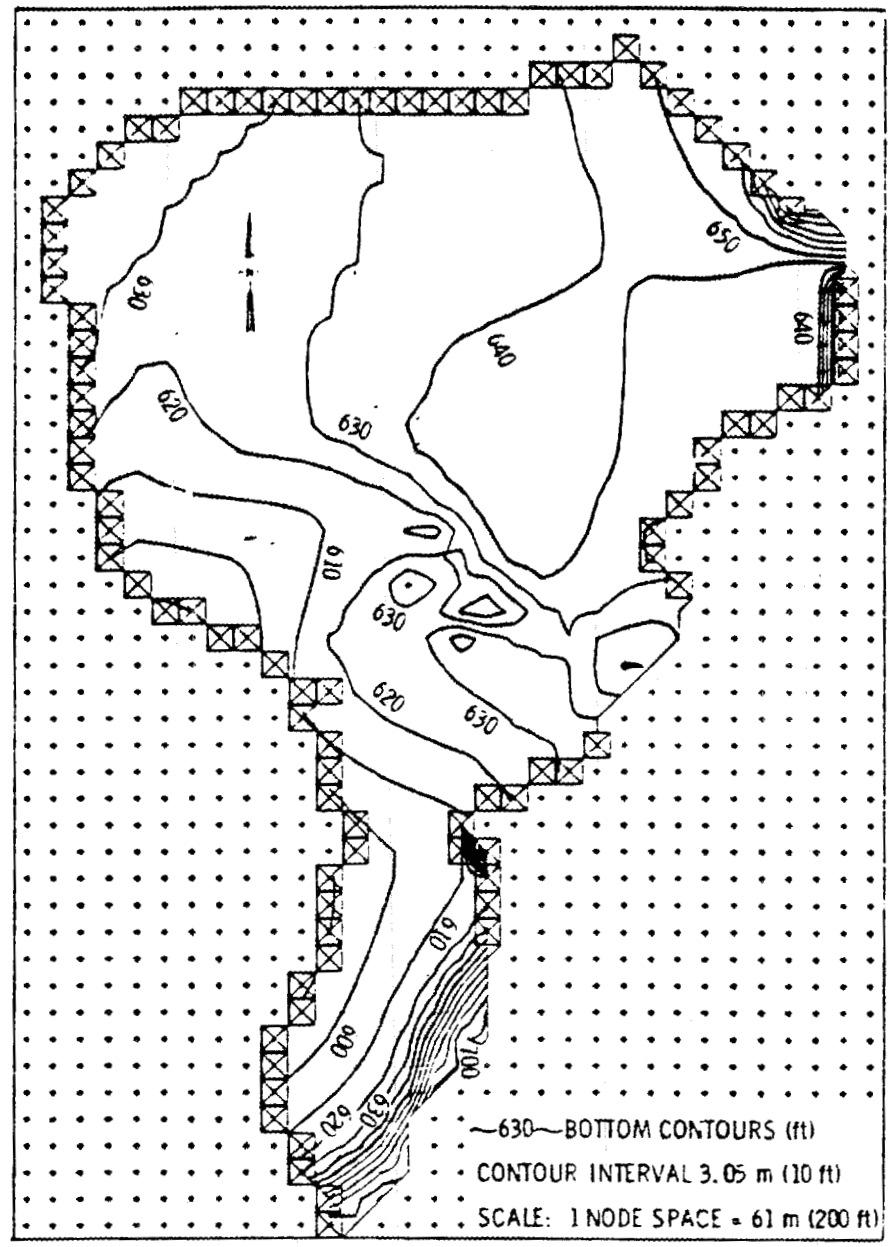

Fig. 14. Conesville unconfined aquifer bottom contours.

ORNL-DWG 86-1560

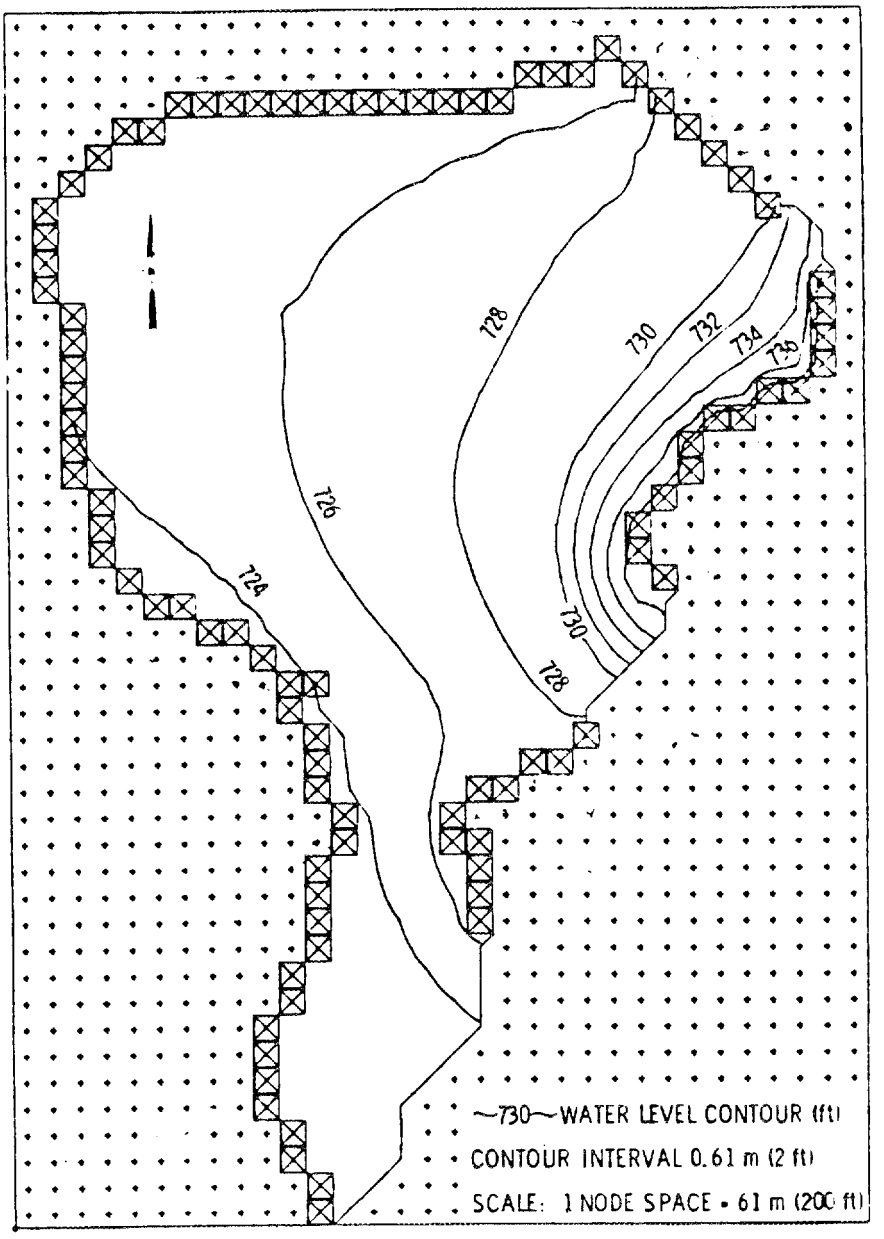

Fig. 15. March 28, 1979, field-measured groundwater potential contours (Bond 1980).

ORNL-DWG 86-1561

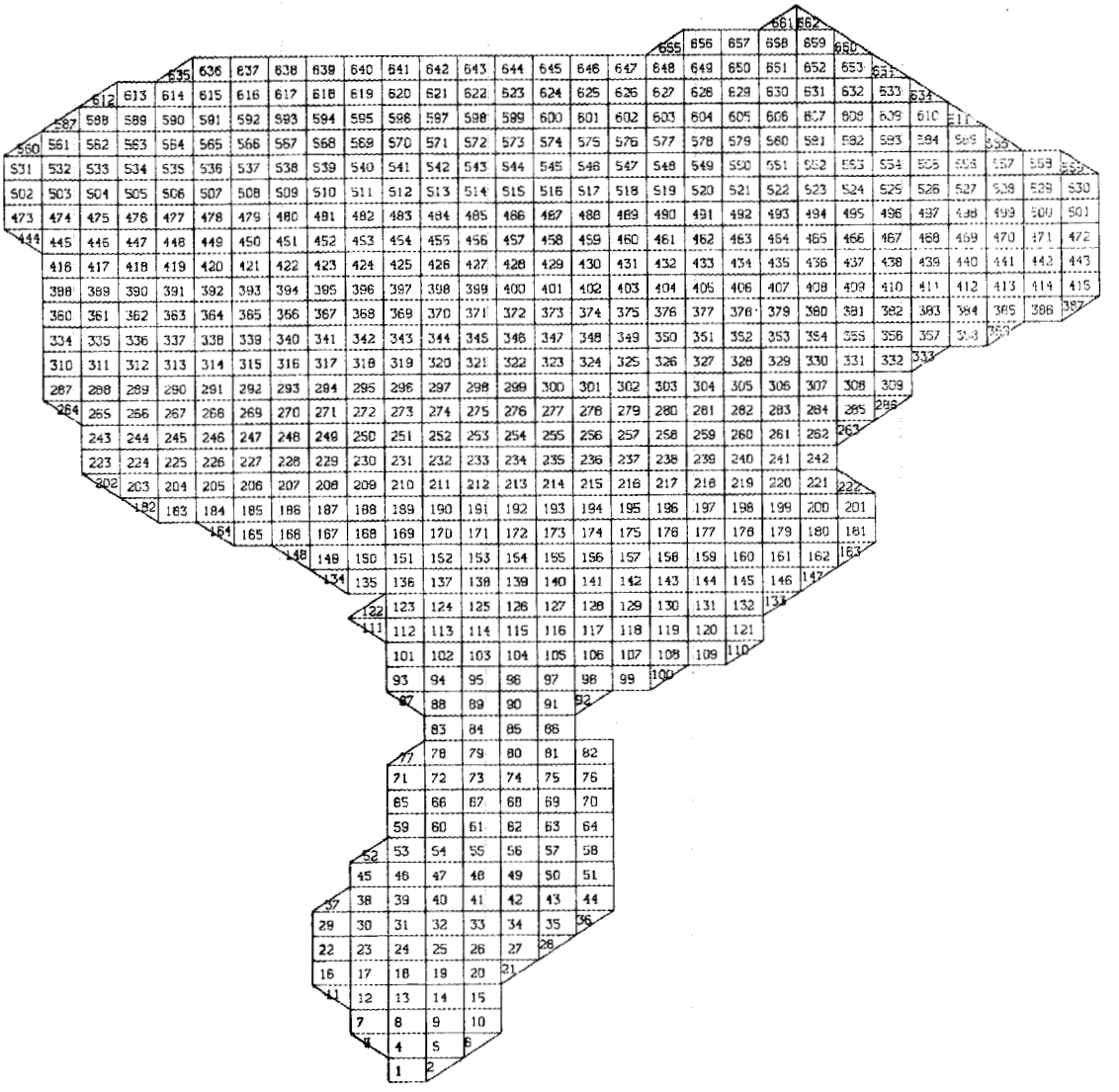

Fig. 16. Finite element array of Conesville area for input to FEWA.

ORNL-DWG 86-1562

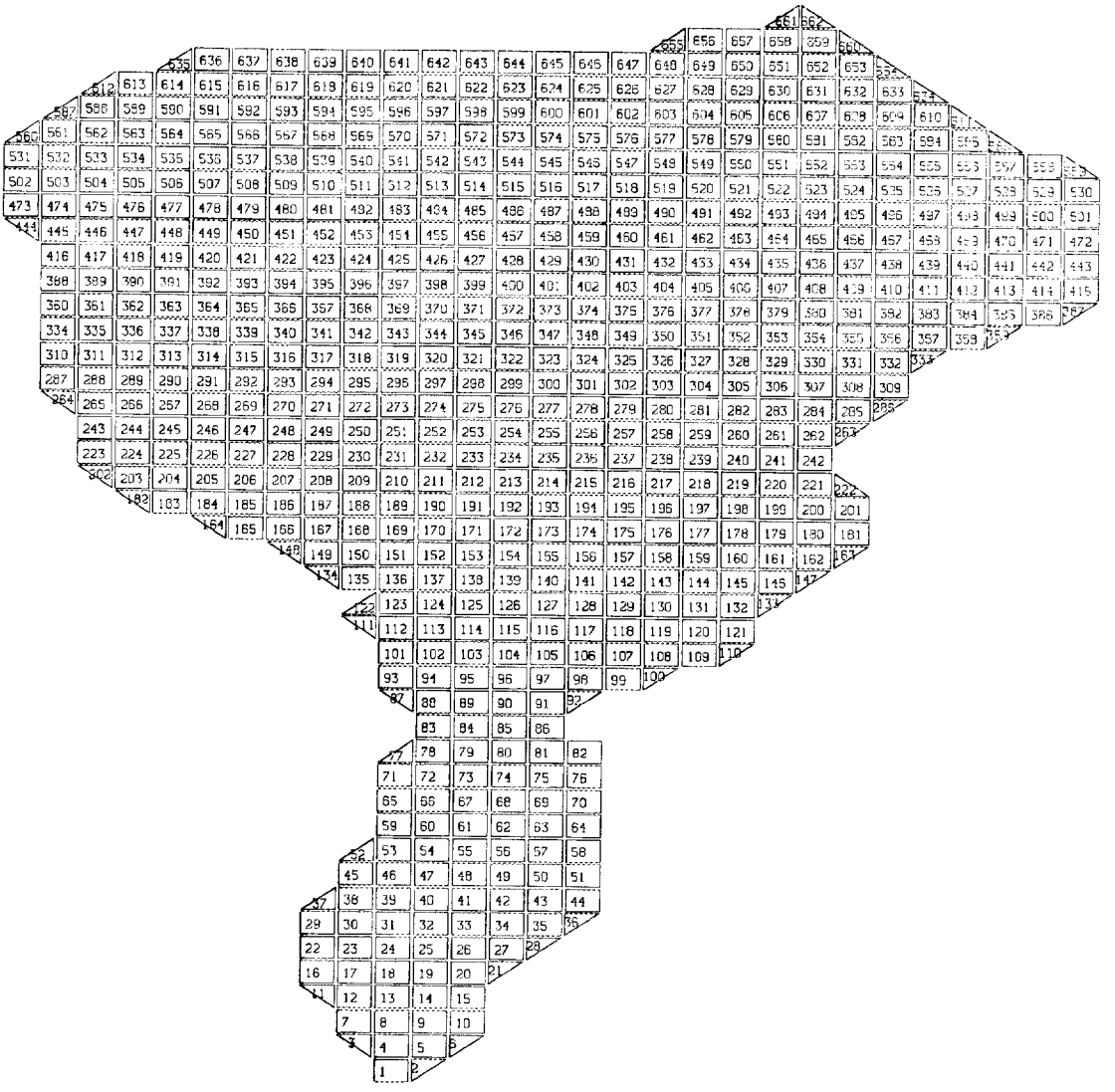

Fig. 17. Finite element grid check of the Conesville area.

4.5 COMPARISON OF RESULTS

The input data for FEWA is presented in Appendix C. The results of the VTT model are plotted in Fig. 18 and those of FEWA are plotted in Fig. 19. The VTT results are hand-interpreted potential contours over the entire model region. The potential contours computed by FEWA are computer-interpolated and computer-drawn, as they were in the previous cases.

The match between the results of FEWA and the field data (Fig. 15) is generally excellent. The match between the results of FEWA and those of the VTT model is almost perfect. In general, both computer models predicted surfaces which were slightly lower than the field-measured surface. The area of greatest discrepancy is in the area of the fly ash pond where the steepest gradient exists. The maximum difference between FEWA-predicted and field-measured potential at any node is about 76.2 cm (2.5 ft). The asymmetric bulge on the 726-ft potentiometric line is due to anisotropy.

ORNL-DWG 86-1563

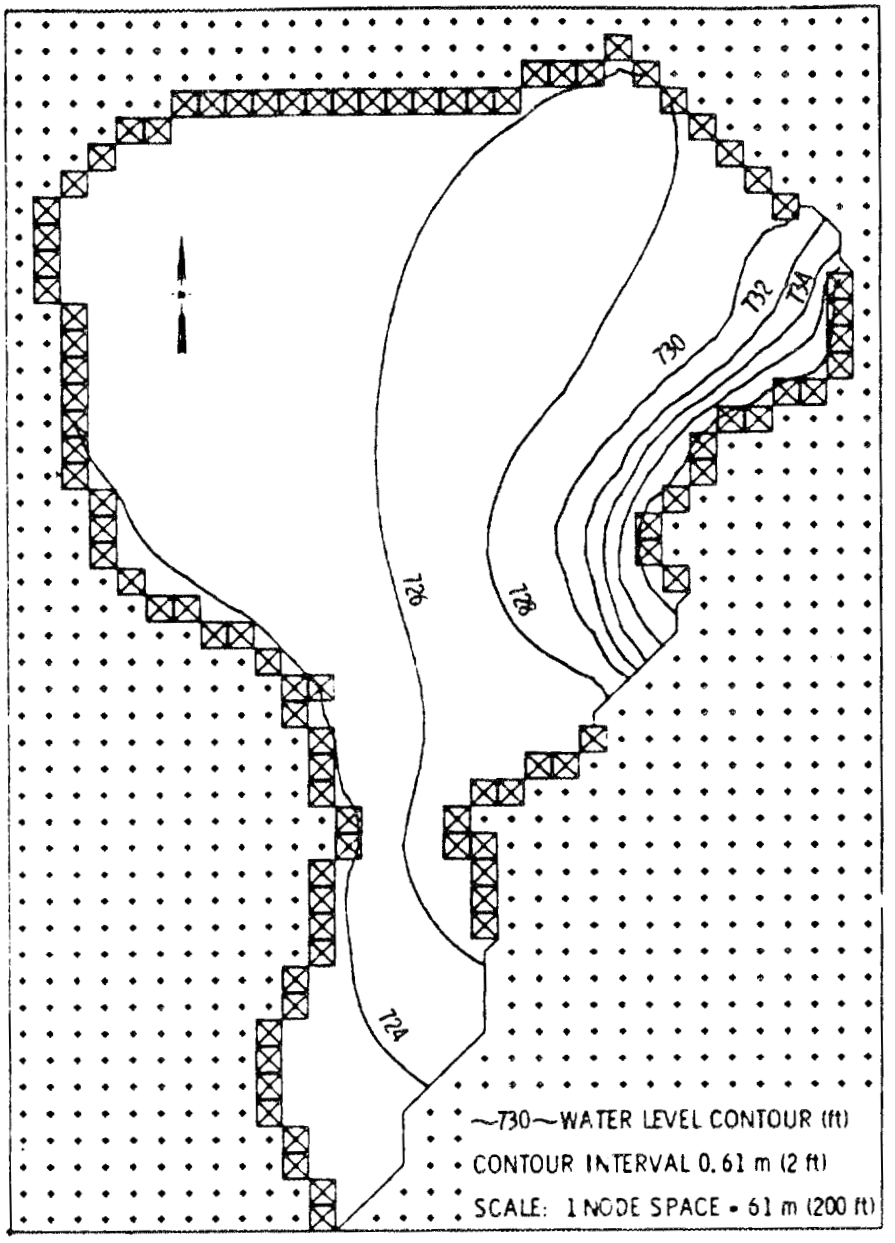

Fig. 18. March 28, 1979, model-predicted groundwater potential contours using VTT model (Bond 1980).

ORNL-DWG 86-1564

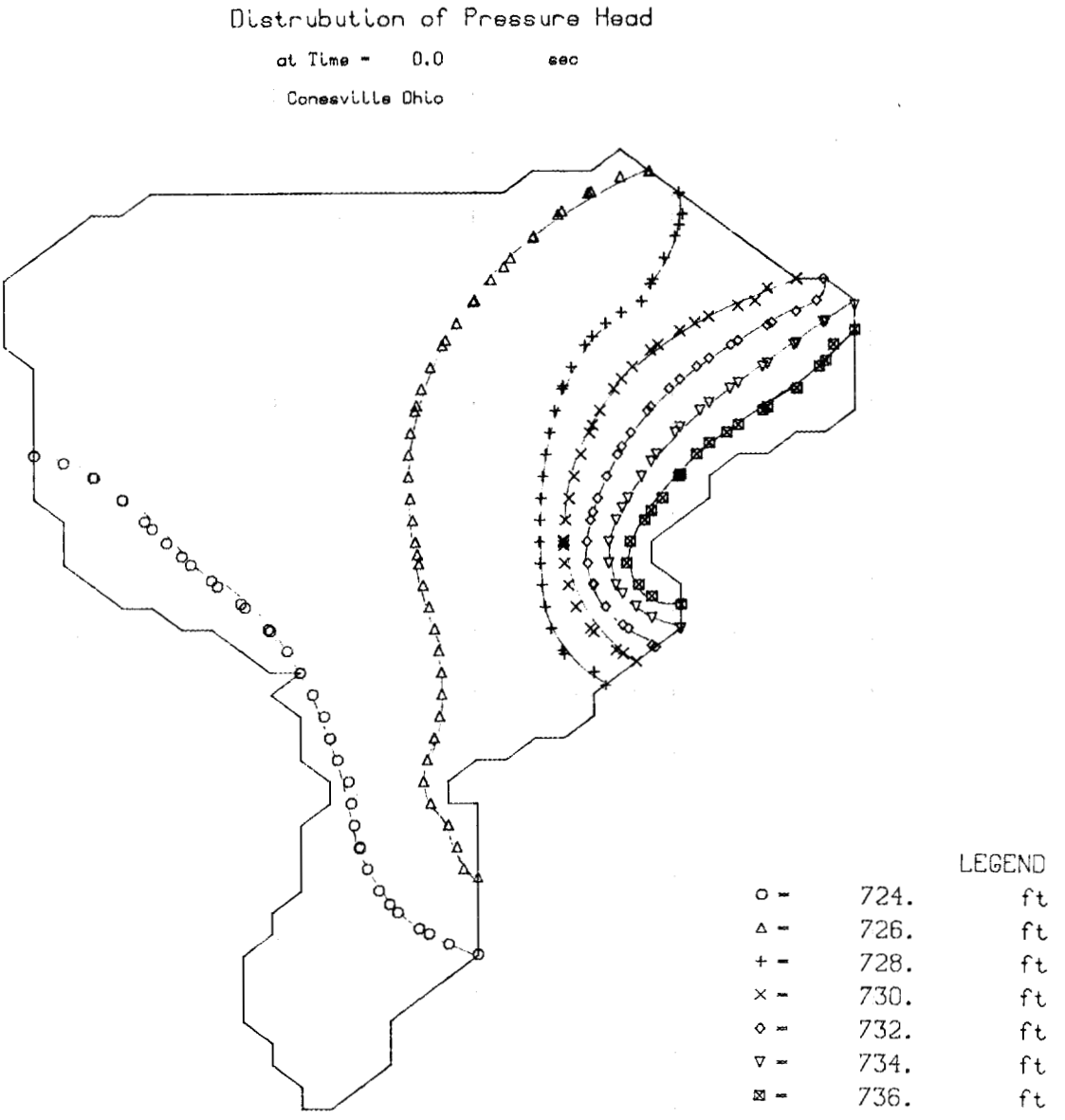

Fig. 19. March 28, 1979, model-predicted groundwater potential contours using FEWA.

5. PREDICTIVE APPLICATION OF FEWA

5.1 INTRODUCTION

In this chapter the predictive capability of FEWA is tested. A hydrologic site is chosen where field data are available for two dates, and information is obtainable for the period between those dates, regarding rainfall, surface runoff and evaporation, pumping rates, and other relevant factors. The first set of field data is used to calibrate the model for one of the required parameters, say hydraulic conductivity (accuracy of experimental determinations of hydraulic conductivity are usually not very good). This is done by matching the calculated potentiometric surface at various values of the parameter with the measured potentiometric surface. After calibration, FEWA is used to integrate over the period using the relevant figures on the net infiltration, pumping rates, etc. The computed potentiometric surface at the second date is then compared to the measured one. A good match establishes the predictive capability of the model.

When the predictive capabilities of FEWA have been established, its usefulness is greatly enhanced. For example, in water management planning it is required to predict the behavior of the aquifer as pumping rates vary to meet demand. The model can be calibrated with current field data. Using the projected pumping rates and known facts about the average rainfall, recharge rates, etc., the model can be used to predict the conditions of the aquifer at any time in the future.

5.2 BISCAYNE AQUIFER

The chief source of fresh groundwater in south Florida is the Biscayne aquifer. This is a highly permeable limestone and sandstone aquifer capable of yielding large quantities of water suitable for municipal, industrial, and agricultural use. The aquifer is recharged by rainfall and a reservoir at Lake Okeechobee, which lies northeast of the three southeastern counties of Palm Beach, Broward, and Dade.

The unconfined aquifer is 24 to 46 m (80 to 150 ft) thick along the west edge of the counties. The groundwater level rises in response to rainfall and surface water inflow, but declines in response to evapotranspiration, surface water outflow, seepage to the ocean, and pumping of wells.

The study area chosen is the Hialeah-Preston wells in Dade County, which supply the cities of Hialeah and Miami Springs with drinking water. Figure 20 shows the measured potentiometric surface of this area on May 3, 1977, and Fig. 21 gives the corresponding data for October 4, 1977. The field data for May 3, 1977, is used for calibration of FEWA, and that for October 4, 1977, used for predictive analysis. The pumping wells are marked as solid squares in Figs. 20 and 21. The Miami canal runs next to and parallel to Okeechobee road marked in Figs. 20 and 21. The Hialeah wells are the wells south of the Miami Canal which runs from northwest to southeast, and the Preston wells are the wells north of the canal. Since Lake Okeechobee acts as a reservoir for the Biscayne aquifer, and the study area is very small compared to the whole aquifer area, any one of the potentiometric lines can be used as a demarcation for the study area.

ORNL-DWG 86-1565

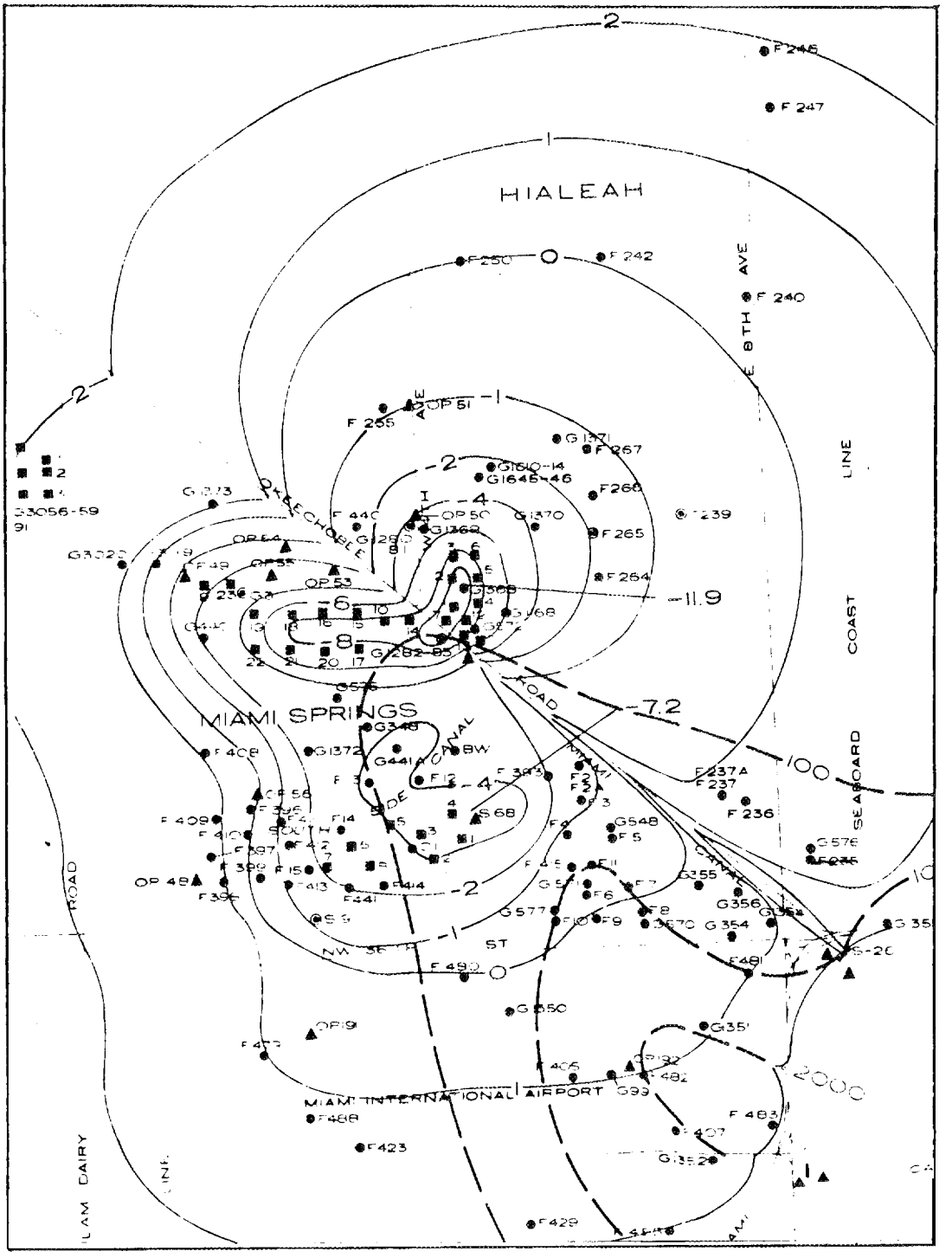

Fig. 20. Measured potentiometric surface of the Hialeah-Preston wells on May 3, 1977.

ORNL-DWG 86-1566

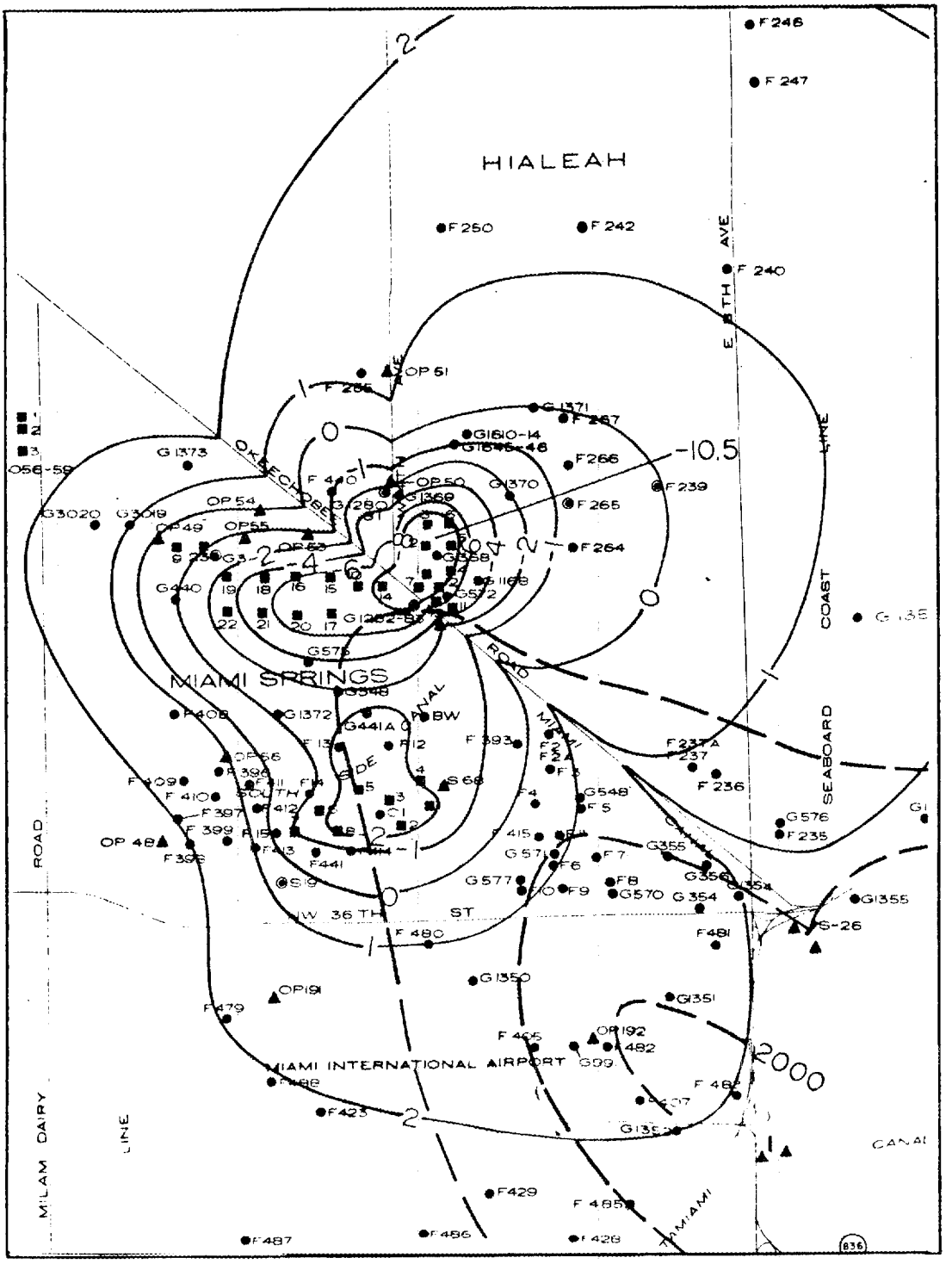

Fig. 21. Measured potentiometric surface of the Hialeah-Preston wells on October 4, 1977.

The bottom of the Biscayne aquifer is underlain by impermeable rock. Figure 22 is the structure contour map of Dade and Broward counties showing the base of the Biscayne aquifer.

5.3 INPUT DATA

The hydraulic conductivity was found to be 36 mm/d (0.12 ft/d) (Miller 1978). This value is used as a starting point of the investigations in this chapter. It has also been estimated by Miller (1978) that 46% of the total well-field pumpage was contributed by infiltration from the canals. It has been previously shown that the Miami canal was not hydraulically connected to the Biscayne aquifer.

Hull (1977, 1978, and 1979) reported rainfall averaged 58.69 in., 1.52 in. above the long-term average. Rainfall on the approximately 2,300-mile^2 Dade County area during 1977 ranged from 51.90 in. at the Miami Beach station to 64.95 in. at the Miami International Airport. Figure 23 shows the monthly rainfall during 1977 and the monthly long-term average. The rainfall was above average in May, August, September, and November. The peak rainfall month was May with 8.20 in. above the long-term average.

The maps provided by the Miami USGS, Figs. 20 and 21, provided information about pumpage. The pumpage for the Hialeah wells for May 1, 2, 3, and 4 was 84, 88.1, 82.7, and 72.2 million gallons/d. The corresponding pumpage for the Preston wells was 40, 41, 40 and 32 million gallons/d. The pumpage for the Hialeah wells for October 1, 2, 3, 4, and 5 was 37, 37, 37, 35, and 36 million gallons/d while those for the Preston wells was 76.5, 76, 79.2, 77.5, and 76.5 million gallons/d.

ORNL-DWG 86-1567

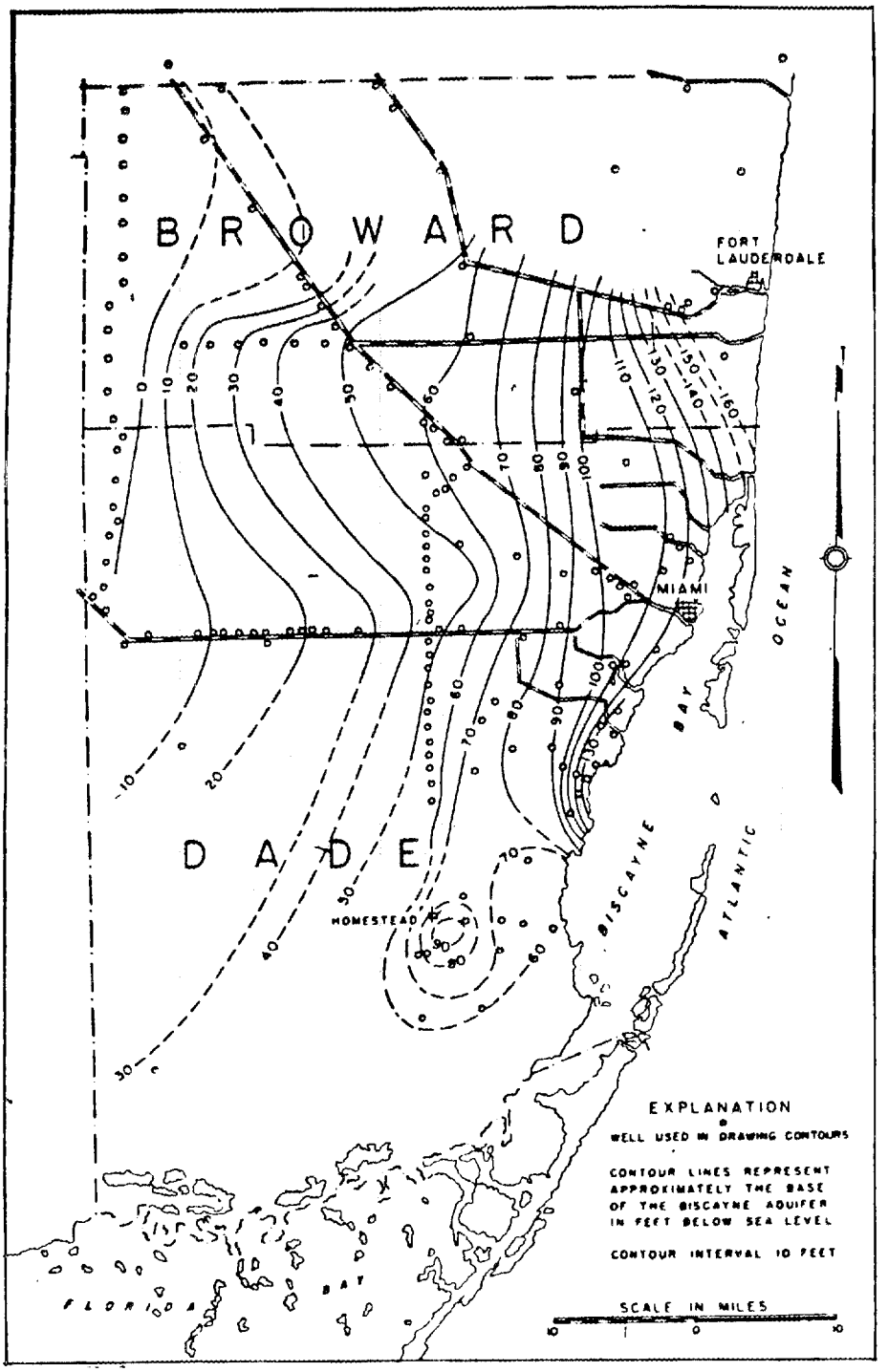

Fig. 22. Structure contour map of Dade and Broward counties showing base of Biscayne aquifer.

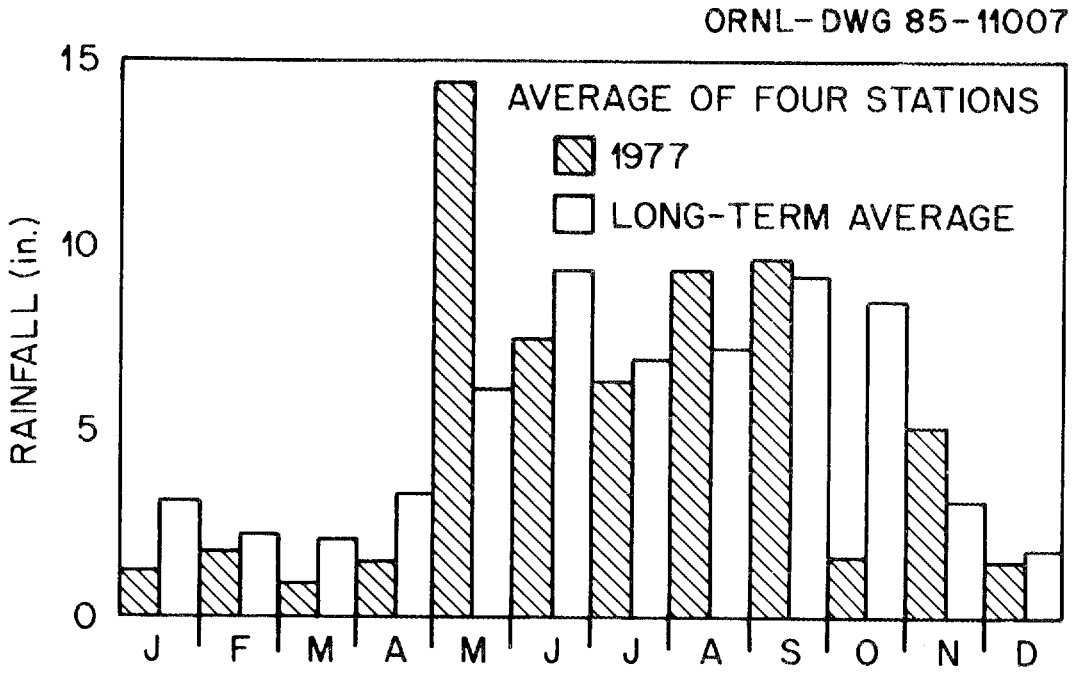

Fig. 23. Monthly rainfall for 1977 and long-term average monthly rainfall.

5.4 MODEL CALIBRATION AND PREDICTION

The 1-ft potentiometric line on May 3, 1977, was selected as the constant head boundary of the study area. The area was divided into finite elements as shown in Fig. 24. Since the potentiometric line was generally circular, the elements had to be chosen fine enough so that the triangular elements on the outer edge could give a fair representation of the boundary. Furthermore, it was ensured that all the pumping wells acted as nodes, and the Miami canal was represented as sides of the finite elements. A grid check was done to ensure that there were no errors in setting up the coordinates. The output from this grid check is presented in Fig. 25.

By trial and error, a value of 2495 ft/day for hydraulic conductivity (2.888×10^{-2} ft/sec) was found to give an acceptable match, but not acceptable around the Preston well area. Various values were then tried for this area until a satisfactory one was found at 120 ft/day (1.388×10^{-3} ft/sec). Thus, the hydraulic conductivity was found to be isotropic and nonhomogeneous. The input data for FEWA is presented in Appendix D.

The model was then integrated from May 3, 1977, to October 4, 1977, using the known values of infiltration and pumpage. The input data for FEWA is presented in Appendix E. By several experimental computer runs it was established that the results were not significantly affected by the infiltration rates. This also meant that the phenomenon of evapotranspiration is not important in the study area. The reason for this is that the high pumpage experienced in the area

ORNL-DWG 86-1568

Fig. 24. Finite element network of the study area.

ORNL-DWG 86-1569

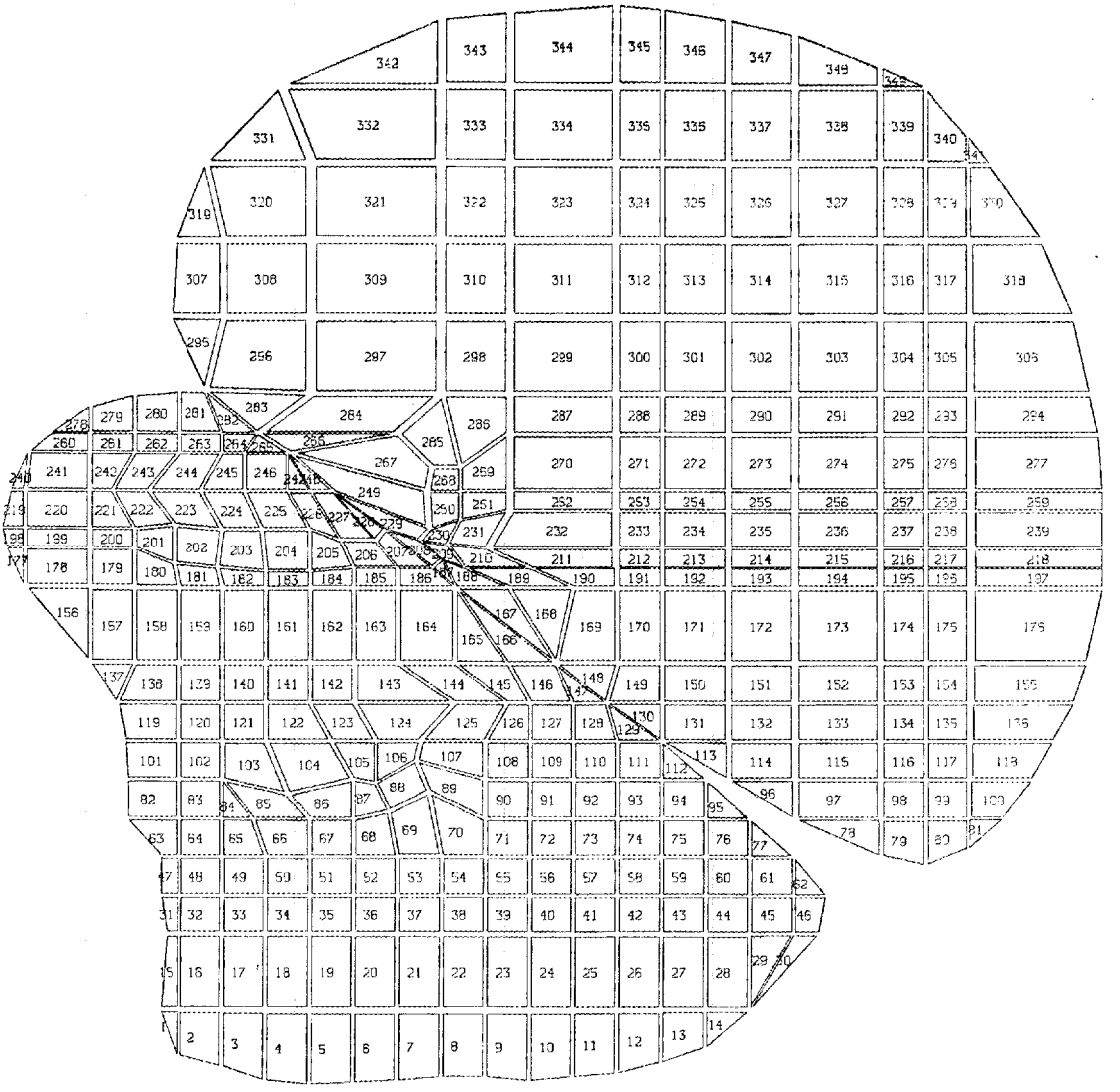

Fig. 25. Grid check of the finite element network.

overwhelms the other components of the water budget. A fact to note about FEWA is that for transient runs, the initial conditions can either be put into the computer manually or computed.

5.5 COMPARISON OF MODELED RESULTS TO FIELD DATA

The results of the calibration run are plotted in Fig. 26, and there appears to be good match to the field data (Fig. 20). It is noted that FEWA correctly predicts the drawdown at the Preston wells, as well as the upper and lower Hialeah wells.

Figure 27 shows the integrated flux at the wells and at the Miami canal drawn to scale. The length of the arrow is a measure of the magnitude of the flux, and the direction of the flux is as shown in the figure. It is interesting to note the rather complex flow in the Preston wells area.

The results of the predictive run are plotted in Fig. 28. In general, the match is good, however, the small drawdown around the lower Hialeah wells is not predicted. This could be due to insufficient detailed information regarding pumpage at these lower Hialeah wells. On the other hand, it could be due to a difference in interpretation.

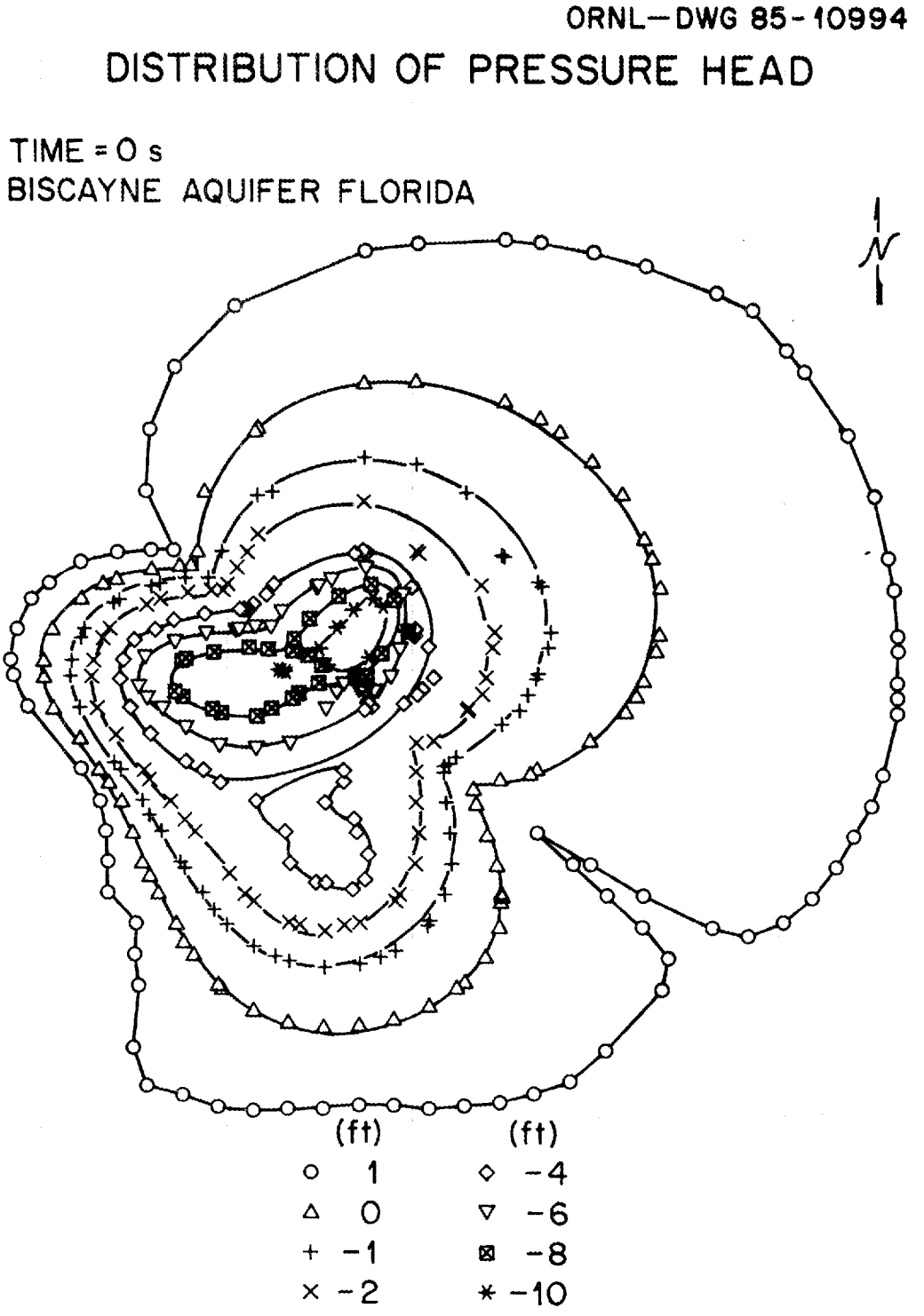

Fig. 26. Computed potentiometric surface of the Hialeah-Preston wells on May 3, 1977.

ORNL-DWG 85-11003

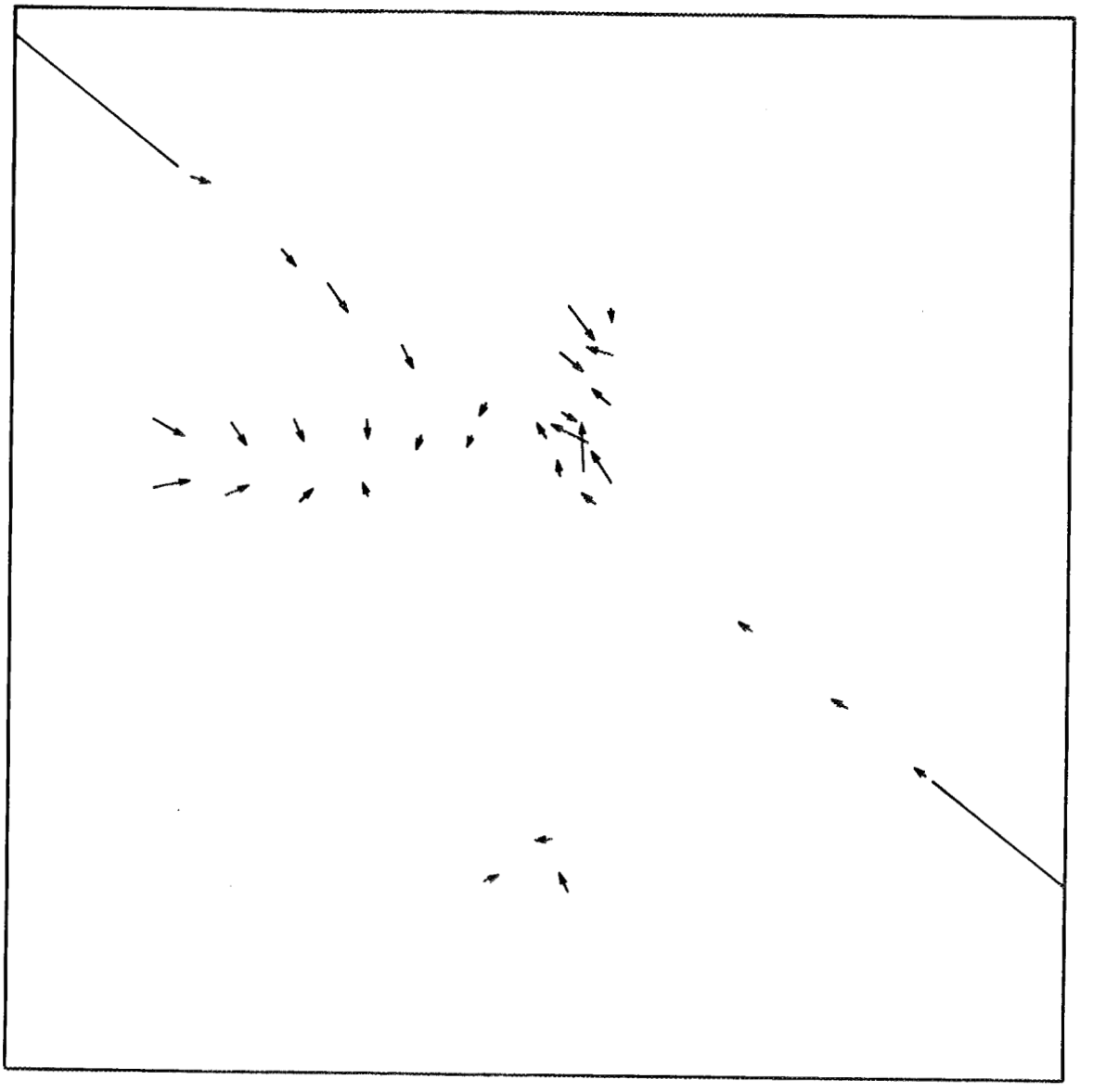

Fig. 27. Integrated flux at the wells and at the Miami Canal, May 3, 1977.

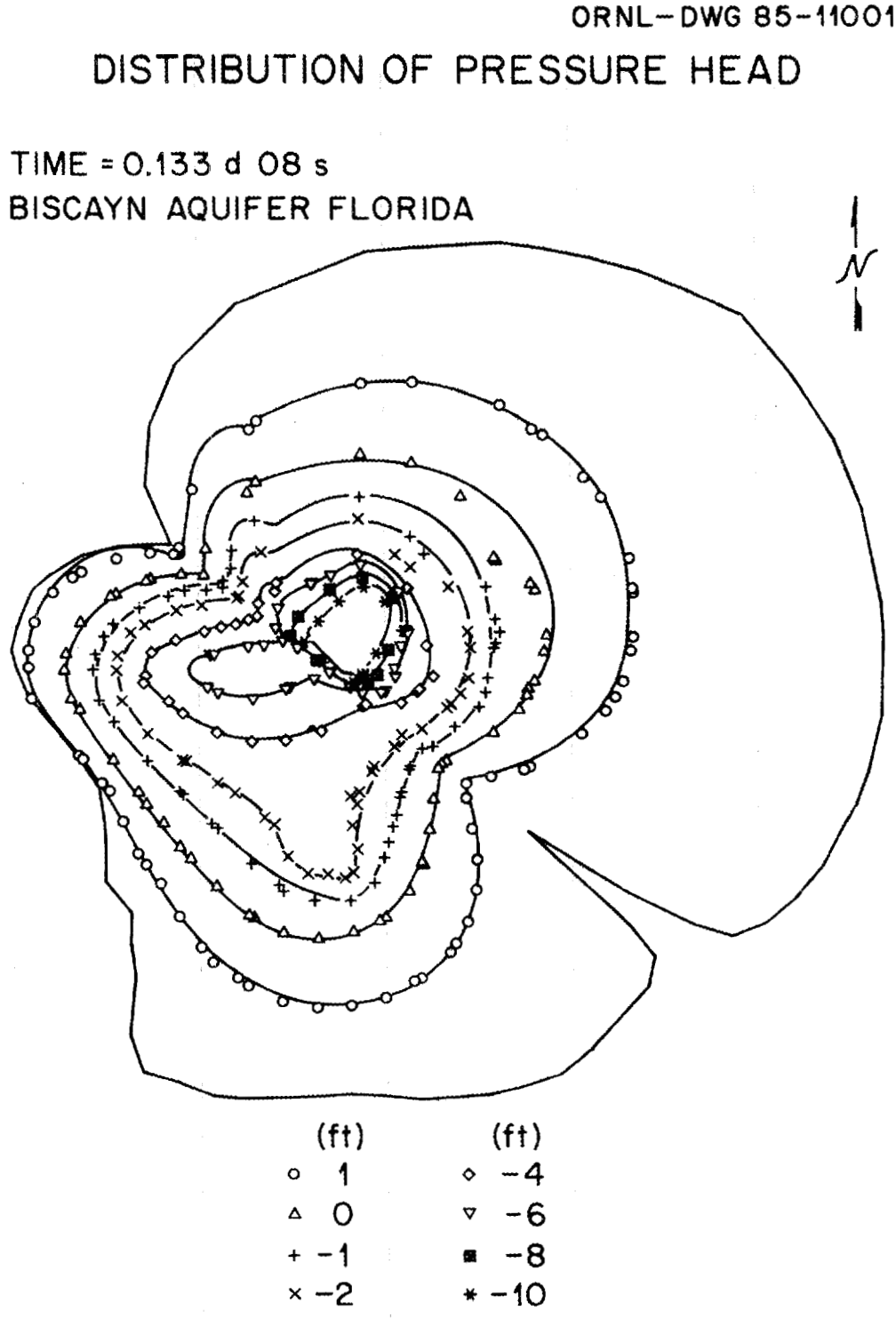

Fig. 28. Predicted potentiometric surface of the Hialeah-Preston wells on October 4, 1977.

6. SUMMARY AND CONCLUSIONS

FEWA: A finite element model of water flow through aquifers, is a simulation model of two-dimensional flow in saturated subsurface media. It has been found in this study to be both efficient and accurate. The ability of FEWA to handle inhomogeneity and anisotropic conditions is an asset.

When compared to the USGS two-dimensional model (Trescott et al. 1976), FEWA was found superior in treating boundary conditions and in handling anisotropic media when the coordinates cannot be made to coincide with the principal directions of hydraulic conductivities. FEWA is a continuous model, whereas the USGS model is a discrete one. This means that in FEWA the velocity field is computed as a continuum, while the velocities are computed at discrete points in the USGS model. Using a continuous velocity in the subsequent contaminant transport modeling, mass conservation will be preserved.

FEWA was calibrated with measured potentiometric surfaces from the Love Canal area, New York, and the Conesville area, Ohio. There were satisfactory matches between computed results and field data. The computer time used for the runs showed that FEWA was efficiently designed, and the results indicated precision in the computation.

The calibration and predictive runs of FEWA were done with the Hialeah-Preston well field data over the Biscayne aquifer in South Florida. The calibration run yielded two values of hydraulic conductivity in the area and the predictive run gave results that

matched well with field data. This illustrated the power of FEWA as a predictive tool, and therefore its usefulness as a tool in groundwater management.

The uses of FEWA as a simulation model go beyond the immediate need as a first and necessary step to simulating contaminant transport in shallow land burial of low-level radioactive wastes. It can be used in many aspects of groundwater study, including predicting future demands on aquifers (studies by USGS), and reservoir simulations which are of immediate interest to U.S. oil companies.

REFERENCES

Bond, F. 1980. Modeling the Fixed Sludge Landfill - Conesville, Ohio (Phase I). CS-1355. Battelle Pacific Northwest Laboratories, Richland, Washington.

Geotrans, Inc. 1981. Final Report on Groundwater Flow Modeling Study of the Love Canal Area, New York. LC1-619-026-14-FR-0000. Geotrans, Inc., Reston, Virginia.

Hull, J. E., and T. R. Beaven. 1977. Summary of Hydrologic Data Collected During 1975 in Dade County, Florida. Open file report FL 77-803, United States Geological Survey, Tallahassee, Florida.

Hull, J. E. 1978. Summary of Hydrologic Data Collected During 1976 in Dade County, Florida. Open file report 78-883, U.S. Geological Survey, Tallahassee, Florida.

Hull, J. E. 1979. Summary of Hydrologic Data Collected During 1977 in Dade County, Florida. Open file report 79-514. U.S. Geological Survey, Tallahassee, Florida.

Jacob, C. E. 1947. Drawdown Test to Determine Effective Radius of Artesian Wells. Trans. Am. Soc. Civil Engrs., Vol. 112, pp. 1047-1070.

Johnston, R. H. 1964. Groundwater in the Niagara Falls Area, New York with Emphasis on the Water-Bearing Characteristics of Bedrock. Bulletin GW-53. State of New York Conservation Department Water Resources Commission.

Kipp, K. L., et al. 1972. Updated (1976). Variable Thickness Transient Groundwater Flow Model - Theory and Numerical Implementation. BNWL-1703. Pacific Northwest Laboratory, Richland, Washington.

Leonard, R. P., P. H. Werthman, and R. C. Ziegler. 1977. Characterization and Abatement of Groundwater Pollution from Love Canal Chemical Landfill. Niagara Falls, New York. Calspan Report No. ND-6097-M-1.

Mercer, J. W., C. R. Faust, and L. R. Silka. 1984. Groundwater Flow Modeling Study of the Love Canal Area, New York. Groundwater Contamination, National Academy Press, Washington, D.C.

Miller, W. L. 1978. Effects of Bottom Sediments in Infiltration from the Miami and Tributary Canals to the Biscayne Aquifer. Dade County, Florida. Water-Resources Investigations 78-36, U.S. Geological Survey, Miami, Florida.

Power Authority of the State of New York (Pasny). 1965. Niagara Power Project Data Statistics, Pasny, New York. 48 pp.

Theis, C. V. 1935. The Relation Between the Lowering of the Piezometric Surface and the Rate and Duration of Discharge of a Well Using Groundwater Storage. Trans. Am. Geophys. Union. Vol. 16, pp. 519-524.

Thornthwaite, C. W., and H. G. Wilm. 1944. Report of the Committee on Transpiration and Evaporation. 1943-44. Trans. Am. Geophys. Union. Vol. 25, Pt.V. pp. 683-693.

Trescott, P. C. 1975. Documentation of Finite-Difference Model for Simulation of Three-Dimensional Groundwater Flow. USGS Open File Report 75-438. U.S. Geological Survey, Reston, Virginia.

Trescott, P. C., G. F. Pinder, and S. P. Larson. 1976. Finite-Difference Model for Aquifer Simulation in Two Dimensions with Results of Numerical Experiments. Book 7, Chapter C1. Technique of Water-Resources Investigations of the United States Geological Survey, U.S. Geological Survey, Reston, Virginia.

U.S. Department of Agriculture. 1972. Soil Survey of Niagara County, New York. U.S. Government Printing Office. 0-459-901.

Yeh, G. T., and D. D. Huff. 1983. FEWA: A Finite Element Model of Water Flow Through Aquifers. ORNL-5976. Oak Ridge National Laboratory, Oak Ridge, Tennessee.

APPENDIX A

FEWA INPUT DATA FOR USGA DATA SET

```
*KVWONG(1).USGSDAT(3) SYM CREATED ON 8 OCT 84 AT 11:09:32
      1  FEWA  APPLIED  TO  USGS  AQUIFER  SIMULATION  EXAMPLE                    1
      THE FOLLOWING CARD CONTAINS THE BASIC INTEGER PARAMETERS
    109   86    4   66    0    0    1    0    0   50    0    0    0    1    1  600
      THE FOLLOWING TWO CARDS CONTAIN THE BASIC REAL PARAMETERS
  0.01      0.0        0.01        9999999.0 0.01       0.003      62.5       32.2
    2.093E-51.0         1.0         1.85
      THE FOLLOWING CARDS CONTAIN PRINTER- AND STORAGE- CONTROL
  33
  11
     1.0D50
      THE FOLLOWING CARDS CONTAIN MATERIAL PROPERTIES
  0.0       0.0        0.3         0.60DE-2  0.600E-20.0        0.0
                       0.3         0.800E-2  0.800E-2
                       0.3         0.400E-2  0.400E-2
                       0.3         0.200E-2  0.200E-2
      THE FOLLOWING CARDS CONTAIN BED ELEVATION AND AQUIFER THICKNESS
      1  108     1      0.0        0.0

      1  108     1      0.0        0.0

      THE FOLLOWING CARDS CONTAIN NODAL COORDINATES
      1                .000000+00
      2                .850000+03
      3                .142500+04
      4                .187500+04
      5                .245000+04
      6                .332500+04
      7                .462500+04
      8                .642500+04
      9                .837500+04
     10                .992500+04
     11                .109750+05
     12                .116750+05
     13                .121750+05
     14                .000000+00
     15                .850000+03
     16                .142500+04
     17                .187500+04
     18                .245000+04
     19                .332500+04
     20                .462500+04
     21                .642500+04
     22                .837500+04
     23                .992500+04
     24                .109750+05
     25                .116750+05
     26                .121750+05
     27                .000000+00
     28                .850000+03
     29                .142500+04
     30                .187500+04
     31                .245000+04
     32                .332500+04
     33                .462500+04
     34                .642500+04
     35                .837500+04
     36                .992500+04
     37                .109750+05
     38                .116750+05
     39                .121750+05
     40                .127250+05
     41                .142500+04
     42                .187500+04
     43                .245000+04
     44                .332500+04
     45                .462500+04
     46                .642500+04
     47                .837500+04
     48                .992500+04
     49                .109750+05
     50                .116750+05
```

51	.121750D+05
52	.127250D+05
53	.142500D+04
54	.187500D+04
55	.245000D+04
56	.332500D+04
57	.462500D+04
58	.642500D+04
59	.837500D+04
60	.992500D+04
61	.109750D+05
62	.116750D+05
63	.121750D+05
64	.127250D+05
65	.142500D+04
66	.187500D+04
67	.245000D+04
68	.332500D+04
69	.462500D+04
70	.642500D+04
71	.837500D+04
72	.992500D+04
73	.109750D+05
74	.116750D+05
75	.121750D+05
76	.127250D+05
77	.142500D+04
78	.187500D+04
79	.245000D+04
80	.332500D+04
81	.462500D+04
82	.642500D+04
83	.837500D+04
84	.992500D+04
85	.109750D+05
86	.116750D+05
87	.121750D+05
88	.127250D+05
89	.142500D+04
90	.187500D+04
91	.245000D+04
92	.332500D+04
93	.462500D+04
94	.642500D+04
95	.837500D+04
96	.992500D+04
97	.109750D+05
98	.116750D+05
99	.121750D+05
100	.127250D+05
101	.187500D+04
102	.245000D+04
103	.332500D+04
104	.462500D+04
105	.837500D+04
106	.992500D+04
107	.109750D+05
108	.116750D+05
109	.121750D+05

```
  1   12    1     0.
 14   12    1     1525.
 27   13    1     2950.
 41   11    1     4075.
 53   11    1     4875.
 65   11    1     5475.
 77   11    1     5900.
 89   11    1     6200.
101    8    1     6575.

 THE FOLLOWING CARDS CONTAIN ELEMENT INCIDENCES AND TYPE
  1    1    2   15   14   -1   12    2
 25   29   30   42   41   -1   11    1
 36   41   42   54   53   -1   11    4
 80   90   91  102  101   -1    3    1
 83   95   96  106  105   -1    4    1

THE FOLLOWING CARDS CONTAIN MATERIAL TYPE CORRECTION
  1    6    1   -2    0
 20    4    1   -2
 25    2    1   -3
 36   10    1   -3
 47    3    1   -4
 51    6    1   -3
 58    3    1   -4
 62    6    1   -3
 69    3    1   -4
 73    6    1   -3
 80    2    1   -4
 83    3    1   -3

THE FOLLOWING CARDS CONTAIN PRE-INITIAL CONDITIONS
  1  108    1    100.     0.

THE FOLLOWING CARD CONTAINS TRANSIENT CONTROLLING INTEGERS
  0    0    0    0    7    1    2    1    2    1    2    1    2    6    2    2
 THE FOLLOWING CARDS CONTAIN SOURCES AND WELLS
0.0          0.02E-6 9999999.0    0.02E-6
  1   85    1    1    0

0.0        0.05      9999999.0 0.05
0.0       -10.       9999999.0 -10.
 30   42   54   66   44   73
  1    3    1    1    0
  5    1    1    2    0

 THE FOLLOWING CARDS CONTAIN DIRICHLET BOUNDARY CONDITIONS
0.0       100.0      9999999.0 100.0
  8    9   10   11   12   13   26
  1    6    1    1    0

 THE FOLLOWING CARDS CONTAIN UPPER LEAKING AQUIFERS
0.0       100.0      9999999.0 100.0
0.0
  1   85    1    1    0

 THE FOLLOWING CARDS CONTAIN LOWER LEAKING AQUIFERS
0.0       100.       9999999.0 100.
  0.3E-8
  1   85    1    1    0
```

APPENDIX B

FEWA INPUT DATA FOR LOVE CANAL, NEW YORK

```
WONG(1).LOVEDAT(1) SYM CREATED ON 6 SEP 84 AT 19:10:21
    1  FLWA  APPLIED  TO  LOVE  CANAL,  NEW  YORK                                    1
    THE  FOLLOWING  CARD  CONTAINS  THE  BASIC  INTEGER  PARAMETERS
  408  363     2  144     0     0     1    -1     0    20     0     0     1     1     1 4000
    THE  FOLLOWING  TWO  CARDS  CONTAIN  THE  BASIC  REAL  PARAMETERS
0.01       0.0        0.01       9999999.0 0.0001      0.0001      62.5       32.2
  2.093E-51.0         1.00       1.85
    THE  FOLLOWING  TWO  CARDS CONTAIN PRINTER-  AND STORAGE-  CONTROL
33
11
   1.00050
    THE FOLLOWING CARDS CONTAIN MATERIAL PROPERTIES
0.0        0.0        0.3        0.00492   0.00492   0.0        0.3
0.0        0.0        0.3        0.000492  0.000492  0.0        0.3
    THE FOLLOWING  CARDS  CONTAIN BED ELEVATION AND AQUIFER THICKNESS
    1  407     1      540.0      0.0

    1  407     1      15.0       0.0

    THE  FOLLOWING  CARDS  CONTAIN  NODAL  COORDINATES
    1                 0.2110+05
    2                 0.2270+05
    3                 0.2530+05
    4                 0.2800+05
    5                 0.3270+05
    6                 0.3750+05
    7                 0.4220+05
    8                 0.1950+05
    9                 0.2010+05
   10                 0.2110+05
   11                 0.2270+05
   12                 0.2530+05
   13                 0.2800+05
   14                 0.3270+05
   15                 0.3750+05
   16                 0.4220+05
   17                 0.9500+04
   18                 0.1210+05
   19                 0.1430+05
   20                 0.1580+05
   21                 0.1690+05
   22                 0.1800+05
   23                 0.1850+05
   24                 0.1900+05
   25                 0.1950+05
   26                 0.2010+05
   27                 0.2110+05
   28                 0.2270+05
   29                 0.2530+05
   30                 0.2800+05
   31                 0.3270+05
   32                 0.3750+05
   33                 0.4220+05
   34                 0.3170+04
   35                 0.6340+04
   36                 0.9500+04
   37                 0.1210+05
   38                 0.1430+05
   39                 0.1580+05
   40                 0.1690+05
   41                 0.1800+05
   42                 0.1850+05
   43                 0.1900+05
   44                 0.1950+05
   45                 0.2010+05
   46                 0.2110+05
   47                 0.2270+05
   48                 0.2530+05
   49                 0.2800+05
   50                 0.3270+05
   51                 0.3750+05
   52                 0.4220+05
```

53	0.0000+00
54	0.3170+04
55	0.6340+04
56	0.9500+04
57	0.1210+05
58	0.1430+05
59	0.1580+05
60	0.1690+05
61	0.1800+05
62	0.1850+05
63	0.1900+05
64	0.1950+05
65	0.2010+05
66	0.2110+05
67	0.2270+05
68	0.2530+05
69	0.2800+05
70	0.3270+05
71	0.3750+05
72	0.4220+05
73	0.0000+00
74	0.3170+04
75	0.6340+04
76	0.9500+04
77	0.1210+05
78	0.1430+05
79	0.1580+05
80	0.1690+05
81	0.1800+05
82	0.1850+05
83	0.1900+05
84	0.1950+05
85	0.2010+05
86	0.2110+05
87	0.2270+05
88	0.2530+05
89	0.2800+05
90	0.3270+05
91	0.3750+05
92	0.4220+05
93	0.0000+00
94	0.3220+04
95	0.6340+04
96	0.9500+04
97	0.1210+05
98	0.1430+05
99	0.1580+05
100	0.1690+05
101	0.1800+05
102	0.1850+05
103	0.1900+05
104	0.1950+05
105	0.2010+05
106	0.2110+05
107	0.2270+05
108	0.2530+05
109	0.2800+05
110	0.3270+05
111	0.3750+05
112	0.4220+05
113	0.0000+00
114	0.3270+04
115	0.6340+04
116	0.9500+04
117	0.1210+05
118	0.1430+05
119	0.1580+05
120	0.1690+05
121	0.1800+05
122	0.1850+05
123	0.1900+05
124	0.1950+05

125	0.2310+05
126	0.2110+05
127	0.2270+05
128	0.2530+05
129	0.2800+05
130	0.3270+05
131	0.3750+05
132	0.4220+05
133	0.0000+00
134	0.3170+04
135	0.6340+04
136	0.9500+04
137	0.1210+05
138	0.1430+05
139	0.1580+05
140	0.1690+05
141	0.1800+05
142	0.1850+05
143	0.1900+05
144	0.1950+05
145	0.2010+05
146	0.2110+05
147	0.2270+05
148	0.2530+05
149	0.2800+05
150	0.3270+05
151	0.3750+05
152	0.4220+05
153	0.0000+00
154	0.3170+04
155	0.6340+04
156	0.9500+04
157	0.1210+05
158	0.1430+05
159	0.1580+05
160	0.1690+05
161	0.1800+05
162	0.1850+05
163	0.1900+05
164	0.1950+05
165	0.2010+05
166	0.2110+05
167	0.2270+05
168	0.2530+05
169	0.2800+05
170	0.3270+05
171	0.3750+05
172	0.4220+05
173	0.0000+00
174	0.3170+04
175	0.6340+04
176	0.9500+04
177	0.1210+05
178	0.1430+05
179	0.1580+05
180	0.1690+05
181	0.1800+05
182	0.1850+05
183	0.1900+05
184	0.1950+05
185	0.2010+05
186	0.2110+05
187	0.2270+05
188	0.2530+05
189	0.2800+05
190	0.3270+05
191	0.3750+05
192	0.4220+05
193	0.0000+00
194	0.3170+04
195	0.6340+04
196	0.8980+04

197	0.121D+05
198	0.143D+05
199	0.158D+05
200	0.169D+05
201	0.180D+05
202	0.185D+05
203	0.190D+05
204	0.195D+05
205	0.201D+05
206	0.211D+05
207	0.227D+05
208	0.253D+05
209	0.280D+05
210	0.327D+05
211	0.375D+05
212	0.422D+05
213	0.000D+00
214	0.317D+04
215	0.634D+04
216	0.950D+04
217	0.121D+05
218	0.143D+05
219	0.158D+05
220	0.169D+05
221	0.180D+05
222	0.185D+05
223	0.190D+05
224	0.195D+05
225	0.201D+05
226	0.211D+05
227	0.227D+05
228	0.253D+05
229	0.280D+05
230	0.327D+05
231	0.375D+05
232	0.422D+05
233	0.000D+00
234	0.317D+04
235	0.634D+04
236	0.950D+04
237	0.121D+05
238	0.143D+05
239	0.158D+05
240	0.169D+05
241	0.180D+05
242	0.185D+05
243	0.190D+05
244	0.195D+05
245	0.201D+05
246	0.211D+05
247	0.227D+05
248	0.253D+05
249	0.280D+05
250	0.327D+05
251	0.375D+05
252	0.422D+05
253	0.000D+00
254	0.317D+04
255	0.634D+04
256	0.950D+04
257	0.121D+05
258	0.143D+05
259	0.158D+05
260	0.169D+05
261	0.180D+05
262	0.185D+05
263	0.190D+05
264	0.195D+05
265	0.201D+05
266	0.211D+05
267	0.227D+05
268	0.253D+05

269	0.2800+05
270	0.3270+05
271	0.3750+05
272	0.4220+05
273	0.0000+00
274	0.3170+04
275	0.6340+04
276	0.9500+04
277	0.1210+05
278	0.1430+05
279	0.1580+05
280	0.1690+05
281	0.1800+05
282	0.1850+05
283	0.1900+05
284	0.1950+05
285	0.2010+05
286	0.2110+05
287	0.2270+05
288	0.2530+05
289	0.2800+05
290	0.3270+05
291	0.3750+05
292	0.4220+05
293	0.0000+00
294	0.3170+04
295	0.6340+04
296	0.9500+04
297	0.1210+05
298	0.1430+05
299	0.1580+05
300	0.1690+05
301	0.1800+05
302	0.1850+05
303	0.1900+05
304	0.1950+05
305	0.2010+05
306	0.2110+05
307	0.2270+05
308	0.2530+05
309	0.2800+05
310	0.3270+05
311	0.3750+05
312	0.4220+05
313	0.0000+00
314	0.3170+04
315	0.6340+04
316	0.9500+04
317	0.1210+05
318	0.1430+05
319	0.1580+05
320	0.1690+05
321	0.1800+05
322	0.1850+05
323	0.1900+05
324	0.1950+05
325	0.2010+05
326	0.2110+05
327	0.2270+05
328	0.2530+05
329	0.2800+05
330	0.3270+05
331	0.3750+05
332	0.4220+05
333	0.0000+00
334	0.3170+04
335	0.6340+04
336	0.9500+04
337	0.1210+05
338	0.1430+05
339	0.1580+05
340	0.1690+05

341	0.1800+05
342	0.1850+05
343	0.1900+05
344	0.1950+05
345	0.2010+05
346	0.2110+05
347	0.2270+05
348	0.2480+05
349	0.2800+05
350	0.3270+05
351	0.3750+05
352	0.4220+05
353	0.1210+05
354	0.1430+05
355	0.1580+05
356	0.1690+05
357	0.1800+05
358	0.1850+05
359	0.1900+05
360	0.1950+05
361	0.2010+05
362	0.2110+05
363	0.2270+05
364	0.2530+05
365	0.2800+05
366	0.3270+05
367	0.3750+05
368	0.4220+05
369	0.0000+00
370	0.3170+04
371	0.6340+04
372	0.9500+04
373	0.1210+05
374	0.1430+05
375	0.1580+05
376	0.1690+05
377	0.1800+05
378	0.1850+05
379	0.1900+05
380	0.1950+05
381	0.2010+05
382	0.2110+05
383	0.2270+05
384	0.2530+05
385	0.2800+05
386	0.3270+05
387	0.3750+05
388	0.4220+05
389	0.0000+00
390	0.3170+04
391	0.6340+04
392	0.9500+04
393	0.1210+05
394	0.1430+05
395	0.1580+05
396	0.1690+05
397	0.1800+05
398	0.1850+05
399	0.1900+05
400	0.1950+05
401	0.2010+05
402	0.2110+05
403	0.2270+05
404	0.2530+05
405	0.2800+05
406	0.3270+05
407	0.3750+05
408	0.4220+05

1	0.0000D+00
2	0.0000D+00
3	0.0000D+00
4	0.0000D+00
5	0.0000D+00
6	0.0000D+00
7	0.0000D+00
8	0.1530D+04
9	0.1530D+04
10	0.1530D+04
11	0.1530D+04
12	0.1530D+04
13	0.1530D+04
14	0.1530D+04
15	0.1530D+04
16	0.1530D+04
17	0.2640D+04
18	0.2640D+04
19	0.2640D+04
20	0.2640D+04
21	0.2640D+04
22	0.2640D+04
23	0.2640D+04
24	0.2640D+04
25	0.2640D+04
26	0.2640D+04
27	0.2640D+04
28	0.2640D+04
29	0.2640D+04
30	0.2640D+04
31	0.2640D+04
32	0.2640D+04
33	0.2640D+04
34	0.3270D+04
35	0.3270D+04
36	0.3270D+04
37	0.3270D+04
38	0.3270D+04
39	0.3270D+04
40	0.3270D+04
41	0.3270D+04
42	0.3270D+04
43	0.3270D+04
44	0.3270D+04
45	0.3270D+04
46	0.3270D+04
47	0.3270D+04
48	0.3270D+04
49	0.3270D+04
50	0.3270D+04
51	0.3270D+04
52	0.3270D+04
53	0.3850D+04
54	0.3850D+04
55	0.3850D+04
56	0.3850D+04
57	0.3850D+04
58	0.3850D+04
59	0.3850D+04
60	0.3850D+04
61	0.3850D+04
62	0.3850D+04
63	0.3850D+04
64	0.3850D+04
65	0.3850D+04
66	0.3850D+04
67	0.3850D+04
68	0.3850D+04
69	0.3850D+04
70	0.3850D+04
71	0.3850D+04
72	0.3850D+04

73	0.4380+04
74	0.4380+04
75	0.4380+04
76	0.4380+04
77	0.4380+04
78	0.4380+04
79	0.4380+04
80	0.4380+04
81	0.4380+04
82	0.4380+04
83	0.4380+04
84	0.4380+04
85	0.4380+04
86	0.4380+04
87	0.4380+04
88	0.4380+04
89	0.4380+04
90	0.4380+04
91	0.4380+04
92	0.4380+04
93	0.4860+04
94	0.4860+04
95	0.4860+04
96	0.4860+04
97	0.4860+04
98	0.4860+04
99	0.4860+04
100	0.4860+04
101	0.4860+04
102	0.4860+04
103	0.4860+04
104	0.4860+04
105	0.4860+04
106	0.4860+04
107	0.4860+04
108	0.4860+04
109	0.4860+04
110	0.4860+04
111	0.4860+04
112	0.4860+04
113	0.5280+04
114	0.5280+04
115	0.5280+04
116	0.5280+04
117	0.5280+04
118	0.5280+04
119	0.5280+04
120	0.5280+04
121	0.5280+04
122	0.5280+04
123	0.5280+04
124	0.5280+04
125	0.5280+04
126	0.5280+04
127	0.5280+04
128	0.5280+04
129	0.5280+04
130	0.5280+04
131	0.5280+04
132	0.5280+04
133	0.5810+04
134	0.5810+04
135	0.5810+04
136	0.5810+04
137	0.5810+04
138	0.5810+04
139	0.5810+04
140	0.5810+04
141	0.5810+04
142	0.5810+04
143	0.5810+04
144	0.5810+04

145	0.5810D+04
146	0.5810D+04
147	0.5810D+04
148	0.5810D+04
149	0.5810D+04
150	0.5810D+04
151	0.5810D+04
152	0.5810D+04
153	0.6340D+04
154	0.6340D+04
155	0.6340D+04
156	0.6340D+04
157	0.6340D+04
158	0.6340D+04
159	0.6340D+04
160	0.6340D+04
161	0.6340D+04
162	0.6340D+04
163	0.6340D+04
164	0.6340D+04
165	0.6340D+04
166	0.6340D+04
167	0.6340D+04
168	0.6340D+04
169	0.6340D+04
170	0.6340D+04
171	0.6340D+04
172	0.6340D+04
173	0.6860D+04
174	0.6860D+04
175	0.6860D+04
176	0.6860D+04
177	0.6860D+04
178	0.6860D+04
179	0.6860D+04
180	0.6860D+04
181	0.6860D+04
182	0.6860D+04
183	0.6860D+04
184	0.6860D+04
185	0.6860D+04
186	0.6860D+04
187	0.6860D+04
188	0.6860D+04
189	0.6860D+04
190	0.6860D+04
191	0.6860D+04
192	0.6860D+04
193	0.7390D+04
194	0.7390D+04
195	0.7390D+04
196	0.7390D+04
197	0.7390D+04
198	0.7390D+04
199	0.7390D+04
200	0.7390D+04
201	0.7390D+04
202	0.7390D+04
203	0.7390D+04
204	0.7390D+04
205	0.7390D+04
206	0.7390D+04
207	0.7390D+04
208	0.7390D+04
209	0.7390D+04
210	0.7390D+04
211	0.7390D+04
212	0.7390D+04
213	0.8450D+04
214	0.8450D+04
215	0.8450D+04
216	0.8450D+04

217	0.845D+04
218	0.845D+04
219	0.845D+04
220	0.845D+04
221	0.845D+04
222	0.845D+04
223	0.845D+04
224	0.845D+04
225	0.845D+04
226	0.845D+04
227	0.845D+04
228	0.845D+04
229	0.845D+04
230	0.845D+04
231	0.845D+04
232	0.845D+04
233	0.950D+04
234	0.950D+04
235	0.950D+04
236	0.950D+04
237	0.950D+04
238	0.950D+04
239	0.950D+04
240	0.950D+04
241	0.950D+04
242	0.950D+04
243	0.950D+04
244	0.950D+04
245	0.950D+04
246	0.950D+04
247	0.950D+04
248	0.950D+04
249	0.950D+04
250	0.950D+04
251	0.950D+04
252	0.950D+04
253	0.111D+05
254	0.111D+05
255	0.111D+05
256	0.111D+05
257	0.111D+05
258	0.111D+05
259	0.111D+05
260	0.111D+05
261	0.111D+05
262	0.111D+05
263	0.111D+05
264	0.111D+05
265	0.111D+05
266	0.111D+05
267	0.111D+05
268	0.111D+05
269	0.111D+05
270	0.111D+05
271	0.111D+05
272	0.111D+05
273	0.132D+05
274	0.132D+05
275	0.132D+05
276	0.132D+05
277	0.132D+05
278	0.132D+05
279	0.132D+05
280	0.132D+05
281	0.132D+05
282	0.132D+05
283	0.132D+05
284	0.132D+05
285	0.132D+05
286	0.132D+05
287	0.132D+05
288	0.132D+05

289	0.1320D+05
290	0.1320D+05
291	0.1320D+05
292	0.1320D+05
293	0.1640D+05
294	0.1640D+05
295	0.1640D+05
296	0.1640D+05
297	0.1640D+05
298	0.1640D+05
299	0.1640D+05
300	0.1640D+05
301	0.1640D+05
302	0.1640D+05
303	0.1640D+05
304	0.1640D+05
305	0.1640D+05
306	0.1640D+05
307	0.1640D+05
308	0.1640D+05
309	0.1640D+05
310	0.1640D+05
311	0.1640D+05
312	0.1640D+05
313	0.2110D+05
314	0.2110D+05
315	0.2110D+05
316	0.2110D+05
317	0.2110D+05
318	0.2110D+05
319	0.2110D+05
320	0.2110D+05
321	0.2110D+05
322	0.2110D+05
323	0.2110D+05
324	0.2110D+05
325	0.2110D+05
326	0.2110D+05
327	0.2110D+05
328	0.2110D+05
329	0.2110D+05
330	0.2110D+05
331	0.2110D+05
332	0.2110D+05
333	0.2590D+05
334	0.2590D+05
335	0.2590D+05
336	0.2590D+05
337	0.2590D+05
338	0.2590D+05
339	0.2590D+05
340	0.2590D+05
341	0.2590D+05
342	0.2590D+05
343	0.2590D+05
344	0.2590D+05
345	0.2590D+05
346	0.2590D+05
347	0.2590D+05
348	0.2590D+05
349	0.2590D+05
350	0.2590D+05
351	0.2590D+05
352	0.2590D+05
353	0.3060D+05
354	0.3060D+05
355	0.3060D+05
356	0.3060D+05
357	0.3060D+05
358	0.3060D+05
359	0.3060D+05
360	0.3060D+05
361	0.3060D+05

```
362                    0.3060+05
363                    0.3060+05
364                    0.3060+05
365                    0.3060+05
366                    0.3060+05
367                    0.3060+05
368                    0.3060+05
369                    0.3540+05
370                    0.3540+05
371                    0.3540+05
372                    0.3540+05
373                    0.3540+05
374                    0.3540+05
375                    0.3540+05
376                    0.3540+05
377                    0.3540+05
378                    0.3540+05
379                    0.3540+05
380                    0.3540+05
381                    0.3540+05
382                    0.3540+05
383                    0.3540+05
384                    0.3540+05
385                    0.3540+05
386                    0.3540+05
387                    0.3540+05
388                    0.3540+05
389                    0.3960+05
390                    0.3960+05
391                    0.3960+05
392                    0.3960+05
393                    0.3960+05
394                    0.3960+05
395                    0.3960+05
396                    0.3960+05
397                    0.3960+05
398                    0.3960+05
399                    0.3960+05
400                    0.3960+05
401                    0.3960+05
402                    0.3960+05
403                    0.3960+05
404                    0.3960+05
405                    0.3960+05
406                    0.3960+05
407                    0.3960+05
408                    0.3960+05

  THE  FOLLOWING  CARDS  CONTAIN  ELEMENT  INCIDENCES  AND  TYPE
  1     1     2    11    10     1     6     1
  7     8     9    26    25     1     8     1
 15    17    18    37    36     1    16     1
 31    34    35    55    54     1    18     1
 49    53    54    74    73     1    19    14
315   337   338   354   353     1    15     1
330   353   354   374   373     1    15     1
345   369   370   390   389     1    19     1

  THE  FOLLOWING  CARDS  CONTAIN  MATERIAL  TYPE  CORRECTION
220   143     1     2     0

  THE  FOLLOWING  CARDS  CONTAIN  PRE-INITIAL  CONDITIONS
  1   407     1     560.     0.

  THE  FOLLOWING  CARD  CONTAINS  TRANSIENT  CONTROLLING  INTEGERS
  0     0     0     0    49    13     2     1     2    10     2     1     2     0     0     0
  THE  FOLLOWING  CARDS  CONTAIN  ELEMENT  WIDE  SOURCES
0.0            1.0E-30  999999.0     1.0E-30
  1   362     1     1     0
```

```
    THE  FOLLOWING  CARDS  CONTAIN  DIRICHLET  BOUNDARY  CONDITIONS
0.0        564.0       999999.0 564.0
0.0        563.0       999999.0 563.0
0.0        562.0       999999.0 562.0
0.0        561.0       999999.0 561.0
0.0        560.0       999999.0 560.0
0.0        559.0       999999.0 559.0
0.0        558.0       999999.0 558.0
0.0        557.0       999999.0 557.0
0.0        556.0       999999.0 556.0
0.0        555.0       999999.0 555.0
0.0        620.0       999999.0 620.0
0.0        640.0       999999.0 640.0
0.0        580.0       999999.0 580.0
    1     2     3     4     5     6     7     8     9    10    17    18    19    20    21    22
   23    24    25    34    35    36    53    54    73    93   113   133   153   173   193   213
  233   253   273   293   313   333   334   335   336   337   353   373   372   371   370   369
  389
    1     9     1     1     0
   11     3     1     2     0
   15     4     1     1     0
   20     4     1     2     0
   25     1     1     3     0
   27     1     1     4     0
   29     1     1     5     0
   31     1     1     6     0
   33     1     1     7     0
   35     0     0     8     0
   36     0     0     9     0
   37     0     0    10     0
   38     0     0    11     0
   39     1     1    12     0
   41     4     1    11     0
   46     1     1    12     0
   48     0     0    11     0
   49     0     0    13     0

    THE  FOLLOWING CARDS  CONTAIN  UPPER  LEAKING  AQUIFERS
0.0        565.        9999999.0 565.
0.0        570.        9999999.0 570.
0.0        580.        9999999.0 580.
0.0        590.        9999999.0 590.
0.0        600.        9999999.0 600.
0.0        610.        9999999.0 610.
0.0        620.        9999999.0 620.
0.0        630.        9999999.0 630.
0.0        640.        9999999.0 640.
0.0        590.        9999999.0 590.
 1.312E-11 1.312E-11 1.312E-11 1.312E-11 1.312E-10 1.312E-10 1.312E-10 1.312E-10
 1.312E-10 1.312E-11
    1   237     1     1     0
  239     1     1     2     0
  241     0     0     3     0
  242     8     1     1     0
  251     2     1     2     0
  254     3     1     1     0
  258     0     0     2     0
  259     1     1     3     0
  261    15     1     2     0
  277     1     1     3     0
  279    16     1     4     0
  296     1     1    10     0
  298     0     0     5     0
  299     2     1     6     0
  302     0     0     7     0
  303    11     1     6     0
  315    29     1     7     0
  345     0     0     5     0
  346     1     1     6     0
  348     4     1     7     0
  353     3     1     8     0
  357     1     1     9     0
  359     0     0     8     0
  360     3     1     7     0

    THE  FOLLOWING  CARDS  CONTAIN  LOWER  LEAKING  AQUIFERS
0.0        540.        9999999.0 540.
0.0
    1   362     1     1     0
```

APPENDIX C

FEWA INPUT DATA FOR CONESVILLE, OHIO

```
VWONG(1).CONESDAT(1) SYM CREATED ON 6 SEP 84 AT 19:02:10
     1  FEWA  APPLIED  TO  CONESVILLE,  OHIO                                                  1
     THE  FOLLOWING  CARD  CONTAINS  THE  BASIC  INTEGER  PARAMETERS
   697  662     2  127     0     0     1     0     0    20     0     0     0     1     1   600
     THE  FOLLOWING  TWO  CARDS  CONTAIN  THE  BASIC  REAL  PARAMETERS
 0.01       0.0          0.01       9999999.0 0.001            1.E-362.5       32.2
   2.093E-51.0           1.00       1.85
     THE  FOLLOWING  TWO  CARDS  CONTAIN  PRINTER-  AND  STORAGE-  CONTROL
 33
 11
    1.00D50
     THE FOLLOWING CARD CONTAINS MATERIAL PROPERTIES
 0.0        0.0          0.3        0.0145     0.0145     0.0        0.3
 0.0        0.0          0.3        0.003      0.003      0.0        0.3
     THE  FOLLOWING  CARDS  CONTAIN  BOTTOM  ELEVATION
      1     1     1      710.       0.
      3     1     1      680.       20.
      5     0     0      710.       0.
      6     1     1      630.       10.
      8     1     1      670.       20.
     10     0     0      700.       0.
     11     2     1      615.       10.
     14     1     1      660.       40.
     16     3     1      605.       5.
     20     1     1      640.       60.
     22     3     1      600.       5.
     26     1     1      625.       25.
     28     0     0      700.       0.
     29     3     1      595.       5.
     33     1     1      618.       17.
     35     1     1      680.       20.
     37     1     1      595.       0.
     39     1     1      600.       5.
     41     1     1      613.       15.
     43     1     1      670.       35.
     45     0     0      710.       0.
     46     1     1      595.       3.
     48     1     1      603.       7.
     50     1     1      620.       20.
     52     1     1      685.       25.
     54     3     1      590.       5.
     58     1     1      615.       15.
     60     1     1      660.       30.
     62     1     1      590.       5.
     64     1     1      605.       5.
     66     1     1      617.       18.
     68     0     0      660.       0.
     69     1     1      590.       5.
     71     2     1      602.       5.
     74     1     1      618.       12.
     76     2     1      590.       5.
     79     1     1      604.       4.
     81     1     1      613.       7.
     83     6     1      590.       4.
     90     0     0      595.       0.
     91     4     1      598.       4.
     96     0     0      598.       0.
     97     3     1      602.       2.
    101     0     0      598.       0.
    102     3     1      601.       3.
    106     2     1      613.       3.5
    109     2     1      604.       4.
    112     3     1      614.       2.
    116     2     1      624.       4.
    119     4     1      610.       2.5
    124     3     1      622.       2.
    128     1     1      632.       4.
    130     3     1      610.       3.33
    134     4     1      622.       2.
    139     1     1      632.       0.
    141     0     0      630.       0.
    142     2     1      612.       4.
```

145	3	1	622.	2.
149	1	1	632.	4.
151	1	1	634.	-4.
153	1	1	640.	0.
155	1	1	605.	7.
157	1	1	617.	5.
159	1	1	620.	0.
161	1	1	629.	-1.
163	1	1	620.	0.
165	1	1	628.	2.
167	1	1	640.	10.
169	0	0	640.	0.
170	2	1	590.	7.
173	1	1	612.	8.
175	3	1	623.	3.
179	1	1	645.	-11.
181	1	1	630.	3.
183	1	1	632.	8.
185	1	1	645.	0.
187	0	0	640.	0.
188	1	1	585.	5.
190	1	1	594.	4.
192	3	1	604.	6.
196	1	1	620.	2.
198	1	1	622.	8.
200	0	0	634.	0.
201	1	1	625.	5.
203	1	1	633.	-3.
205	2	1	635.	0.
208	4	1	596.	2.5
213	1	1	604.	4.
215	1	1	613.	5.
217	1	1	628.	12.
219	1	1	630.	-10.
221	1	1	624.	6.
223	1	1	638.	-2.
225	1	1	634.	-2.
227	1	1	630.	2.
229	1	1	600.	-2.
231	1	1	597.	1.
233	1	1	600.	2.
235	1	1	605.	2.
237	2	1	612.	3.
240	2	1	620.	0.
243	1	1	622.	21.
245	1	1	642.	-2.
247	2	1	638.	-4.
250	0	0	603.	0.
251	1	1	602.	0.
253	3	1	603.	1.
257	1	1	608.	2.
259	1	1	614.	4.
261	1	1	630.	0.
263	0	0	625.	0.
264	1	1	640.	2.
266	0	0	643.	0.
267	3	1	642.	-4.
271	0	0	608.	0.
272	1	1	600.	0.
274	1	1	608.	1.
276	1	1	609.	1.
278	4	1	612.	2.
283	1	1	630.	0.
285	0	0	642.	0.
286	1	1	643.	.5
288	1	1	645.	7.
290	2	1	638.	-1.
293	1	1	614.	-3.
295	1	1	609.	2.
297	4	1	612.	1.
302	1	1	610.	0.
304	1	1	620.	0.

306	1	1	636.	5.
308	1	1	642.	1.
310	0	0	643.5	0.
311	1	1	643.	-1.
313	3	1	639.	-1.
317	2	1	618.	-2.
320	3	1	614.	2.
324	3	1	622.5	2.5
328	1	1	635.	5.
330	2	1	641.	1.
333	1	1	643.5	0.
335	1	1	643.	-1.
337	3	1	639.	-1.
341	2	1	622.	-2.
344	1	1	617.	1.
346	3	1	625.	2.
350	3	1	631.	3.
354	2	1	641.	1.
357	1	1	643.5	0.
359	1	1	643.	-1.
361	4	1	640.	-1.
366	0	0	636.	0.
367	1	1	626.	-6.
369	1	1	618.	0.
371	4	1	625.	2.5
376	4	1	632.2	2.2
381	1	1	642.	1.
383	1	1	643.5	0.
385	1	1	643.	-1.
387	4	1	640.	-1.
392	2	1	636.	2.
395	2	1	630.	-5.
398	5	1	619.	2.
404	4	1	631.2	2.2
409	1	1	642.	1.
411	1	1	643.5	0.
413	1	1	643.	-1.
415	4	1	640.	-1.
420	2	1	636.	2.
423	0	0	690.	0.
424	1	1	631.	-3.
426	1	1	622.	0.
428	1	1	624.	2.
430	2	1	627.	1.
433	5	1	631.	2.
439	1	1	642.	1.
441	0	0	643.5	0.
442	1	1	643.	-1.
444	4	1	640.	-1.
449	2	1	636.	2.
452	0	0	690.	0.
453	2	1	631.	-2.
456	1	1	626.	-2.
458	5	1	626.	1.
464	5	1	632.5	1.5
470	1	1	642.	1.
472	1	1	643.	-3.
474	3	1	639.	-1.
478	2	1	636.	2.
481	0	0	690.	0.
482	2	1	632.	-1.
485	2	1	628.	-2.
488	4	1	626.	1.
493	8	1	632.	1.
502	1	1	643.	-3.
504	2	1	639.	0.
507	2	1	636.	0.
510	1	1	640.	50.
512	0	0	635.	0.
513	2	1	632.	-1.
516	1	1	628.	-4.
518	5	1	626.	1.

524	7	1	631.	1.
532	1	1	640.	3.
534	3	1	642.	0.
538	3	1	640.	0.
542	4	1	634.	-1.
547	1	1	628.	-4.
549	4	1	626.	1.
554	8	1	632.	1.
563	5	1	642.	1.6
569	1	1	660.	10.
571	0	0	670.	0.
572	1	1	635.	-1.
574	2	1	632.	-1.
577	1	1	628.	-4.
579	4	1	628.	1.
584	8	1	632.	1.
593	4	1	642.	2.
598	0	0	660.	0.
599	1	1	700.	0.
601	1	1	635.	-1.
603	2	1	632.	-1.
606	1	1	628.	-4.
608	4	1	628.	1.
613	7	1	631.25	1.25
621	3	1	642.	3.
625	1	1	657.	23.
627	1	1	635.	-1.
629	2	1	632.	-1.
632	2	1	628.	-2.
635	2	1	628.	1.
638	6	1	631.2	1.2
645	3	1	641.	3.
649	1	1	654.	4.
651	1	1	635.	-1.
653	2	1	632.	-1.
656	1	1	628.	-2.
658	1	1	628.	2.
660	7	1	631.25	1.25
665	2	1	642.	2.
671	1	1	652.	2.
673	1	1	634.	-2.
675	1	1	631.	-1.
677	2	1	626.	2.
680	7	1	631.25	1.25
688	3	1	643.	3.
692	4	1	638.	3.
697	0	0	648.	0.
1	696	1	50.0	0.0

THE FOLLOWING CARDS CONTAIN NODAL COORDINATES

1	1	1	2200.	200.	0.
2	2	1	2200.	200.	0.
6	3	1	2000.	200.	0.
11	4	1	2000.	200.	0.
16	5	1	1800.	200.	0.
22	6	1	1800.	200.	0.
29	7	1	1800.	200.	0.
37	8	1	1800.	200.	0.
46	7	1	2000.	200.	0.
54	7	1	2000.	200.	0.
62	6	1	2200.	200.	0.
69	6	1	2200.	200.	0.
76	6	1	2200.	200.	0.
83	6	1	2200.	200.	0.
90	5	1	2400.	200.	0.
96	4	1	2400.	200.	0.
101	7	1	2200.	200.	0.
107	9	1	2200.	200.	0.
119	10	1	2200.	200.	0.
130	11	1	2000.	200.	0.
142	12	1	2000.	200.	0.

155	14	1	1300.	200.	0.
170	17	1	1400.	200.	0.
188	19	1	1000.	200.	0.
208	20	1	800.	200.	0.
229	20	1	600.	200.	0.
250	20	1	600.	200.	0.
271	21	1	600.	200.	0.
293	23	1	600.	200.	0.
317	23	1	400.	200.	0.
341	25	1	400.	200.	0.
367	27	1	400.	200.	0.
395	28	1	400.	200.	0.
424	28	1	400.	200.	0.
453	28	1	400.	200.	0.
482	29	1	200.	200.	0.
512	29	1	200.	200.	0.
542	29	1	200.	200.	0.
572	28	1	200.	200.	0.
601	25	1	400.	200.	0.
627	23	1	600.	200.	0.
651	21	1	800.	200.	0.
673	18	1	1200.	200.	0.
692	4	1	3800.	200.	0.
697	0	0	4400.	0.	0.
1	1	1	0.	0.	0.
3	2	1	200.	0.	0.
6	4	1	400.	0.	0.
11	4	1	600.	0.	0.
16	5	1	800.	0.	0.
22	6	1	1000.	0.	0.
29	7	1	1200.	0.	0.
37	8	1	1400.	0.	0.
46	7	1	1600.	0.	0.
54	7	1	1800.	0.	0.
62	6	1	2000.	0.	0.
69	6	1	2200.	0.	0.
76	6	1	2400.	0.	0.
83	6	1	2600.	0.	0.
90	5	1	2800.	0.	0.
96	4	1	3000.	0.	0.
101	7	1	3200.	0.	0.
109	9	1	3400.	0.	0.
119	10	1	3600.	0.	0.
130	11	1	3800.	0.	0.
142	12	1	4000.	0.	0.
155	14	1	4200.	0.	0.
170	17	1	4400.	0.	0.
188	19	1	4600.	0.	0.
208	20	1	4800.	0.	0.
229	20	1	5000.	0.	0.
250	20	1	5200.	0.	0.
271	21	1	5400.	0.	0.
293	23	1	5600.	0.	0.
317	23	1	5800.	0.	0.
341	25	1	6000.	0.	0.
367	27	1	6200.	0.	0.
395	28	1	6400.	0.	0.
424	28	1	6600.	0.	0.
453	28	1	6800.	0.	0.
482	29	1	7000.	0.	0.
512	29	1	7200.	0.	0.
542	29	1	7400.	0.	0.
572	28	1	7600.	0.	0.
601	25	1	7800.	0.	0.
627	23	1	8000.	0.	0.
651	21	1	8200.	0.	0.
673	18	1	8400.	0.	0.
692	4	1	8600.	0.	0.
697	0	0	8200.	0.	0.

THE FOLLOWING CARDS CONTAIN ELEMENT INCIDENCES AND TYPE

1	1	2	4	3	-1	0	0
2	2	5	4	0	-1	0	0
3	3	7	6	0	-1	0	0
4	3	4	8	7	-1	2	1
6	5	10	9	0	-1	0	0
7	6	7	12	11	-1	4	1
11	11	17	16	0	-1	0	0
12	11	12	18	17	-1	4	1
16	16	17	23	22	-1	5	1
21	21	28	27	0	-1	0	0
22	22	23	30	29	-1	6	1
28	28	36	35	0	-1	0	0
29	29	30	38	37	-1	7	1
36	36	45	44	0	-1	0	0
37	37	38	46	0	-1	0	0
38	38	39	47	46	-1	7	1
45	46	47	55	54	-1	7	1
52	54	55	62	0	-1	0	0
53	55	56	63	62	-1	6	1
59	62	63	70	69	-1	6	1
65	69	70	77	76	-1	6	1
71	76	77	84	83	-1	6	1
77	83	84	90	0	-1	0	0
78	84	85	91	90	-1	5	1
83	90	91	97	96	-1	4	1
87	96	102	101	0	-1	0	0
88	96	97	103	102	-1	4	1
92	100	107	106	0	-1	0	0
93	101	102	110	109	-1	7	1
100	108	117	116	0	-1	0	0
101	109	110	120	119	-1	9	1
110	118	129	128	0	-1	0	0
111	119	131	130	0	-1	0	0
112	119	120	132	131	-1	10	1
122	130	131	143	0	-1	0	0
123	131	132	144	143	-1	10	1
133	141	154	153	0	-1	0	0
134	142	156	155	0	-1	0	0
135	142	143	157	156	-1	12	1
147	154	169	168	0	-1	0	0
148	155	172	171	0	-1	0	0
149	155	156	173	172	-1	14	1
163	169	187	186	0	-1	0	0
164	170	190	189	0	-1	0	0
165	170	171	191	190	-1	17	1
182	188	209	208	0	-1	0	0
183	188	189	210	209	-1	19	1
202	208	230	229	0	-1	0	0
203	208	209	231	230	-1	19	1
222	227	228	249	0	-1	0	0
223	229	230	251	250	-1	20	1
243	250	251	272	271	-1	20	1
263	270	292	291	0	-1	0	0
264	271	294	293	0	-1	0	0
265	271	272	295	294	-1	21	1
286	292	316	315	0	-1	0	0
287	293	294	318	317	-1	23	1
310	317	318	342	341	-1	23	1
333	340	365	364	0	-1	0	0
334	341	342	368	367	-1	25	1
359	366	393	392	0	-1	0	0
360	367	368	396	395	-1	27	1
387	394	423	422	0	-1	0	0
388	395	396	425	424	-1	24	1
416	424	425	454	453	-1	28	1
444	453	483	482	0	-1	0	0
445	453	454	484	483	-1	28	1
473	482	483	513	512	-1	29	1
502	512	513	543	542	-1	29	1
531	542	543	573	572	-1	28	1
559	570	571	600	0	-1	0	0

```
560  572  573  601    0   -1    0    0
561  573  574  602  601   -1   25    1
586  598  599  626    0   -1    0    0
587  601  602  627    0   -1    0    0
588  602  603  628  627   -1   23    1
611  625  626  650    0   -1    0    0
612  627  628  651    0   -1    0    0
613  628  629  652  651   -1   21    1
634  649  650  672    0   -1    0    0
635  652  653  673    0   -1    0    0
636  653  654  674  673   -1   16    1
654  671  672  691    0   -1    0    0
655  685  686  692    0   -1    0    0
656  686  687  693  692   -1    4    1
660  690  691  696    0   -1    0    0
661  694  695  697    0   -1    0    0
662  695  696  697    0   -1    0    0

  THE  FOLLOWING  CARDS  CONTAIN  MATERIAL  TYPE  CORRECTION
144    3    1   -2    0
159    4    1   -2    0
177    4    1   -2    0
197    4    1   -2    0
218    4    1   -2    0
239    3    1   -2    0
259    4    1   -2    0
281    5    1   -2    0
304    5    1   -2    0
327    6    1   -2    0
351    8    1   -2    0
377   10    1   -2    0
405   10    1   -2    0
433   10    1   -2    0
462   10    1   -2    0
491   10    1   -2    0
520   10    1   -2    0

  THE  FOLLOWING  CARDS  CONTAIN  PRE-INITIAL  CONDITIONS
  1  696    1     730.     0.

  THE  FOLLOWING  CARD  CONTAINS  TRANSIENT  CONTROLLING  INTEGERS
  2    3    1    2   94   18    2    1    2    1    2    1    2    0    0    0
  THE  FOLLOWING  CARDS  CONTAIN  ELEMENT  WIDE  SOURCES
0.0          1.5E-8  999999.0      1.5E-8
  1  661    1    1    0

  THE  FOLLOWING  CARDS  CONTAIN  DIRICHLET  BOUNDARY  CONDITIONS
0.0        722.5      9999999.0  722.5
0.0        723.0      9999999.0  723.0
0.0        723.5      9999999.0  723.5
0.0        724.0      9999999.0  724.0
0.0        724.5      9999999.0  724.5
0.0        725.0      9999999.0  725.0
0.0        725.5      9999999.0  725.5
0.0        726.0      9999999.0  726.0
0.0        726.5      9999999.0  726.5
0.0        727.0      9999999.0  727.0
0.0        727.5      9999999.0  727.5
0.0        728.0      9999999.0  728.0
0.0        728.5      9999999.0  728.5
0.0        729.0      9999999.0  729.0
0.0        729.5      9999999.0  729.5
0.0        730.0      9999999.0  730.0
0.0        738.0      9999999.0  738.0
0.0        740.0      9999999.0  740.0
  1    3    6   11   16   22   29   37   46   54   62   69   76   83   90   96
101  109  119  130  143  142  155  171  170  189  188  208  229  250  271  293
317  341  367  395  424  453  482  512  542  572  601  627  651  652  673  674
675  676  677  678  679  680  681  682  683  684  685  692  693  694  697  696
691  672  650  626  599  511  481  452  423  394  393  366  365  340  316  292
270  249  228  129  118  117  108  107  100   94   95   89   82   75
```

```
  1     7     1     1     0
  9     5     1     2     0
 15     5     1     3     0
 21     0     0     4     0
 22    11     1     3     0
 34     0     0     4     0
 35    11     1     5     0
 47    12     1     6     0
 60     3     1     7     0
 64     0     0     8     0
 65     0     0    12     0
 66     0     0    13     0
 67     0     0    14     0
 68     0     0    15     0
 69     0     0    16     0
 70    11     1    17     0
 82     1     1    18     0
 84     2     1    11     0
 87     2     1    10     0
 90     4     1     9     0

  THE  FOLLOWING  CARDS  CONTAIN  NEUMANN  BOUNDARY  CONDITIONS
0.0        -0.001929 9999999.0 -0.001929
 541  571   600
  1     2     1     1     0

  1     1     1     2     1     1

  THE  FOLLOWING  CARDS  CONTAIN  UPPER  LEAKING  AQUIFERS
0.0        800.       9999999.0 800.
0.0
  1  661     1     1     0

  THE  FOLLOWING  CARDS  CONTAIN  LOWER  LEAKING  AQUIFERS
0.0        585.       9999999.0 800.
0.0
  1  661     1     1     0
```

APPENDIX D

FEWA INPUT DATA FOR HIALEAH-PRESTON WELLS, MAY 3, 1977

```
   1  FEWA  APPLIED  TO  HIALEAH-PRESTON  WELLS, BISCAYNE  AQUIFER, FLORIDA    1
   THE  FOLLOWING  CARD  CONTAINS  THE  BASIC  INTEGER  PARAMETERS
 366  349     2   10     0     0     1     0     0  600     0     0     0     1     1  600
   THE  FOLLOWING  TWO  CARDS  CONTAIN  THE  BASIC  REAL  PARAMETERS

.01       0.0        0.01        9999999.0 0.010      0.010      62.5       32.2
 2.093E-51.0         1.0         1.00
   THE  FOLLOWING  TWO  CARDS  CONTAIN  PRINTER-  AND  STORAGE-  CONTROL
3
1
  1.00050
   THE  FOLLOWING  CARD  CONTAINS  MATERIAL  PROPERTIES

.0        0.0        0.35          2.888E-2  2.888E-20.0        0.35

.0        0.0        0.35          1.388E-3  1.388E-30.0        0.35
   THE  FOLLOWING  CARDS  CONTAIN  BOTTOM  ELEVATION
   1  365     1      -105.       0.0
   1  365     1      0.0         0.0
   THE  FOLLOWING  CARDS  CONTAIN  NODAL  COORDINATES
   1                .310600+04
   2                .385200+04
   3                .465900+04
   4                .543500+04
   5                .621200+04
   6                .698800+04
   7                .776500+04
   8                .854100+04
   9                .931800+04
  10                .100940+05
  11                .108710+05
  12                .116470+05
  13                .124240+05
  14                .279500+04
  15                .310600+04
  16                .385200+04
  17                .465900+04
  18                .543500+04
  19                .621200+04
  20                .698800+04
  21                .776500+04
  22                .854100+04
  23                .931800+04
  24                .100940+05
  25                .108710+05
  26                .116470+05
  27                .124240+05
  28                .132000+05
  29                .291200+04
  30                .310600+04
  31                .385200+04
  32                .465900+04
  33                .543500+04
  34                .621200+04
  35                .698800+04
  36                .776500+04
  37                .854100+04
  38                .931800+04
  39                .100940+05
  40                .108710+05
  41                .116470+05
  42                .124240+05
  43                .132000+05
  44                .139770+05
  45                .144420+05
  46                .279500+04
  47                .310600+04
  48                .385200+04
  49                .465900+04
  50                .543500+04
  51                .621200+04
  52                .698800+04
  53                .776500+04
  54                .854100+04
  55                .931800+04
  56                .100940+05
  57                .108710+05
  58                .116470+05
  59                .124240+05
  60                .132000+05
  61                .139770+05
```

62	.145590+[illegible]
63	.279500+04
64	.310600+04
65	.323200+04
66	.465300+04
67	.543500+04
68	.621200+04
69	.698300+04
70	.776500+04
71	.854100+04
72	.931200+04
73	.100940+05
74	.108710+05
75	.116470+05
76	.124240+05
77	.132000+05
78	.139770+05
79	.155290+05
80	.163060+05
81	.170820+05
82	.217400+04
83	.310600+04
84	.320200+04
85	.442600+04
86	.543500+04
87	.621200+04
88	.683300+04
89	.753200+04
90	.854100+04
91	.931200+04
92	.100940+05
93	.108710+05
94	.116470+05
95	.124240+05
96	.132000+05
97	.139770+05
98	.155290+05
99	.163060+05
100	.170820+05
101	.177240+05
102	.217400+04
103	.310600+04
104	.380200+04
105	.504700+04
106	.621200+04
107	.660000+04
108	.729900+04
109	.854100+04
110	.931200+04
111	.100940+05
112	.108710+05
113	.116470+05
114	.124240+05
115	.123120+05
116	.139770+05
117	.155290+05
118	.163060+05
119	.170820+05
120	.182470+05
121	.213700+04
122	.310600+04
123	.385200+04
124	.465900+04
125	.582400+04
126	.660000+04
127	.737700+04
128	.854100+04
129	.931200+04
130	.100940+05
131	.108710+05
132	.116470+05
133	.123120+05

134	.139770+05
135	.155290+05
136	.163060+05
137	.170820+05
138	.186350+05
139	.201900+04
140	.310600+04
141	.383200+04
142	.465900+04
143	.543500+04
144	.621200+04
145	.799800+04
146	.892900+04
147	.931900+04
148	.100940+05
149	.108770+05
150	.116470+05
151	.128120+05
152	.139770+05
153	.155290+05
154	.163060+05
155	.170820+05
156	.190240+05
157	.155290+04
158	.232900+04
159	.310600+04
160	.383200+04
161	.465900+04
162	.543500+04
163	.621200+04
164	.698800+04
165	.799800+04
166	.892900+04
167	.973800+04
168	.100940+05
169	.116470+05
170	.128120+05
171	.139770+05
172	.155290+05
173	.163060+05
174	.170820+05
175	.192570+05
176	.388000+05
177	.155290+04
178	.232900+04
179	.310600+04
180	.383200+04
181	.465900+04
182	.543500+04
183	.621200+04
184	.698800+04
185	.799800+04
186	.892900+04
187	.100940+05
188	.108710+05
189	.116470+05
190	.128120+05
191	.139770+05
192	.155290+05
193	.163060+05
194	.170820+05
195	.192670+05
196	.778000+06
197	.388200+05
198	.155290+04
199	.232900+04
200	.302300+04
201	.380500+04
202	.465900+04
203	.543500+04
204	.621200+04
205	.698800+04

206	.760000+04
207	.775500+04
208	.815300+04
209	.931900+04
210	.108710+05
211	.116470+05
212	.128120+05
213	.139770+05
214	.155290+05
215	.163060+05
216	.170820+05
217	.195670+05
218	.000000+00
219	.388000+03
220	.155300+04
221	.232900+04
222	.302800+04
223	.388200+04
224	.458100+04
225	.543500+04
226	.597900+04
227	.660000+04
228	.675500+04
229	.737700+04
230	.784200+04
231	.854100+04
232	.108710+05
233	.116470+05
234	.128120+05
235	.139770+05
236	.155290+05
237	.163060+05
238	.170820+05
239	.195670+05
240	.155000+05
241	.388000+03
242	.155300+04
243	.194100+04
244	.255200+04
245	.349400+04
246	.427100+04
247	.504700+04
248	.543500+04
249	.582400+04
250	.757100+04
251	.807500+04
252	.892900+04
253	.108710+05
254	.116470+05
255	.128120+05
256	.139770+05
257	.155290+05
258	.163060+05
259	.170820+05
260	.195670+05
261	.465000+03
262	.155300+04
263	.232900+04
264	.310600+04
265	.388200+04
266	.427100+04
267	.504700+04
268	.753200+04
269	.807500+04
270	.892900+04
271	.108710+05
272	.116470+05
273	.128120+05
274	.139770+05
275	.155290+05
276	.163060+05
277	.170820+05

278	.195670+05
279	.854000+03
280	.155300+04
281	.232900+04
282	.310600+04
283	.388200+04
284	.450400+04
285	.698800+04
286	.760900+04
287	.807500+04
288	.892900+04
289	.108710+05
290	.116470+05
291	.128120+05
292	.139770+05
293	.155290+05
294	.163060+05
295	.170820+05
296	.194890+05
297	.155300+04
298	.232900+04
299	.310600+04
300	.357200+04
301	.543500+04
302	.776500+04
303	.892900+04
304	.108710+05
305	.116470+05
306	.128120+05
307	.139770+05
308	.155290+05
309	.163060+05
310	.170820+05
311	.193340+05
312	.295100+04
313	.388200+04
314	.543500+04
315	.776500+04
316	.892900+04
317	.108710+05
318	.116470+05
319	.128120+05
320	.139770+05
321	.155290+05
322	.163060+05
323	.170820+05
324	.190230+05
325	.302800+04
326	.388200+04
327	.543500+04
328	.776500+04
329	.892900+04
330	.108710+05
331	.116470+05
332	.128120+05
333	.139770+05
334	.155290+05
335	.163060+05
336	.170820+05
337	.184410+05
338	.357200+04
339	.543500+04
340	.776500+04
341	.892900+04
342	.108710+05
343	.116470+05
344	.128120+05
345	.139770+05
346	.155290+05
347	.163060+05
348	.170820+05
349	.174710+05

350			.489200*04
351			.776500*04
352			.892900*04
353			.108710*05
354			.116470*05
355			.128120*05
356			.139770*05
357			.155290*05
358			.163060*05
359			.170820*05
360			.776500*04
361			.892900*04
362			.108710*05
363			.116470*05
364			.128120*05
365			.139770*05
366			.155290*05
1			621.
2			388.
3			78.
4			0.
5			39.
6			78.
7			155.
8			155.
9			78.
10			155.
11			233.
12			466.
13			777.
14	14	1	1553.
29	16	1	3106.
45	16	1	3882.
63	16	1	4659.
80			4465.
81			4014.
82	5	1	5435.
88			5591.
89			5979.
90	11	1	5435.
102	2	1	6212.
105			5901.
106			6212.
107			6134.
108			6000.
109	11	1	6212.
121	17	1	6988.
139	17	1	7765.
157	18	1	8541.
176	19	1	10094.
196	3	1	10871.
200			10560.
201			10482.
202	1	1	10405.
204	2	1	10482.
207			10633.
208	9	1	10482.
219	3	1	11259.
222			11337.
223	2	1	11259.
226	1	1	11026.
228			11259.
229			11026.
230			10948.
231	6	1	10871.
240	9	1	12035.
250			11259.
251			11453.
252	8	1	11647.
261	8	1	12812.
268	10	1	12035.
279	6	1	13200.

286	1	1	12501.
289	0	1	13200.
297			13744.
298			13977.
299	1	1	14054.
301	10	1	13977.
312	12	1	15629.
325	12	1	17032.
338	11	1	18635.
350	0	1	20183.
359			19173.
360			21565.
361			21741.
362			21845.
363			21813.
364			21586.
365			21275.
366			20574.

THE FOLLOWING CARDS CONTAIN ELEMENT INCIDENCES AND TYPE

1	1	15	14	0	-1		
2	1	2	16	15	-1	12	1
14	13	28	27	0	-1		
15	14	15	30	29	-1	14	1
29	28	44	43	0	-1		
30	28	45	44	0	-1		
31	29	30	47	46	-1	16	1
47	46	47	64	63	-1	15	1
62	61	62	78	0	-1		
63	63	64	83	82	-1	14	1
77	77	78	98	0	-1		
78	79	98	97	0	-1		
79	79	80	99	98	-1	2	1
81	81	101	100	0	-1		
82	82	83	103	102	-1	2	1
84	84	85	104	0	-1		
85	85	86	105	104	-1	10	1
95	95	96	114	0	-1		
96	97	116	115	0	-1		
97	97	98	117	116	-1	4	1
101	102	103	122	121	-1	11	1
112	113	114	132	0	-1		
113	115	133	132	0	-1		
114	115	116	134	133	-1	5	1
119	121	122	140	139	-1	13	1
129	131	132	149	0	-1		
130	132	150	149	0	-1		
131	132	133	151	150	-1	6	1
137	139	158	157	0	-1		
138	139	140	159	158	-1	3	1
147	148	149	167	0	-1		
148	149	168	167	0	-1		
149	149	150	169	168	-1	7	1
156	157	177	176	0	-1		
157	157	158	178	177	-1	8	1
165	166	186	185	0	-1		
166	166	187	185	0	-1		
167	167	186	185	0	-1		
168	167	187	186	0	-1		
169	167	188	186	187	-1	9	1
177	178	197	196	0	-1		
178	178	177	198	197	-1	9	1
187	189	207	206	0	-1		
188	189	186	208	207	-1	10	1
198	198	197	219	218	-1	21	1
219	218	219	241	240	-1	9	1
228	227	228	249	0	-1		
229	228	229	250	249	-1	11	1
240	240	241	261	0	-1		
241	241	242	262	261	-1	9	1
247	247	248	267	0	-1		
248	248	249	267	0	-1		
249	249	250	268	267	-1	11	1

```
260  261  262  280  279   -1    5    1
265  266  267  284    0   -1
266  267  285  284    0   -1
267  267  268  286  285   -1   11    1
278  279  280  297    0   -1
279  280  281  298  297   -1    3    1
282  283  284  300    0   -1
283  284  301  300    0   -1
284  284  285  302  301   -1
285  285  286  287  302   -1
286  287  288  303  302   -1    9    1
295  300  313  312    0   -1
296  300  301  314  313   -1   11    1
307  312  313  326  325   -1   12    1
319  325  326  338    0   -1
320  326  327  339  338   -1   11    1
331  338  339  350    0   -1
332  339  340  351  350   -1    9    1
341  348  349  359    0   -1
342  350  351  360    0   -1
343  351  352  361  360   -1    6    1
349  357  358  366    0   -1
  THE  FOLLOWING  CARDS  CONTAIN  MATERIAL  TYPE  CORRECTION
207    1    1   -2    0
229    1    1   -2    0
250    1    1   -2    0
268    1    1   -2    0
286    1    1   -2    0
  THE  FOLLOWING  CARDS  CONTAIN  PRE-INITIAL  CONDITIONS
  1  365    1    1.    0.
  THE  FOLLOWING  CARD  CONTAINS  TRANSIENT  CONTROLLING  INTEGERS
  0    0    0    0   72    1    2    1    2    1    2    1    2   33    4    2
  THE  FOLLOWING  CARDS  CONTAIN  SOURCES  AND  WELLS

.0        0.0        9999999.0 0.0
  1  348    1    1    0

.0       -10.486     9999999.0 -10.486

.0       -6.344      9999999.0 -6.344

.0        8.3536     9999999.0 8.3536

.0       16.7072     9999999.0 16.7072
 89  107  108  227  226  225  224  223  222  200  201  202  203  208  207  230
251  269  287  286  268  250  229  132  149  167  206  228  249  267  284  300
185
  1   12    1    1    0
 14    9    1    2    0
 24    8    1    3    0
 33    0    1    4    0
  THE  FOLLOWING  CARDS  CONTAIN  DIRICHLET  BOUNDARY  CONDITIONS

.0        1.         9999999.0 1.
  1    2    3    4    5    6    7    8    9   10   11   12   13   28   45   62
 79   96  114  132  115   97   79   80   81  101  120  138  156  175  195  217
239  260  278  296  311  324  337  349  359  358  366  365  364  363  362  361
360  350  338  325  312  300  299  293  297  279  261  240  218  196  176  157
139  121  102   82   63   44   29   14
  1   71    1    1    0
  THE  FOLLOWING  CARDS  CONTAIN  UPPER  LEAKING  AQUIFERS

.0        1.0        9999999.0 1.0

.0
  1  348    1    1    0
  THE  FOLLOWING  CARDS  CONTAIN  LOWER  LEAKING  AQUIFERS

.0        0.0        9999999.0 0.0

.0
  1  348    1    1
```

APPENDIX E

FEWA INPUT DATA FOR HIALEAH-PRESTON WELLS

```
VWONG(1),BISCNDAT(10) SYM CREATED ON 28 SEP 84 AT 10:59:23
     1  FEWA  APPLIED  TO  HIALEAH-PRESTON  WELLS, BISCAYNE  AQUIFER, FLORIDA    1
     THE  FOLLOWING  CARD  CONTAINS  THE  BASIC  INTEGER  PARAMETERS
   366  349    2   10    40    0    1    0    0  600    0    0    0    1    1  600
     THE  FOLLOWING  TWO  CARDS  CONTAIN  THE  BASIC  REAL  PARAMETERS
 332640.    0.0        500000.   13305600. 0.001      0.001      62.5       32.2
  2.093E-51.0           1.0        1.00
     THE  FOLLOWING  TWO  CARDS  CONTAIN  PRINTER-  AND  STORAGE-  CONTROL
 3111111111111111111311111111111111111113
 1000000000000000000103000000000000000001
    1.00E20
     THE  FOLLOWING  CARD  CONTAINS  MATERIAL  PROPERTIES
 0.0        0.0        0.35        2.888E-2  2.888E-20.0        0.35
 0.0        0.0        0.35        1.388E-3  1.388E-30.0        0.35
     THE  FOLLOWING  CARDS  CONTAIN  BOTTOM  ELEVATION
     1  365    1       -105.       0.0

     1  365    1       0.0         0.0

     THE  FOLLOWING  CARDS  CONTAIN  NODAL  COORDINATES
     1                .31060D+04
     2                .38820D+04
     3                .46590D+04
     4                .54350D+04
     5                .62120D+04
     6                .69880D+04
     7                .77650D+04
     8                .85410D+04
     9                .93180D+04
    10                .10094D+05
    11                .10871D+05
    12                .11647D+05
    13                .12424D+05
    14                .27950D+04
    15                .31060D+04
    16                .38820D+04
    17                .46590D+04
    18                .54350D+04
    19                .62120D+04
    20                .69880D+04
    21                .77650D+04
    22                .85410D+04
    23                .93180D+04
    24                .10094D+05
    25                .10871D+05
    26                .11647D+05
    27                .12424D+05
    28                .13200D+05
    29                .29120D+04
    30                .31060D+04
    31                .38820D+04
    32                .46590D+04
    33                .54350D+04
    34                .62120D+04
    35                .69880D+04
    36                .77650D+04
    37                .85410D+04
    38                .93180D+04
    39                .10094D+05
    40                .10871D+05
    41                .11647D+05
    42                .12424D+05
    43                .13200D+05
    44                .13977D+05
    45                .14442D+05
    46                .27950D+04
    47                .31060D+04
    48                .38820D+04
    49                .46590D+04
    50                .54350D+04
    51                .62120D+04
    52                .69880D+04
```

53	.776500D+04
54	.854100D+04
55	.931800D+04
56	.100940D+05
57	.108710D+05
58	.116470D+05
59	.124240D+05
60	.132000D+05
61	.139770D+05
62	.145590D+05
63	.279500D+04
64	.310600D+04
65	.388200D+04
66	.465900D+04
67	.543500D+04
68	.621200D+04
69	.698800D+04
70	.776500D+04
71	.854100D+04
72	.931800D+04
73	.100940D+05
74	.108710D+05
75	.116470D+05
76	.124240D+05
77	.132000D+05
78	.139770D+05
79	.155290D+05
80	.163060D+05
81	.170820D+05
82	.217400D+04
83	.310600D+04
84	.368200D+04
85	.442600D+04
86	.543500D+04
87	.621200D+04
88	.683300D+04
89	.753200D+04
90	.854100D+04
91	.931800D+04
92	.100940D+05
93	.109710D+05
94	.116470D+05
95	.124240D+05
96	.132000D+05
97	.139770D+05
98	.155290D+05
99	.163060D+05
100	.170820D+05
101	.177040D+05
102	.217400D+04
103	.310600D+04
104	.388200D+04
105	.504700D+04
106	.621200D+04
107	.660000D+04
108	.729900D+04
109	.854100D+04
110	.931800D+04
111	.100940D+05
112	.108710D+05
113	.116470D+05
114	.124240D+05
115	.128120D+05
116	.139770D+05
117	.155290D+05
118	.163060D+05
119	.170820D+05
120	.182470D+05
121	.213500D+04
122	.310600D+04
123	.388200D+04
124	.465900D+04

125	.58240D+04
126	.66000D+04
127	.73770D+04
128	.85410D+04
129	.93180D+04
130	.10094D+05
131	.10871D+05
132	.11647D+05
133	.12812D+05
134	.13977D+05
135	.15529D+05
136	.16306D+05
137	.17082D+05
138	.18635D+05
139	.20190D+04
140	.31060D+04
141	.38820D+04
142	.46590D+04
143	.54350D+04
144	.62120D+04
145	.79980D+04
146	.89290D+04
147	.93180D+04
148	.10094D+05
149	.10677D+05
150	.11647D+05
151	.12812D+05
152	.13977D+05
153	.15529D+05
154	.16306D+05
155	.17082D+05
156	.19024D+05
157	.15530D+04
158	.23290D+04
159	.31060D+04
160	.38820D+04
161	.46590D+04
162	.54350D+04
163	.62120D+04
164	.69880D+04
165	.79980D+04
166	.89290D+04
167	.97830D+04
168	.10871D+05
169	.11647D+05
170	.12812D+05
171	.13977D+05
172	.15529D+05
173	.16306D+05
174	.17082D+05
175	.19257D+05
176	.38800D+03
177	.15530D+04
178	.23290D+04
179	.31060D+04
180	.38820D+04
181	.46590D+04
182	.54350D+04
183	.62120D+04
184	.69880D+04
185	.79980D+04
186	.89290D+04
187	.10094D+05
188	.10871D+05
189	.11647D+05
190	.12812D+05
191	.13977D+05
192	.15529D+05
193	.16306D+05
194	.17082D+05
195	.19567D+05
196	.77600D+02

197	.388200D+03
198	.155290D+04
199	.232900D+04
200	.302800D+04
201	.380500D+04
202	.465900D+04
203	.543500D+04
204	.621200D+04
205	.698800D+04
206	.760900D+04
207	.776500D+04
208	.815300D+04
209	.931800D+04
210	.108710D+05
211	.116470D+05
212	.128120D+05
213	.139770D+05
214	.155290D+05
215	.163060D+05
216	.170820D+05
217	.195670D+05
218	.000000D+00
219	.388000D+03
220	.155300D+04
221	.232900D+04
222	.302800D+04
223	.388200D+04
224	.458100D+04
225	.543500D+04
226	.597900D+04
227	.660000D+04
228	.675500D+04
229	.737700D+04
230	.784200D+04
231	.854100D+04
232	.108710D+05
233	.116470D+05
234	.128120D+05
235	.139770D+05
236	.155290D+05
237	.163060D+05
238	.170820D+05
239	.195670D+05
240	.155000D+03
241	.368000D+03
242	.155300D+04
243	.194100D+04
244	.256200D+04
245	.349400D+04
246	.427100D+04
247	.504700D+04
248	.543500D+04
249	.582400D+04
250	.757100D+04
251	.807500D+04
252	.892900D+04
253	.108710D+05
254	.116470D+05
255	.128120D+05
256	.139770D+05
257	.155290D+05
258	.163060D+05
259	.170820D+05
260	.195670D+05
261	.466000D+03
262	.155300D+04
263	.232900D+04
264	.310600D+04
265	.368200D+04
266	.427100D+04
267	.504700D+04
268	.753200D+04

269	.80750D+04
270	.89290D+04
271	.10871D+05
272	.11647D+05
273	.12812D+05
274	.13977D+05
275	.15529D+05
276	.16306D+05
277	.17082D+05
278	.19567D+05
279	.85400D+03
280	.15530D+04
281	.23290D+04
282	.31060D+04
283	.38820D+04
284	.45040D+04
285	.69880D+04
286	.76090D+04
287	.80750D+04
288	.89290D+04
289	.10871D+05
290	.11647D+05
291	.12812D+05
292	.13977D+05
293	.15529D+05
294	.16306D+05
295	.17082D+05
296	.19489D+05
297	.15530D+04
298	.23290D+04
299	.31060D+04
300	.35720D+04
301	.54350D+04
302	.77650D+04
303	.89290D+04
304	.10871D+05
305	.11647D+05
306	.12812D+05
307	.13977D+05
308	.15529D+05
309	.16306D+05
310	.17082D+05
311	.19334D+05
312	.29510D+04
313	.38820D+04
314	.54350D+04
315	.77650D+04
316	.89290D+04
317	.10871D+05
318	.11647D+05
319	.12812D+05
320	.13977D+05
321	.15529D+05
322	.16306D+05
323	.17082D+05
324	.19023D+05
325	.30280D+04
326	.38820D+04
327	.54350D+04
328	.77650D+04
329	.89290D+04
330	.10871D+05
331	.11647D+05
332	.12812D+05
333	.13977D+05
334	.15529D+05
335	.16306D+05
336	.17082D+05
337	.18441D+05
338	.35720D+04
339	.54350D+04
340	.77650D+04

341			.89290D+04
342			.10871D+05
343			.11647D+05
344			.12812D+05
345			.13977D+05
346			.15529D+05
347			.16306D+05
348			.17082D+05
349			.17471D+05
350			.48920D+04
351			.77650D+04
352			.89290D+04
353			.10871D+05
354			.11647D+05
355			.12812D+05
356			.13977D+05
357			.15529D+05
358			.16306D+05
359			.17082D+05
360			.77650D+04
361			.89290D+04
362			.10871D+05
363			.11647D+05
364			.12812D+05
365			.13977D+05
366			.15529D+05
1			621.
2			388.
3			78.
4			0.
5			39.
6			78.
7			155.
8			155.
9			78.
10			155.
11			233.
12			466.
13			777.
14	14	1	1553.
29	16	1	3106.
46	16	1	3882.
63	16	1	4659.
80			4465.
81			4814.
82	5	1	5435.
88			5591.
89			5979.
90	11	1	5435.
102	2	1	6212.
105			5901.
106			6212.
107			6134.
108			6600.
109	11	1	6212.
121	17	1	6988.
139	17	1	7765.
157	18	1	8541.
176	19	1	10094.
196	3	1	10871.
200			10560.
201			10482.
202	1	1	10405.
204	2	1	10482.
207			10638.
208	9	1	10482.
218	3	1	11259.
222			11337.
223	2	1	11259.
226	1	1	11026.
228			11259.

229			11026.
230			10948.
231	8	1	10871.
240	9	1	12035.
250			11259.
251			11453.
252	8	1	11647.
261	6	1	12812.
268	10	1	12035.
279	6	1	13200.
286	1	1	12501.
288	8	1	13200.
297			13744.
298			13977.
299	1	1	14054.
301	10	1	13977.
312	12	1	15529.
325	12	1	17082.
338	11	1	18635.
350	8	1	20188.
359			19179.
360			21586.
361			21741.
362			21896.
363			21819.
364			21586.
365			21275.
366			20576.

THE FOLLOWING CARDS CONTAIN ELEMENT INCIDENCES AND TYPE

1	1	15	14	0	-1		
2	1	2	16	15	-1	12	1
14	13	28	27	0	-1		
15	14	15	30	29	-1	14	1
29	28	44	43	0	-1		
30	28	45	44	0	-1		
31	29	30	47	46	-1	16	1
47	46	47	64	63	-1	15	1
62	61	62	78	0	-1		
63	63	64	83	82	-1	14	1
77	77	78	96	0	-1		
78	79	98	97	0	-1		
79	79	80	99	98	-1	2	1
81	81	101	100	0	-1		
82	82	83	103	102	-1	2	1
84	84	85	104	0	-1		
85	85	86	105	104	-1	10	1
95	95	96	114	0	-1		
96	97	116	115	0	-1		
97	97	98	117	116	-1	4	1
101	102	103	122	121	-1	11	1
112	113	114	132	0	-1		
113	115	133	132	0	-1		
114	115	116	134	133	-1	5	1
119	121	122	140	139	-1	10	1
129	131	132	149	0	-1		
130	132	150	149	0	-1		
131	132	133	151	150	-1	6	1
137	139	158	157	0	-1		
138	139	140	159	158	-1	9	1
147	148	149	167	0	-1		
148	149	168	167	0	-1		
149	149	150	169	168	-1	7	1
156	157	177	176	0	-1		
157	157	158	178	177	-1	8	1
165	165	166	185	0	-1		
166	166	167	185	0	-1		
167	167	186	185	0	-1		
168	167	187	186	0	-1		
169	167	168	188	187	-1	8	1
177	176	197	196	0	-1		
178	176	177	198	197	-1	9	1

```
187  185  207  206    0   -1
188  185  186  208  207   -1   10    1
198  196  197  219  218   -1   21    1
219  218  219  241  240   -1    9    1
228  227  228  249    0   -1
229  228  229  250  249   -1   11    1
240  240  241  261    0   -1
241  241  242  262  261   -1    6    1
247  247  248  267    0   -1
248  248  249  267    0   -1
249  249  250  268  267   -1   11    1
260  261  262  280  279   -1    5    1
265  266  267  284    0   -1
266  267  285  284    0   -1
267  267  268  286  285   -1   11    1
278  279  280  297    0   -1
279  280  281  298  297   -1    3    1
282  283  284  300    0   -1
283  284  301  300    0   -1
284  284  285  302  301   -1
285  285  286  287  302   -1
286  287  288  303  302   -1    9    1
295  300  313  312    0   -1
296  300  301  314  313   -1   11    1
307  312  313  326  325   -1   12    1
319  325  326  338    0   -1
320  326  327  339  338   -1   11    1
331  338  339  350    0   -1
332  339  340  351  350   -1    9    1
341  348  349  359    0   -1
342  350  351  360    0   -1
343  351  352  361  360   -1    6    1
349  357  358  366    0   -1

   THE  FOLLOWING  CARDS  CONTAIN  MATERIAL  TYPE  CORRECTION
207    1    1   -2    0
229    1    1   -2    0
250    1    1   -2    0
268    1    1   -2    0
286    1    1   -2    0

   THE  FOLLOWING  CARDS  CONTAIN  PRE-INITIAL  CONDITIONS
   1  365    1    1.        0.

   THE  FOLLOWING  CARD  CONTAINS  TRANSIENT  CONTROLLING  INTEGERS
   0    0    0    0   72    7    4    1   13    1    2    1    2   33    4    4
   THE  FOLLOWING  CARDS  CONTAIN  SOURCES  AND  WELLS
 0.0        0.0        86400.        2.72E-72419200.      2.72E-72419210.      2.00E-7
 5011200.      2.00E-75011210.      0.81E-77689600.      0.81E-77689610.      1.29E-7
10368000.     1.29E-710368010.     1.13E-712960000.     1.13E-712960100.     0.0
13306000. 0.0
   1  348    1    1    0

0.0        -10.486    12972900. -10.486    12972960. -4.1660    13306000. -4.166
0.0        -6.344     12972900. -6.3440    12972960. -11.992    13306000. -11.992
0.0        8.3536     12972900. 8.3536     12972960. 7.2800     13306000. 7.280
0.0        16.7072    12972900. 16.7072    12972960. 14.56      13306000. 14.56
  89  107  108  227  226  225  224  223  222  200  201  202  203  208  207  230
 251  269  287  286  268  250  229  132  149  167  206  228  249  267  284  300
 185
   1   12    1    1    0
  14    9    1    2    0
  24    8    1    3    0
  33    0    1    4    0

   THE  FOLLOWING  CARDS  CONTAIN  DIRICHLET  BOUNDARY  CONDITIONS
0.0        1.0        332640.   1.1        12972960. 1.1        13306000. 1.1
0.0        1.0        332640.   1.3        12972960. 1.3        13306000. 1.3
0.0        1.0        332640.   1.5        12972960. 1.5        13306000. 1.5
0.0        1.0        332640.   1.6        12972960. 1.6        13306000. 1.6
0.0        1.0        332640.   1.7        12972960. 1.7        13306000. 1.7
0.0        1.0        332640.   1.8        12972960. 1.8        13306000. 1.8
0.0        1.0        332640.   2.0        12972960.  2.0        13306000. 2.0
```

```
  1    2    3    4    5    6    7    8    9   10   11   12   13   28   45   62
 78   96  114  132  115   97   79   80   81  101  120  138  156  175  195  217
239  260  278  296  311  324  337  349  359  358  366  365  364  363  362  361
360  350  338  325  312  300  299  298  297  279  261  240  218  196  176  157
139  121  102   82   63   46   29   14
  1    3    1    6    0
  5    8    1    5
 14              6
 15   13    1    7
 29    1    1    6
 31    1    1    5
 33    2    1    4
 36    8    1    3
 45    2    1    4
 48    1    1    5
 50    3    1    7
 54    8    1    2
 63    1    1    1
 65              2
 66              3
 67              5
 68    1    1    7
 70    2    1    6

  THE  FOLLOWING  CARDS  CONTAIN  UPPER  LEAKING  AQUIFERS
0.0       1.0        13306000. 1.0
0.0
  1  348    1    1    0

  THE  FOLLOWING  CARDS  CONTAIN  LOWER  LEAKING  AQUIFERS
0.0       0.0        13306000. 0.0
0.0
  1  348    1    1    0
```

INTERNAL DISTRIBUTION

1. S. I. Auerbach
2. J. S. Baldwin
3. W. J. Boegly, Jr.
4. R. O. Chester
5. R. B. Clapp
6. N. H. Cutshall
7. E. C. Davis
8. L. R. Dole
9. S. G. Hildebrand
10. D. D. Huff
11. R. S. Lowrie
12. T. W. Oakes
13. F. G. Pin
14. D. E. Reichle
15. C. R. Richmond
16. E. D. Smith
17. B. P. Spalding
18-27. L. E. Stratton
28. R. G. Wymer
29-33. G. T. Yeh
34. Central Research Library
35-49. ESD Library
50-51. Laboratory Records Department
52. Laboratory Records-ORNL-RC
53. ORNL Patent Section
54. ORNL Y-12 Technical Library

EXTERNAL DISTRIBUTION

55. M. Barainca, Program Manager, Low-Level Waste Management Program, U.S. Department of Energy, 550 Second Street, Idaho Falls, ID 83401
56. J. J. Blakeslee, Program Manager, Nuclear Waste Processing, Rocky Flats Plant, Rockwell International, P.O. Box 464, Golden, CO 80401
57. J. Thomas Callahan, Associate Director, Ecosystem Studies Program, Room 336, 1800 G Street, NW, National Science Foundation, Washington, DC 20550
58. T. C. Chee, R&D and Byproducts Division, DP-123 (GTN), U.S. Department of Energy, Washington, DC 20545
59. A. T. Clark, Jr., Division of Fuel Material Safety, U.S. Nuclear Regulatory Commission, Washington, DC 20555
60. Peter Colombo, Group Leader, Nuclear Waste Research, Brookhaven National Laboratory, Bldg. 701, Upton, NY 11973
61. E. F. Conti, Office of Nuclear Regulatory Research, Nuclear Regulatory Commission, MS-1130-SS, Washington, DC 20555
62. J. E. Dieckhoner, Acting Director, Operations and Traffic Division, DP-122 (GTN), U.S. Department of Energy, Washington, DC 20545
63. G. J. Foley, Office of Environmental Process and Effects Research, U.S. Environmental Protection Agency, 401 M Street, SW, RD-682, Washington, DC 20460
64. Carl Gertz, Director, Radioactive Waste Technology Division, Idaho Operations Office, U.S. Department of Energy, 550 Second Street, Idaho Falls, ID 83401
65. C. R. Goldman, Professor of Limnology, Director of Tahoe Research Group, Division of Environmental Studies, University of California, Davis, CA 94616

66. W. H. Hannum, Director, West Valley Project Office, U.S. Department of Energy, P.O. Box 191, West Valley, NY 14171
67. J. W. Huckabee, Project Manager, Environmental Assessment Department, Electric Power Research Institute, 3412 Hillview Avenue, P.O. Box 10412, Palo Alto, CA 94303
68. E. A. Jennrich, Program Manager, Low-Level Waste Management Program, EG&G Idaho, Inc., P.O. Box 1625, Idaho Falls, ID 83415
69. J. J. Jicha, Director, R&D and Byproducts Division, DP-123 (GTN), U.S. Department of Energy, Washington, DC 20545
70. E. A. Jordan, Low Level Waste Program Manager, Division of Storage and Treatment Projects, NE-25 (GTN), U.S. Department of Energy, Washington, DC 20545
71. George Y. Jordy, Director, Office of Program Analysis, Office of Energy Research, ER-30, G-226, U.S. Department of Energy, Washington, DC 20545
72. J. Howard Kittel, Manager, Office of Waste Management Programs, Argonne National Laboratory, 9700 S. Cass Ave., Bldg. 205, Argonne, IL 60439
73. L. T. Lakey, Waste Isolation, Pacific Northwest Laboratory, Richland, WA 99352
74. Leonard Lane, Los Alamos National Laboratory, P.O. Box 1663, Los Alamos, NM 87545
75. D. B. Leclaire, Director, Office of Defense Waste and Byproducts Management, DP-12 (GTN), U.S. Department of Energy, Washington, DC 20545
76. Helen McCammon, Director, Ecological Research Division, Office of Health and Environmental Research, Office of Energy Research, MS-E201, ER-75, Room E-233, Department of Energy, Washington, DC 20545
77. Michael McFadden, Waste Management, Albuquerque Operations Office, U.S. Department of Energy, Albuquerque, NM 37115
78. G. L. Meyer, Environmental Protection Agency, 401 M Street SW, MS-ANR459, Washington, DC 20460
79. Edward O'Donnell, Division of Radiation Programs and Earth Sciences, U.S. Nuclear Regulatory Commission, Mail Stop 1130 SS, Washington, DC 20555
80. J. W. Patterson, Program Director, Waste Management Program Office, Rockwell Hanford Operations, P.O. Box 800, Richland, WA 99352
81. Irwin Remson, Department of Applied Earth Sciences, Stanford University, Stanford, CA 94305
82. Paul G. Risser, Office of the Chief, Illinois Natural History Survey, Natural Resources Building, 607 E. Peabody Ave., Champaign, IL 61820
83. Jackson Robertson, USGS, 410 National Center, Reston, VA 22092
84. E. M. Romney, University of California, Los Angeles, 900 Veteran Avenue, Los Angeles, CA 90024

85. R. J. Starmer, HLW Technical Development Branch, Office of Nuclear Material Safety and Safeguards, Nuclear Regulatory Commission, Room 427-SS, Washington, DC 20555
86. J. G. Steger, Environmental Sciences Group, Los Alamos Scientific Laboratory, MS-K495, P.O. Box 1663, Los Alamos, NM 87545
87. R. J. Stern, Director, Office of Environmental Compliance, MS PE-25, FORRESTAL, U.S. Department of Energy, 1000 Independence Avenue, SW, Washington, DC 20585
88. J. A. Stone, Savannah River Laboratory, E. I. DuPont de Nemours and Company, Bldg. 773-A, Room E-112, Aiken, SC 29808
89. Leonard H. Weinstein, Program Director of Environmental Biology, Cornell University, Boyce Thompson Institute for Plant Research, Ithaca, NY 14853
90. Raymond G. Wilhour, Chief, Air Pollution Effects Branch, Corvallis Environmental Research Laboratory, U.S. Environmental Protection Agency, 200 SW 35th Street, Corvallis, OR 97330
91. Frank J. Wobber, Ecological Research Division, Office of Health and Environmental Research, Office of Energy Research, MS-E201, Department of Energy, Washington, DC 20545
92. M. Gordon Wolman, The Johns Hopkins University, Department of Geography and Environmental Engineering, Baltimore, MD 21218

93-97. K-F. V. Wong, University of Miami, Coral Gables, FL 33124

98. Robert W. Wood, Director, Division of Pollutant Characterization and Safety Research, U.S. Department of Energy, Washington, DC 20545
99. Office of Assistant Manager for Energy Research and Development, Oak Ridge Operations, P. O. Box E, U.S. Department of Energy, Oak Ridge, TN 37831

100-126. Technical Information Center, Oak Ridge, TN 37831